Conductive Thermoplastic Composite Blends for Flow Field Plates for Use in Polymer Electrolyte Membrane Fuel Cells (PEMFC)

by

Yuhua Wang

A thesis
presented to the University of Waterloo
in fulfillment of the
thesis requirement for the degree of
Master of Applied Science
in
Chemical Engineering

Waterloo, Ontario, Canada, 2006

I hereby declare that I am the sole author of this thesis. This is a true copy of the thesis, including any required final revisions, as accepted by my examiners.

I understand that my thesis may be made electronically available to the public.

Abstract

This project is aimed at developing and demonstrating highly conductive, lightweight, and low-cost thermoplastic blends to be used as flow field bipolar plates for polymer electrolyte membrane (PEM) fuel cells.

The research is focused on designing, prototyping, and testing carbon-filled thermoplastic composites with high electrical conductivity, as well as suitable mechanical and process properties.

The impact of different types of fillers on the composite blend properties was evaluated, as well as the synergetic effect of mixtures of fill types within a thermoplastic polymer matrix. A number of blends were produced by varying the filler percentages. Composites with loadings up to 65% by weight of graphite, conductive carbon black, and carbon fibers were investigated. Research results show that three-filler composites exhibit better performance than single or two-filler composites.

Injection and compression molding of the conductive carbon filled polypropylene blend was used to fabricate the bipolar plates. A Thermal Gravimetric Analysis (TGA) was used to determine the actual filler loading of composites. A Scanning Electron Microscope (SEM) technique was use as an effective way to view the microstructure of composite for

properties such as edge effects, porosity, and fiber alignment. Density and mechanical properties of conductive thermoplastic composites were also investigated. During this study, it was found that 1:1:1 SG-4012/VCB/CF composites showed better performance than other blends. The highest conductivity, 1900 S/m in in-plane and 156 S/m in through plane conductivity, is obtained with the 65% composite. Mechanical properties such as tensile modulus, tensile strength, flexural modulus and flexural strength for 65% 1:1:1 SG-4012/VCB/CF composite were found to be 584.3 MPa, 9.50 MPa, 6.82 GPa and 47.7 MPa, respectively, and these mechanical properties were found to meet minimum mechanical property requirements for bipolar plates. The highest density for bipolar plate developed in this project is 1.33 g/cm^3 and is far less than that of graphite bipolar plate.

A novel technique for metal insert bipolar plate construction was also developed for this project. With a copper sheet insert, the in-plane conductivity of bipolar plate was found to be significantly improved. The performance of composite and copper sheet insert bipolar plates was investigated in a single cell fuel cell. All the composites bipolar plates showed lower performance than the graphite bipolar plate on current-voltage (I-V) polarization curve testing. Although the copper sheet insert bipolar plates were very conductive in in-plane conductivity, there was little improvement in single cell performance compared with the composite bipolar plates.

This work also investigated the factors affecting bipolar plate resistance measurement,

which is important for fuel cell bipolar plate design and material selection. Bipolar plate surface area (S) and surface area over thickness (S/T) ratio was showed to have significant effects on the significance of interfacial contact resistances. At high S/T ratio, the contact resistance was found to be most significant for thermoplastic blends. Other factors such as thickness, material properties, surface geometry and clamping pressure were also found to affect the bipolar plate resistance measurements significantly.

Acknowledgements

I wish to express my sincere appreciation to my thesis supervisor Dr. Michael Fowler for his valuable guidance, encouragement and support for this project. I also wish to express my great appreciation to Dr. Costas Tzoganakis and Dr. Leonardo Simon for their valuable guidance and great support for me to fulfill this project. I would like to thank my industrial supervisors at Polymer Technology Inc., in particular Chris Bennet, for giving me the opportunity to apply practical industrial R&D experience in this academic study.

I would also like to acknowledge the work of all the students whose work is included in this project. In particular, Taylor Mali, Rungsima, and Sumit Kundu for their great help in experiments, as well as support from all the group members, in the Fuel Cell research team.

Furthermore, I would like to thank everyone who has helped and encouraged me.

Table of Contents

List of Tables

List of Figures

Nomenclature and Abbreviations

Nomenclature

Symbol	Description	units
$E^0_{25℃}$	Half cell potential measured against a standard hydrogen electrode at 25℃	V
S	Surface area of sample	mm^2
T	Thickness of sample	mm
W	Width of sample	mm
L	Length of sample	mm
S/T	Surface area over thickness	mm
P	Clamping Pressure	Psi
R_{Meau}	Measured resistance	Ω
R_{Plate}	Resistance of bipolar plate sample	Ω
R_{GDL}	Resistance of carbon cloth	Ω
$R_{Au\text{-}Cu}$	Resistance of gold-nickel-copper plate	Ω
$R_{Au/GDL}$	Contact resistance caused by an interface of GDL and gold plate	Ω
$R_{P/GDL}$	Contact resistance caused by an interface of GDL and bipolar plate sample	Ω
V	Voltage	Volt
I	Current	Amps

Abbreviation

CB	Carbon black
CF	Carbon fiber
DOE	Design of experiment
GDL	Gas diffusion layer
LCP	Liquid crystal polymer
MEA	Membrane electrolyte assembly
NCG	Nickel coated graphite
PP	Polypropylene
SG	Synthetic graphite
VCB	Vulcan carbon black
PEMFC	Polymer Electrolyte Membrane Fuel Cell

Chapter 1: Introduction

1.1 Project Objectives

The polymer electrolyte membrane (PEM) fuel cell is one of the most promising power sources for stationary and transportation applications in the future due to many attractive features. These features include high efficiency, high power density, relatively low operating temperature, convenient fuel supply and long lifetime **[1, 2]**. However, the high cost of PEM fuel cells have became one of the major barriers to fuel cell commercialization **[3]**.

In order to make the PEM fuel cell more economically feasible, processing and material costs need to be reduced. This reduction extends to the cost associated with bipolar plates. As a commonly used component in the PEM fuel cell, bipolar plates account for approximately 80% of the fuel cell volume, 70% of the fuel cell weight, and as much as 60% of the entire stack cost **[4]**. This means that dramatic reductions in size, weight, and cost can be achieved by focusing on bipolar plate materials and production methods. In particular, finding an inexpensive mass production method would be an ideal way to lower cost. One approach to reduce the cost of PEM fuel cell bipolar plates is to develop new materials such as a thermoplastic polymer matrix composite to lower manufacturing cost. With polymer composites, Bar-On et. al. **[5]** estimated that the cost of

bipolar plates would be only 15%~29% of the stack cost.

The aim of this thesis was to develop highly conductive, lightweight, and low cost thermoplastic blends and demonstrate their use as bipolar plates for PEM fuel cell. In order to develop ideal conductive composite for bipolar plate use, different aspects were investigated in this project. Firstly, different conductive composites where developed and investigated for their conductivity and mechanical properties, then a novel metal sheet insert technique was investigated to significantly improve the conductivity of a bipolar plate. Finally, in-situ (i.e. in a fuel cell) properties of composite and metal sheet insert bipolar plates were investigated within the scope of this project.

1.2 Introduction to PEM Fuel Cell Technology

The polymer electrolyte membrane (PEM) fuel cell is an electrochemical energy conversion device that converts chemical energy of fuel directly into electric energy. PEM fuel cells are extremely attractive as power sources for transportation, distributed power, and portable electrical devices **[3, 4]**. They offer the potential of a solid state, lightweight, high power density, and low temperature power source **[6]**. There has been a significant increase in PEM fuel cell research in the past five years. The automotive industry has invested considerable effort in the commercialization of PEM fuel cell for cars, which are expected to eventually compete with internal combustion engine vehicles **[7]**. However, there continues to be barriers to commercialization of PEM fuel cells,

specifically, lack of hydrogen production and distribution infrastructure, low on-board hydrogen storage densities, durability of PEM fuel cell stacks, and the high cost. As one of the key components of the PEM fuel cell, new materials and designs of bipolar plates are essential to meet the required cost and weight reduction in fuel cells.

1.2.1 Structure of a PEM Fuel Cell

Figure 1.1 shows the major components in a single PEM fuel cell, which includes: the membrane electrolyte assembly (MEA) (which is an electrolyte membrane with catalyst layer on both sides), gas diffusion layers, gaskets, bipolar plates, current collectors and endplates. A PEM fuel cell consists of four primary components as shown in Table 1.1 **[8]**.

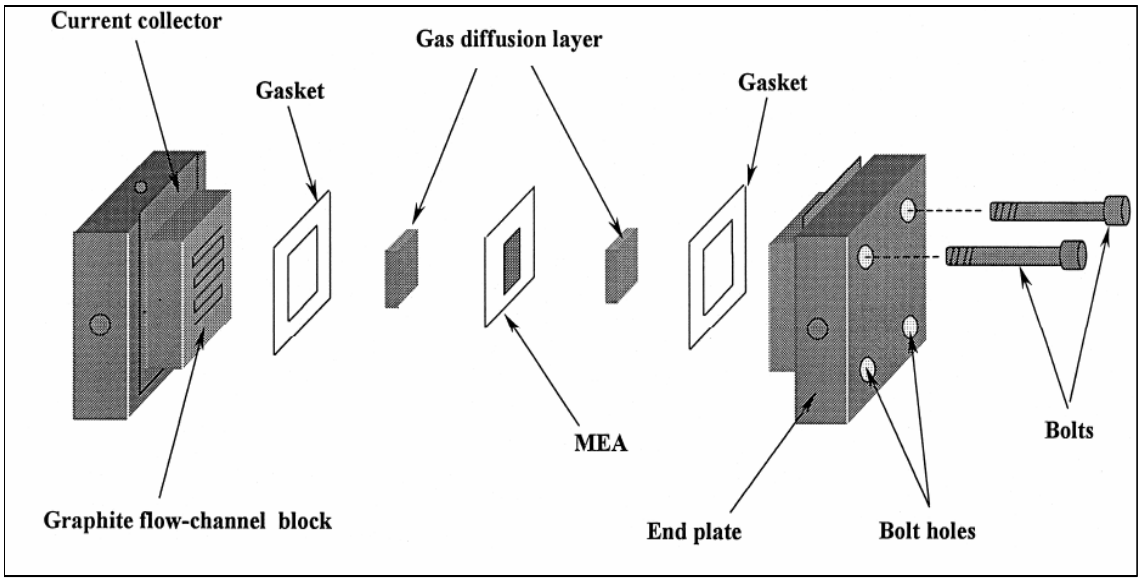

Figure 1.1: Structure diagram of polymer electrolyte membrane fuel cell

Table 1.1: Primary components of a PEM fuel cell [8]

Component	Material	Functionality
Membrane electrode Assembly (MEA)	Solid polymer electrolyte impregnated with catalyst layers for the anode and cathode Porous carbon paper or cloth for gas diffusion layer (GDL)	Consists of the two electrodes, a membrane electrolyte and two GDLs. The membrane separates (with a gas barrier) the two half-cell reactions and allows protons to pass through from anode to the cathode. The dispersed catalyst layers on the electrodes promote each half reaction. The GDL evenly distributes gases to the catalyst on the membrane, conducts electrons from the active area to the bipolar plates and assists in water management.
Bipolar plate	Graphite, stainless steel, or thermoplastic materials	Distributes gases over the active area of the membrane. Conducts electrons from the anode of one electrode pair to the cathode of next electrode pair. Carries water away from each cell.
Endplate	Material with good mechanical strength (normally steel or aluminum)	Provides integrated assembly for the entire fuel cell stack.
Current collector	Metal material with good electric contact and conductivity, normally copper.	Collects and transfers the current from the stack to an external circuit.

1.2.2 Electrochemistry of a PEM Fuel Cell

Humidified hydrogen or hydrogen-rich gas normally serves as the fuel in a PEM fuel cell, and humidified oxygen serves as the oxidant. From the anode, hydrogen diffuses

through the gas diffusion layer (GDL) to the catalyst layer in which hydrogen molecules are split into protons and electrons according to the following half cell electrochemical reaction **[9]**:

$$H_2 \rightarrow 2H^+ + 2e^- \qquad E^0_{25^\circ C} = 0.00\ V \qquad (1.1)$$

Where $E^0_{25^\circ C}$ is the half cell potential measured against a standard hydrogen electrode at temperature of 25° C. The protons travel through the electrolyte membrane to the cathode while the electrons are conducted to the cathode through the external circuit.

At the cathode, oxygen diffuses through the cathode GDL to the cathode catalyst. At the catalyst, oxygen reacts with protons and electrons forming water and producing heat via this half reaction shown in Eqn. (1.2):

$$2H^+ + {}^1/_2\, O_2 + 2e^- \rightarrow H_2O \qquad E^0_{25^\circ C} = +1.229\ V \qquad (1.2)$$

The overall reaction of the PEM fuel cell is presented below:

$$H_2 + {}^1/_2\, O_2 \rightarrow H_2O \qquad E^0_{25^\circ C} = +1.229\ V \qquad (1.3)$$

Figure 1.2 illustrates the diagram of a typical PEM fuel cell **[10]**.

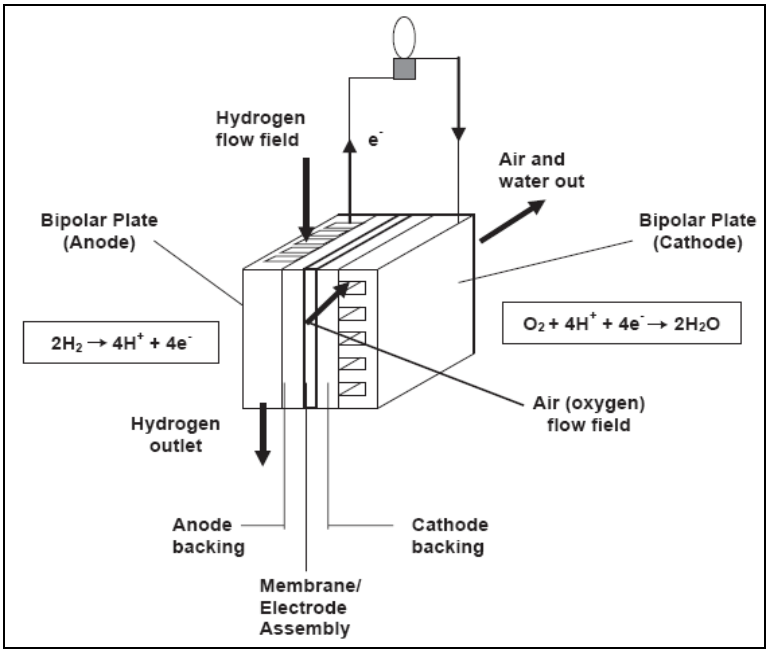

Figure 1.2: Schematic diagram of a polymer electrolyte membrane fuel cell [10]

In the operation of a PEM fuel cell, the bipolar plates serve a number of functions, including: the distribution of gases over the membrane, the conduction of electrons to and from the anode and cathode electrodes, the conduction of heat to and from the electrodes (and they often contain cooling channels to aid in thermal management), the removal of product water away from each cell, the gas barrier between different cells; and, the structural stability of the cell itself.

In the following sections, a detailed discussion about the functionality of bipolar plates within the PEM fuel cell will be given.

1.3 Introduction to the Bipolar Plate

Bipolar plate, also called flow field plate or separator plate, is used as an electrical connection between two electrodes with opposite polarities, thereby implementing the serial addition of the electrochemical potential of different cells in the fuel cell stack. The bipolar plate is made of gas-impermeable and electrically conductive material, serving as current collectors, and forming the supporting structure of the stack. The bipolar plates are commonly made from graphite, coated metals such as aluminum, stainless steel, titanium and nickel, or composite plates such as metal or carbon based plates **[10]**. Gas flow channels are machined or molded into the plates to provide paths for reactant gases. Figure 1.3 shows a photograph of a graphite bipolar plate with flow channels for PEM fuel cell.

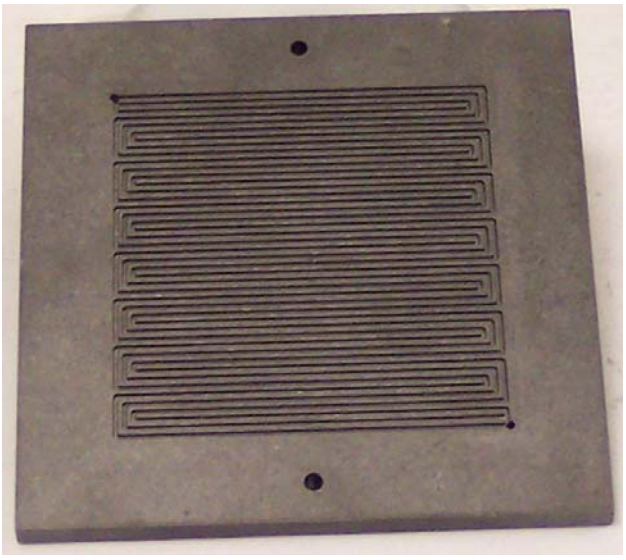

Figure 1.3: Photograph of a graphite bipolar plate with flow channels

As one of the key components in a PEM fuel cell, bipolar plates represent a significant part of the total capital cost and most of the weight of a fuel cell stack. Critical to transportation and portable application of fuel cells are the design characteristics of volume density, energy, and power densities. Bipolar plates represent approximately 80% of total weight and 45% stack cost, and thus are critical to fuel cell design **[10]**. Since there is a relatively large amount of material mass used in bipolar plates, the cost of the material itself is critical. To date, almost all flow path manufacturing involves the machining of the flow path into a plate 'blank', which is a very costly process. This results is in approximately 29% of the fuel cell cost [5] being attributed to the plate. As a key factor to affect the commercialization of PEM fuel cells, it is desirable that bipolar plates be inexpensive, thin, and as lightweight as possible to reduce the weight, volume, and cost of fuel cell. Note that in transportation applications, weight is especially critical because additional weight reduces fuel efficiency, range, and effects handling. The materials suitable for bipolar plates must also allow for the ability to be mass produced at low costs with the flow path on the surface of bipolar plate. A typical fuel cell in vehicle application will include 200 – 400 plates. In this case, proper material selection and processing methodology for bipolar plates is necessary if they are to be widely used in the automotive industry **[11]**. New materials for bipolar plates must have high electrical conductivity and a lower density compared to the available materials such as steel, aluminum, and graphite, and must be able to be mass produced **[12]**.

1.3.1 Functionality of Bipolar Plates

A typical PEM fuel cell (Fig. 1.1) essentially consists of an anode backing, membrane/electrode assembly (MEA) and cathode backing sandwiched between two bipolar plates (anode and cathode) [9]. Bipolar plates serve multiple functions in the operation environment of PEM fuel cells, and are therefore required to exhibit certain material properties.

The primary functions of bipolar plates include [8, 13]:

- the ability to conduct electrons to complete the circuit, including:
  - collecting and transporting electrons from the anode and cathode,
  - connecting individual fuel cells in series to form a fuel cell stack with required voltage (i.e. fuel cell are typically arranged in a bi-polar configurations);
- providing a flow path for gas transport to distribute the gases over the entire electrode area uniformly;
- separating oxidant and fuel gases and feeding H_2 to the anode and O_2 to the cathode, while removing product water;
- providing mechanical strength and rigidity to support thin membrane and electrodes and clamping forces for the stack assembly; and
- providing thermal conduction to help regulate fuel cell temperature and removing heat from the electrode to the cooling channels.

For an ideal bipolar plate, the required material properties are described in Table1.2.

Table 1.2: Material Property Requirements for an Ideal Bipolar Plate [1]

Parameters	Requirement
Volume Conductivity	> 10000 S/m
Strength	Able to withstand clamping pressure of 200 Psi
Weight	Maximum of 200 g per plate
Volume	1 litre/kW/stack
Cost	< \$0.0045/cm^2
Current Density Decay	< 10% per 5000 h. operation
Permeability	Maximum H_2 leakage of 10^{-4} $cm^3/s\text{-}cm^2$
Corrosion	$8*10^{-7}$ mol/cm^2 per 5000hr or 0.0016 mA/cm^2 per 5000hr

1.3.2 Materials for Bipolar Plates

There are a range of materials that could be used as materials for bipolar plates, which include: metals or metal alloys with or without coatings, graphite, carbon/polymer composites and carbon/carbon composites. Table 1.3 and Figure 1.3 generalize the existing materials suitable for bipolar plates **[14].**

A number of options can be considered, including metal-based bipolar plate **[15]**, carbon-filled polymers **[16],** and carbon/carbon composite **[17]**. Metal plates are often

coated with corrosion-resistant layers on the surface, while graphite plates are impregnated with a sealant treatment to lower the gas permeability. In recent years, extensive research has been conducted for low cost, lightweight and high performance bipolar plates in order to replace high cost graphite bipolar plates.

Table 1.3: Possible PEM fuel cells bipolar plate materials [14]

Types of Materials	Properties
Graphite	-Impregnate with polymer -Highly conductive -Brittle and thick -High costs for machining flow path
Metals or Metal Alloys	-Stainless steel - Al alloys -Ni-Cr alloy -Ti steel -Highly conductive -Corrosion problem -High cost of machining flow path
Composite Materials	-Graphite/ Carbon composite -Carbon/carbon composite -Light and low cost -Low conductivity compare to graphite and metal plate
Conductive Plastics	- Liquid Crystal Polymer (e.g. LCP) - relative low conductivity

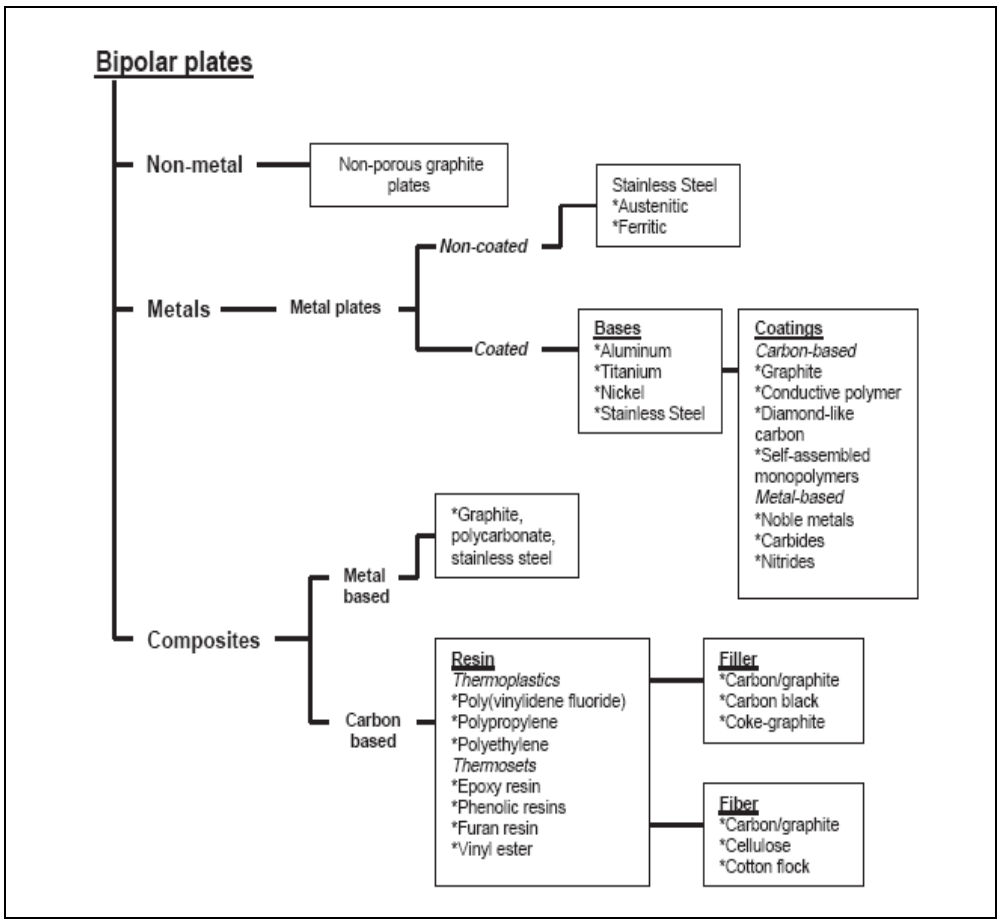

Figure 1.4: Classification of materials for bipolar plates used in PEM fuel cells [10]

1.3.2.1 Graphite Bipolar Plates

The most popular bipolar plates used in PEM fuel cell are graphite plates. Graphite bipolar plates possess good electrical conductivity, excellent corrosion resistance, and a lower density than metal plates. The problems of graphite plates are their brittleness and lower density than metal plates. The problems of graphite plates are their brittleness and porous structure as well as the high cost. The high cost of graphite bipolar plate is

associated with the machining of gas flow channels on the surface of plates and post processing such as resin impregnation to make the plate impermeable to the fuel and oxygen**.**

Because of the brittleness of graphite, graphite plates should be a few millimeters thick in order to maintain sufficient mechanical strength for machining flow channels and stacking assembly. Thus, the weight and volume of the graphite bipolar plate causes the fuel-cell stack to be heavy and of a large volume. As a result of machining costs, graphite plates are too expensive (>US$10/plate) to be used in the automotive industry cost structures. However, graphite bipolar plates set the standard for conductivity and corrosion resistance with which to benchmark other materials.

1.3.2.2 Metallic Bipolar Plates

Pure metals and stainless steel **[18, 19, 20]**, either with or without a protective and conductive coating, are being researched as possible bipolar plate materials. Use of metallic components has several advantages over the conventionally used graphite plates. Metallic materials include stainless steel, titanium, and aluminum. Stainless steel is considered the most promising material for bipolar plate **[21]** because it is a widely used commercial material with well understood properties.

Metallic bipolar plates offer good electrical and thermal conductivity, excellent mechanical properties, as well as negligible gas permeability. However, one problem with metallic bipolar plates is the high machining cost for gas flow channels. New techniques such as continuous rolling or batch stamping have also been developed to facilitate the mass production of metallic bipolar plates, but these plates are still in the research stage. Also, the weight of metal plates is a disadvantage in transportation applications.

Metallic bipolar plates also have corrosion problems because of the release of cations which can poison the electrode catalysts or the electrolyte, thus decreasing of cell performance. Metal plates are also prone to passivity, in that they form an oxide surface layer which leads to increasing contact resistance and an associated ohmic loss due to the extra resistance. The membrane electrolyte assembly (MEA) in PEM fuel cell is a strong acid, and the product water is ion free, and both of these factors lead to the leaching of cations from metals.

High machining cost and corrosion problems affect the potential application of metallic bipolar plates in PEM fuel cells. In order to improve the corrosion resistance of metallic bipolar plates, surface treatments have become one of the key technologies in metallic bipolar plate development. Surface treatments include coating with a conductive and corrosion-resistant layer (such as a titanium nitride layer) on the surface of metallic

bipolar plate [22]. Woodman [23] has developed electroplated aluminum plates to improve the corrosion problem of aluminum alloy. Davies et. al. [24] studied coating on stainless steel and titanium for PEM fuel cells. They reported the coated film could effectively protect bipolar plates, although in this reference it was noted that there remains significant cation leaching, and the impact of this contamination on the MEA was not considered. Wind et al. [25] had investigated the effects of coating materials on reducing metallic ions in membrane electrolyte assembly (MEA). Lee et. al. [26] studied different coating materials by a physical vapor deposition (PVD) process to analyze their corrosion resistance improvement. The corrosion rates of all materials were tested in a simulated fuel cell environment. Results of the corrosion tests in this publication indicated that the coating materials had good corrosion resistance and were stable in the simulated fuel cell environment, although no lifetime durability testing was conducted. The results of the above researchers indicated that coating materials did affect the protection mechanism while demonstrating their effectiveness. However, it is very difficult and costly to perform surface treatment of metallic bipolar plates, and little durability evaluation has been conducted.

1.3.2.3 Polymer -Carbon Composite Bipolar Plates

To reduce the weight of a fuel cell, new materials for bipolar plates are necessary. Recently, polymer matrix composites have been investigated for use in the manufacture

of bipolar plates since polymer-carbon composites are less expensive and light in weight compare to the available materials such as steel, aluminum and graphite.

Processability is also an important issue for the mass production of bipolar plates. Therefore, thermoplastic polymer–carbon composites are an interesting alternative to metal or graphite bipolar plates. Ideally, the composite plates should meet the following requirements **[27]**:

- high electrical conductivity (DOE target of 100 S/cm **[28]**)**;**
- hydrogen permeability equal to or below the range of the permeability of the ionic conducting membrane;
- good mechanical properties;
- thermal stability at fuel cell working conditions (-40 to 120℃ for fuel cell driven vehicles);
- low density;
- chemical stability in the presence of fuel, oxidant and product water, which may be slightly acidic (corrosion < 16 μ Acm^{-2});
- corrosion resistant;
- low permeability to fuel and oxidant (H_2 permeability< $2*10^{-6}$ 16 cm^3/cm^2 s);
- low thermal expansion;
- reproducibility, specifically able to have a reproducible flow path manufactured into the plate within engineering tolerances;

- easy finished to acceptable quality standards; and
- recyclability, or simple end of life management of the material.

With proper selection of the polymer matrix, the polymer carbon composite can provide chemical inertness and gas tightness. Thermo-set and thermoplastic polymer resins can be selected as composites polymer matrix, and mixed with conductive fillers such as carbon black, carbon fibers, graphite, metal coated graphite or low melting metal alloys. Compression molding or injection molding is used to fabricate bipolar plates with gas flow channels on the surfaces, and the process methodology greatly reduces the cost of bipolar plates.

As a promising alternative to fulfill these requirements for PEM bipolar plates, the development of carbon composites have been attempted. Besmann et. al. **[17]** fabricated a plate by using carbon fibers bound with thermo-set phenolic resin. Chemical vapor infiltration as an additional surface treatment was used to seal and remove porosity on the plate surface. Thermo-set conductive blends could be a promising alternative material for bipolar plates, since their thermal and chemical stability is matched by good mechanical strength and dimensional stability values. Thermo-set polymers still do pose some challenges in a mass production, high material volume manufacturing environment.

Additional advantages could be gained if thermoplastic resins can be used, as this would

enable the use of high-productivity, conventional molding processes such as injection molding or compression injection molding. Furthermore, the use of thermoplastic resins would provide recyclability and improved chemical stability over thermo-set composites. Graphite mixing with polymer matrix is another way to improve the conductivity of polymer carbon composites. Kuan **[29]** developed a novel composite bipolar plate for a polymer electrolyte fuel cell by a bulk-molding compound (BMC) process. The electrical resistance of the composite material decreases from 20,000 to 5.8 S/m when the graphite content increases from 60 to 80 wt%. Polymer mixes with higher loadings of graphite can lead to the higher conductivity of composites.

Moreover, mixing a polymer matrix with multiple conductive fillers is another effective way to develop higher conductivity composites. Mighri **[30]** developed highly conductive, lightweight, and low-cost bipolar plates for use in proton exchange membrane fuel cells. Injection and compression molding were applied to fabricate plates with carbon-filled polyphenylene sulfide (PPS). Loadings up to 60 wt% in the form of graphite, conductive carbon black, and carbon fibers were investigated. A volume resistivity of around 0.06 Ohm-cm was attained with injection molded plates made of the PPS-based blend.

A new high performance, low cost, heterogeneous composite bipolar plate **[31]** has been fabricated by Ming-San Lee et. al.. This new plate has its “ribs” made of flexible and

loose carbon fiber bunches while the rest of the plate is unfilled resin. This design shows many advantages: low contact resistance acquired under very low compression force; reduced stack weight and volume; full electrode utilization; high performance and low cost.

Intrinsically conductive polymers have also been applied to develop highly conductive bipolar plates for PEM fuel cell. For example, Zenite, a new liquid crystal polymer (LCP) resin material for electronic connectors from DuPont, promises suitable strength, toughness, and precision for electronic connectors and other molded components **[32]**.

DuPont™ Zenite® LCP liquid crystal polymer resin excels in all-around performance and molding productivity. The aim of choosing LCP resin is to replace ceramics, thermosets or PPS in order to downsize automotive parts, upgrade performance, accelerate production, reduce costs, and develop new markets **[33]**. The features of Zenite include high-temperature electrical/electronic assembly; design freedom; excellent chemical resistance, low mold shrinkage, low thermal expansion, super-fast cycling molding speed, excellent balance of stiffness, strength, and toughness. Typical applications include a wide range of components such as electrical/electronics, lighting, telecommunications, auto ignition and fuel handling, aerospace, fiber optics, motors, imaging devices, sensors, ovenware, and fuel or gas barrier structures **[32]**.

Wolf [34] developed an electrically conductive LCP-carbon composite with low carbon content for bipolar plate application in PEM fuel cells. Lightweight polymer-carbon composites with high specific electrical conductivity at carbon content below 40% were developed. However, liquid crystal polymer resins are too expensive for the high volume applications in manufacturing of bipolar plates for automotive applications.

Although thermoplastic polymer/carbon composite bipolar plates have advantages in that they can be mass produced, these materials have had great difficultly in meeting the resistance and thickness target, as well as mechanical properties, because most polymer resins intrinsically have very low electric conductivity, which then require a higher filler loading to meet with the desired conductivity target for bipolar plates (the minimum overall plate conductivity should be 10,000 S/m [28]). In turn, higher filler loading within the polymer matrix will lead to poorer mechanical properties of bipolar plates. However, from the literature review, it is clear that achieving this level of conductivity with thermoplastic composites is a challenging task. In the following sections, detailed discussion will focus on polymer carbon composites, a promising alternative for bipolar plates in PEM fuel cell.

1.3.3 Polymer-Carbon Composites

Polymer carbon composites, or electrically conductive polymer composites (CPC), are obtained by blending an insulating polymer matrix with conductive fillers like carbon black, carbon fiber or metal particles. Whatever the nature of particles, current circulation is obtained through 'percolation' of the filler through the polymer resin, forming conductive pathways throughout the material. Bipolar plates made from polymer carbon composite are light in weight and have low gas permeability, and can reduce manufacturing cost by mass production.

1.3.3.1 Percolation Threshold

1.3.3.1.1 Concept of Percolation Threshold

Most polymer resins are intrinsically insulating, and their conductivity values are approximately $10^{-14} \sim 10^{-17}$ S/cm. The electrical conductivity of polymeric materials can be increased by the addition of conductive carbon fillers, such as carbon fibers, carbon black, and synthetic graphite. This practice, however, often results in poor mechanical properties of bipolar plates **[35, 36, 37]**. Compared to isotropic high-quality graphite plates, carbon-filled polymer composites have generally lower conductivity. Typical conductivity values for polymers, conductive fillers and metals are summarized in Table 1.4. Compared to metals, polymers and carbon based polymer composites have much lower conductivity. When conductive carbon fillers (conductivity $10^2 \sim 10^5$ S/m)

are mixed with polymers, the corresponding composite might have higher conductivity than that of pure, electrically insulating polymer matrix, but the conductivity of composites will depend on the shape, particle size, and properties of conductive fillers applied. The dispersion of the particles and the formation of a continuous network of the conductive fill are also critical to conductivity.

Table 1.4: Typical conductive Values for different materials [38]

Materials	**Conductivity (S/cm)**
Polymers	$10^{-14} \sim 10^{-17}$
Conductive Carbon fillers	$10^{2} \sim 10^{5}$
Metals	10^{6}

Many studies have been conducted with the intent of reducing the "percolation threshold" so that high material toughness and high conductivity can be achieved. The concept of "percolation threshold" is explained by Matthew et. al. **[38]** in details. Matthew stated that the electrical conductivity of a composite is generally characterized by its dependence on the fill volume fraction.

Figure 1.4 **[38]** shows the trend of the three main regions of a typical composite electrical

conductivity curve. From Figure 1.4, at lower filler loadings, the conductivity of the composite is very close to that of electrically insulating pure polymer matrix. However, at some critical loading, the conductivity increases many orders of magnitude with very little increase in the filler loading, which is called the "percolation threshold".

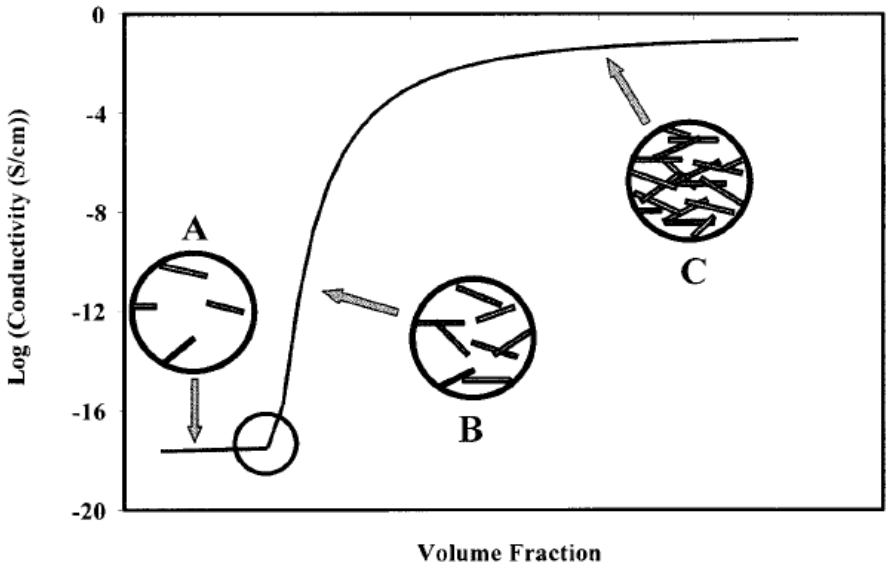

Figure 1.5: Dependence of electrical conductivity on the filler volume fraction [38]

After the region of significant increase, the conductivity of composite levels off and approaches to that of the filler material. At the percolation threshold, enough filler has been added so that it begins to form a continuous conductive network through the composite.

1.3.3.1.2 Effect of Filler Properties on Percolation Threshold

The properties of the fillers, which include type, size, shape, as well as orientation within the polymer matrix, play a significant role in determining the percolation threshold and the conductivity of the composite **[38]**.

For example, carbon fibers and carbon black, the different shapes of carbon, have different inherent conductivities. Their inherent conductivities typically control the upper bound of the conductivity curve shown in Figure 1.4. In the region of higher filler loadings, the composite conductivity should level off to a value slightly lower than that of fillers.

Different forms of carbon generally have different microstructures and, therefore, will affect electrical conductivity in different ways. For spherical particles, smaller particles have been reported to lower the percolation threshold **[39]**. For fillers with an aspect ratio (length/diameter) >1, carbon fiber for instance, a broader range of aspect ratios and larger aspect ratios have been shown to lower the percolation threshold **[40, 41]**.

The surface properties of filler and polymer also have a significant effect on composite conductivity **[42]**. Differences of surface energies between the filler and polymer indicate how well the polymer can wet the surface of the filler. The smaller of the differences between the two surface energy values, the better wetting of the filler by the polymer.

Better wetting effect means that larger amounts of the polymer coat the filler surface and that the filler has better and uniform dispersion within the composite.

However, this increases the composite percolation threshold because larger amounts of filler are required before the particles come in contact with one another. This can also result in increased composite electrical conductivity once the percolation threshold is reached **[39, 43]**.

Matthew **[38]** studied the electrical conductivity of carbon-filled polymers by the addition of three single fillers to nylon 6, 6 and polycarbonate in increasing concentrations. The fillers chosen were carbon black, synthetic-graphite particles, and milled pitch-based carbon fibers. At the high filler volume fractions, the carbon black produced a composite conductivity of approximately 10^{-1} S/cm in both polycarbonate (6.9 vol %) and nylon (6.6 vol %), and the percolation threshold for the carbon-black composite can be approximated to be at a volume fraction of 2.5 vol % for both polycarbonate and nylon. For synthetic graphite composite, the percolation threshold can be approximated to be 11 vol % for both nylon and polycarbonate, and 9.0 vol % for pitch-based carbon fiber for both nylon 6,6 and polycarbonate-based composites.

Although those studies were successful in reducing the percolation thresholds and in developing materials with resistivities sufficient for antistatic, electrostatic painting, and

electromagnetic interference shielding applications, these composites are not conductive enough for bipolar plate applications. Extensive research work was carried out to develop high conductivity polymer carbon composite by using different shape, size fillers.

Blunk et al. **[44]** investigated the use of low loadings of high-aspect-ratio conductive particles such as carbon/graphite fibers, flakes and carbon black, an alignment process **[45]**, and a conductive tie layer **[46]** to meet plate conductivity, thickness and toughness targets.

Zou **[47]** studied the influences of different conductive graphite, resin, pressures and temperature on the properties of polymer/graphite composite bipolar plates for PEM fuel cell. Results show that the components of conductive filler and the type and content of resin have a larger effect on the composite properties than do the pressure and temperature. They found that bipolar plates using a mixture of natural graphite and electro-graphite as conductive filler are better than using a single component. The composite bipolar plates obtained have a conductivity of 300 S/m.

Zhang **[48]** studied the effect of graphite particle size and shape on the bipolar plate performance. With decreasing of graphite particle size, bulk electrical conductivity and thermometric conductivity decreased, but flexural strength of bipolar plate was enhanced.

1.3.3.2 Polymer Matrix

Thermoplastic resins such as Polypropylene (PP), PE, Poly (vinylidene fluoride) (PVDF), and thermosetting resins such as phenolics, epoxies and vinyl esters have been used in fabricating composite bipolar plates **[10]**. The polymer resin not only plays a matrix role in the bipolar plate fabrication process, but is also one of the main factors affecting bipolar plate performance, such as electrical conductivity and flexural strength. Other conductive polymer such as liquid crystalline polymer (LCP), poly (phylene sulfide) (PPS) can also be chosen as polymer matrix.

1.3.3.3 Conductive Fillers

Most composites bipolar plates have electrical conductivity which is far below the DOE target of 100 S/cm **[28]**. As outlined below, some research efforts have been made towards increasing the conductivity of bipolar plates by applying different conductive fillers. Fillers used for conductive composites include graphite/synthetic graphite, carbon black, carbon fiber, as well as carbon nano-tube or nano-carbon fiber.

1.3.3.3.1 Carbon Black

Carbon black filled thermoplastic composites are widely used as antistatic, electrostatic dissipative, and semi conductive materials. In these applications, moderate electrical resistivity in the range of 10^6 to 10^9 Ohm-cm is required.

Carbon black with high surface area can lead to electrical current percolation at lower concentrations and to form a conductive carbon network; however, the porous structure of carbon black can decrease mechanical properties of composites, hence, carbon black filler loading within a polymer matrix is limited **[31]**.

The first large scale use of carbon black in polymer composites dates to the 1930s, when PVC (polyvinyl chloride) and PE (polyethylene) insulation shielding were first produced **[49].** These compounds were typically loaded with 30% to 40% carbon black. Since then, development in the carbon black fabrication process has led to important changes in the carbon black primary size and in the manner that those particles are fused together to form aggregates. In polymer composites, this leads to the ability to achieve electrical percolation at lower concentrations. These developments have enabled the fabrication of composites with resistivity in the 1-10 Ohm-cm range that has found application in electromagnetic shielding. Mighri **[30]** applied carbon black and graphite as conductive fillers, and PP/PPS as polymer matrix to develop high strength composite materials, and obtained resistivity in the range of 10^{-3}-10^{-2} Ohm-cm.

Since carbon black addition reduces processiblility and usually adds costs to the composite, numerous studies have aimed at reducing the percolation threshold. This can be achieved in polymer blends if the carbon black can be preferentially located in one of the continuous polymer phases or at polymer-blend interface in co-continuous polymer

blends. Initial work in this field was carried out on polyethylene/natural rubber blends. For the same carbon loading, it was observed that the resistivity of the polymer/rubber blends in the co-continuous, i.e., 30%-70%, composition range, was several orders of magnitude lower than that of the single polymer/carbon black composites **[50]**.

1.3.3.3.2 Graphite

Graphite based composite bipolar plates are made from a combination of graphite and a polymer resin with conventional polymer processing methods like compression molding or injection molding. Natural, flake-shape graphite has better electrical performance than other kinds of graphite. As one of the commonly used conductive carbon fillers, graphite not only has good conductivity but is also helpful for improving processability due to its lubricating effect in the melt.

Since most polymers are intrinsically insulating materials, excessive graphite fillers which are over 60 wt% have to be incorporated into the composite to meet the minimum requirement on electrical conductivities. It was reported that the typical conductivity values for polymer/graphite materials are 100 S/cm in the in-plane direction and 20 S/cm in the through-plane direction **[28]**.

Scholta **[51]** developed a novel low-cost graphite thermo-set composite bipolar plate, and test results concerning electrical conductivity, corrosion, chemical compatibility, gas

tightness, and mechanical strength showed that the investigated graphite composite appears to be a good choice for stable high performance PEM fuel cell bipolar plates.

Huang **[27]** developed a potential method for economic fuel cell bipolar plates with high conductivity and mechanical properties from graphite filled wet-lay thermoplastic composite materials. Poly (phenylene sulfide) (PPS) was chosen as polymer matrix, and composite plates have in-plane conductivity of 200–300 S/cm, tensile strength of 57MPa, flexural strength of 96MPa and impact strength of 81 Jm^{-1}. These values well exceed industrial as well as Department of Energy requirements and targets.

As well as traditional graphites, a novel graphite product developed from Inco-Novame, nickel-coated graphite, combines the benefits of a low density graphite core with a highly conductive pure nickel outer layer, and can be incorporated into resins, such as silicone, to produce electrically conductive composites **[52]**. Compared to other more expensive fillers, silver coated fillers, for example, the overall performance of nickel-coated graphite in this application is very favorable. These materials can also be used in conductive sealants as well as plasma spray friction applications. Hence, nickel-coated graphite from Inco-Novamet was chosen as one of conductive fillers in this project, and compared with synthetic graphite to develop thermoplastic conductive composite for bipolar plates for PEM fuel cell.

1.3.3.3.3 Carbon Fibers

Usually, carbon fibers are used for mixing with polymer for reinforcement to improve mechanical properties. Recently, extensive studies have focused on the effect of carbon fibers for developing conductive thermoplastic composites.

It is known that carbon fibers or flakes with finite aspect ratios will be 1~3 orders of magnitude more conductive along their long axes **[53]** and will align preferentially in the direction of flow in most injection and compression molding operations due to flow-induced forces.

Extensive studies have been performed on fiber orientation in injection and compression molding **[54]**. In injection molding, the fiber orientation is most affected by the shape of the mold cavity. In a molded plate with a rib, the fibers near the rib base are aligned in the thickness direction. By selecting a plate geometry having an arrangement of grooves and lands, it is possible to get a significant amount of alignment between the top and bottom land regions of the plate, because in those regions the high conductivity is needed.

Based on this concept, Blunk **[45]** investigated the use of low loadings of high aspect-ratio conductive particles such as carbon/graphite fibers, flakes, to meet plate conductivity, thickness, and toughness targets. Through controlled fiber orientation, the bipolar plate conductivity and toughness were increased.

Song [55] developed a short carbon fiber reinforced electrically conductive aromatic polydisulfide/expanded graphite nano-composite, which showed superior mechanical properties and good electrical conductivity, and can be used as electrically conductive materials to prepare the bipolar plates of PEM fuel cells.

1.3.4 Bipolar Plate Conductivity Measurement

Bipolar plate conductivity is one of most important properties of bipolar plate. In general, there are two methods to measure bipolar plate conductivity: one is in-plane conductivity, another is through-plane conductivity recommended by U.S. Fuel Cell Council [56]. However, very few research efforts focus on the development of conductivity measurement procedures and factors that can significantly affect the conductivity measurement results. This project also investigated the effect of different measurement method as well as sample dimensions, thickness, clamping pressure on conductivity of bipolar plate.

1.3.4.1 Conductivity Measurement

The resistance of a material with thickness T and surface area A can be calculated by Eqn. (1.4)

$$R_{\text{Material}} = \rho_{z\ \text{bulk}}\ T / A \qquad (1.4)$$

Where R_{Material} is the material's electrical through-plane sheet resistance (ohm cm^2) and ρ_z

$_{bulk}$ refers to the through-plane electrical resistivity (ohm-cm). From Eqn. (1.4), one can determine that thickness T and surface area A of the material affect the material through-plane resistance. However, among composites bipolar plate conductivity testing results, there are no detailed descriptions on the conductivity measurement procedures, especially on the information of test sample dimensions such as shape, thickness and surface area. Recently, Cunningham **[57]** described an apparatus for measuring through-plane conductivity and calibration methods. They found that some factors can affect measurement accuracy and reproducibility such as the method used to polish the copper electrodes as well as the contact between the electrodes and the sample. They pointed out that in standard experiments the measured resistance is caused not only by the resistance of sample (R_{Material}) but also by the contact resistances of all interfaces in the measured system. Derived equations to calculate the measured resistance of testing system are as follows:

$$R_{\text{Meas}} = V_{\text{Meas}} / I_{\text{Meas}} = R_{\text{Material}} + R_{\text{System}} \tag{1.5}$$

$$R_{\text{System}} = R_{\text{Inst}} + R_{\text{Interfaces}} \tag{1.6}$$

Combine Eqn. (1.5) and (1.6),

$$R_{\text{Meas}} = R_{\text{Material}} + R_{\text{Inst}} + R_{\text{Interfaces}} \tag{1.7}$$

where V_{Meas} and I_{Meas} refer to the measured voltage and current, respectively, R_{Inst} is the systematic error caused by the instruments and $R_{Interfaces}$ includes all the interfacial resistances and the intrinsic resistances of carbon cloth or gold plates. However, most research efforts use Eqn. (1.8) **[58]** to calculate the bulk resistance of the measured material (R_{Plate}):

$$R_{Plate} = V_{Meas} A_{Plate} / I_{Meas} \quad (1.8)$$

As Cunningham **[57]** pointed out, it is impossible to distinguish the resistance caused by the system from the bulk resistance of the measured material. Mishra and Yang **[59]** found that the electrical contact resistance between gas diffusion layers and bipolar plate flow channel is one of the important factors contributing to the operational voltage drop in PEM fuel cells. The measured contact resistances are reported over a range of clamping pressure for various paper-based and cloth-based gas diffusion layers.

1.3.4.2 Factors Affect Conductivity Measurement

The potential factors that could affect bipolar plate conductivity measurement include sample dimensions, thickness, surface area over thickness, clamping pressure and testing method.

In this work, it was also found that interfacial contact resistances such as interfacial resistance between bipolar plates and the gas diffusion layer may have a more significant

effect on measured resistance. As the range of materials used for bi-polar plate broadens, there is a need to understand the contributions that come from various phenomena. For example, thermoplastic polymers are often injection molded, and as a result there will likely be filler orientation, especially if fibers are used, which will lead to non-uniform conductivity properties. Other issues, such as distribution may increase contact resistance if the conductive filler does not fully disperse to the surface. Different bi-polar plate materials and fuel cell flow path geometries may perform differently if the gas diffusion layer materials (GDL) are changed.

This work investigated the effect of sample thickness (T) and surface area (S) on resistance of bipolar plates, and special attention was devoted to reduce all interfacial contact resistances. The effect of loading pressure applied in the test system also was investigated in this research.

1.4 Costs Analysis of Bipolar plate

The PEM fuel cell is the most suitable fuel cell technology for transportation applications due to its low operating temperature, quick response time, CO_2 tolerance by the electrolyte and a combination of high power density and high energy conversion efficiency **[60]**. However, significant barriers are present before this fuel cell technology can be fully embraced for automotive applications. One of the major barriers is the high

cost of PEM fuel cells estimated at about \$200 kW^{-1} **[5].** In order to become economically competitive over the internal combustion engine, the cost of PEM fuel cell needs to be reduced to \$25 kW^{-1} **[5, 17].** A recent technical cost analysis **[5]** indicates that the cost for platinum electrode accounts for about 50% of the PEM fuel cell cost, whereas the bipolar plates rank second or third in the cost, depending on the model used to estimate the cost. Thus, widespread applications of PEM fuel cells rely heavily on the breakthrough in the cost reduction of both electrodes and bipolar plates.

Cost reduction is expected through the application of high volume manufacturing processes or high efficiency materials. The cost of bipolar plates represents a significant part of overall manufacturing cost, and is targeted to cost 29% (\$10 kW^{-1}) of the fuel cell stack cost.

For the cost evaluation of bipolar plate, the Alternative Fuel Economics Laboratory (AFEL) used cost models developed at the Materials Systems Laboratory at MIT to evaluate the designs outlined in the reports by Direct Technologies Inc. (DTI) and the Authur D. Little (ADL) model which was prepared for US department of Energy Transportation Fuel Cell program in 2000. The assumptions for an injection mold composite bipolar plates are as follows **[5]**:

- production is 500,000 units per year, and product life is 5 years;
- the material is a high purity graphite composite at a material cost of \$4.65 kg^{-1};

and,

- there is no sensitivity to changes in assumptions for the processing parameters such as die temperature, heat capacity, and others.

The results show that material cost has the largest effect in reducing the cost from \$25 to \$16.85 kW^{-1} for a 19% decrease in material cost. Even the best case, 7.5s cycle time and materials price is \$4.00 kg^{-1}, the cost of cell is \$15.34 kW^{-1}, which is still far from the goal of \$10 kW^{-1}. The total cost of a bipolar plate cell shows that material cost of bipolar plate is dominant at about 60% for the DTI design and about 75% for the ADL design. For the cost goal of \$10 kW^{-1}, the cost of material needs to be reduced through a reduction in material unit cost or through a reduction of the amount of material used. This can be accomplished through design changes, but new materials are also needed.

The bipolar plates could be thinner, or the area of plate could be reduced, which would require an increase in current density from the electrode. From the results of reduction of thickness or area of plate, it can be seen that reducing the thickness is the only strategy that would accomplish the goal of \$10 kW^{-1}.

Chapter 2: Experimental

2.1 Experimental Overview

The main objective of this research was to develop highly conductive, lightweight, and low cost thermoplastic composite bipolar plates. The experimental procedures used in this work are documented in the section below, and these procedures have evolved from previous work conducted in this field.

Composites were fabricated with polymer matrix Polypropylene (PP) mixed with different conductive fillers such as Vulcan Carbon Black (VCB), Carbon Fiber (CF) and Synthetic Graphite (SG). The processing procedures included design of experiment (DOE) sample design process, compounding through a twin-screw extruder or batch mixer, bipolar plates prototyping via injection or compression molding, and then followed by bipolar plate properties testing, which included investigations of conductivity, mechanical properties, density, microscopy and in-situ properties in a fuel cell.

There are two principal differences in methodology used in this study compared to previous studies in this lab. Specifically, different conductive fillers were used (instead of acetylene carbon black, synthetic graphite and nickel coated graphite was used in this project). Also, composite compounding was conducted via a batch mixer instead of a

twin-screw extruder in order to reduce breakage of carbon fibers. The detailed information with respect to the experimental program is discussed in the following section.

2.2 Experimental Apparatus

Experimental apparatus used in this project included a batch mixer, injection molding machine, hot press molding, and properties testing apparatus such as, TGA, SEM, Mini-mat tensile tester and a fuel cell stack testing station. The specific models for experimental apparatus are detailed in Table 2.1.

Table 2.1: Experimental Apparatus Model

Apparatus	Model
Batch Mixer	Haake Batch Mixer
Injection Molding Machine	Polymer Technology Inc Engel 85 Ton Injection Molder
Hot-pressing	Carver hydraulic press
Grinder	Allen Bradley Co.
TGA	TA SDT 2960 Simultaneous DTA-TGA
SEM	LEO1530 field emission SEM with a Gemini column
Mini-Mat	Rheometric Scientific Mini-Mat
Fuel Cell Testing Station	University of Waterloo custom built test Station

The reasons for the selection of these apparatus are discussed in detail as follows:

1. Batch Mixer:

The batch mixer was used for composites compounding. The advantage of choosing a batch mixer is that it allowed for mixing a small amount of composite up to 220 g. Since the first step was to identify the better composites with a certain weight percent of conductive fillers and polymer, smaller samples were needed. Using the batch mixer to compound different composites reduced material waste and the sample preparation. Another reason for use of the batch mixer is that there was a concern with respect to carbon fiber breakage in the course of compounding via twin-screw extruder. During batch mixer compounding, the temperature of chamber, rotor speed and torque of composite can be closely monitored, and an operator can also more closely control the sequence of adding conductive fillers to make sure the fillers are well mixed within the polymer matrix.

2. Grinder:

A grinder was used to mill composites fabricated in the batch mixer. With different sieve sizes, composites could be milled to the desired size and then used for sample prototyping via injection molding or compression molding. However, using of a grinder might lead to the breakage of carbon fibers in composite, and it is suggested to further study in the future.

3. Hot Press:

A Carver hydraulic press with heated plates was used for various functions in this work. First, it was used for compression molding bipolar plates with the desired temperature and pressure. Those bipolar plates then were tested for conductivity to identify the composites with higher conductivity through the batch mixer to prepare more specific composites for injection molding of bipolar plates. Second, Carver hydraulic press was also used for bipolar plate conductivity measurement, which is one of the most important properties of bipolar plates. A description of bipolar plate conductivity measurement procedures can be found later in this section.

4. Injection Molding Machine:

In this project, all injection molded bipolar plates (blanks and plates) were fabricated at Polymer Technology Inc. using an Engel 85 Ton Injection Molder. Composite materials selected for injection molding were chosen based on the compression molding results for those materials that produced plates with higher conductivity. One objective of this research was to reduce the cost of bipolar plates by mass production, and injection molding is an effective way to fulfill this target.

5. Thermal Gravimetric Analysis (TGA):

Thermal gravimetric analysis was performed on a “TA SDT 2960 Simultaneous DTA-TGA”. TGA was used to identify the actual wt% of carbon black within the

VCB/PP master batch. The powdery carbon black chosen has very fine particles which significantly increase the processing difficulties in compounding. Preparation of a master batch of CB/PP was necessary to simplify composite processing and decrease the associated required clean-up of the equipment. With TGA, the actual wt% of carbon black in master batch could be identified, and thus it became easier to make composites with the desired filler ratio and weight concentration based on carbon black concentration of the master batch.

6. SEM:

The samples were freeze-fractured in order to observe the interior material morphology. This involved taking a small bar of a sample and submerging it in liquid nitrogen. Once frozen, the sample was broken in half while still submerged or immediately on removal. At this point, one of the halves was chosen for mounting. Samples of the composite materials were fixed to an aluminum stub with double sided tape or conductive adhesive. The presence of conductive paths from the material of interest to the aluminum stub is important to prevent charging.

7. Rheometric Scientific Mini-Mat Tensile Tester:

In addition to acquiring higher conductivity, materials for bipolar plates also require sufficient mechanical strength in the PEM fuel cell environment. The Mini-mat tensile material tester was used to testing mechanical properties including tensile strength,

tensile modulus, yield strength, flexural modulus and compression modulus.

8. Single Cell Tests Apparatus:

A fuel cell test station is an essential apparatus for testing of on fuel cell materials. The test station is where materials can be tested and fuel cell performance monitored. As Figure 2.1 shows, the test station consists of many different parts. For this work, the test station constructed for an earlier work was used **[61]**. The reactant gases first flow through Omega flow meters and pressure transducers before entering the reactant stream hydrators. PERMA PURE hydrators were used in this system. The photograph and schematic diagram of fuel cell test station used in this work are shown in Figure 2.1 (A) and (B), respectively.

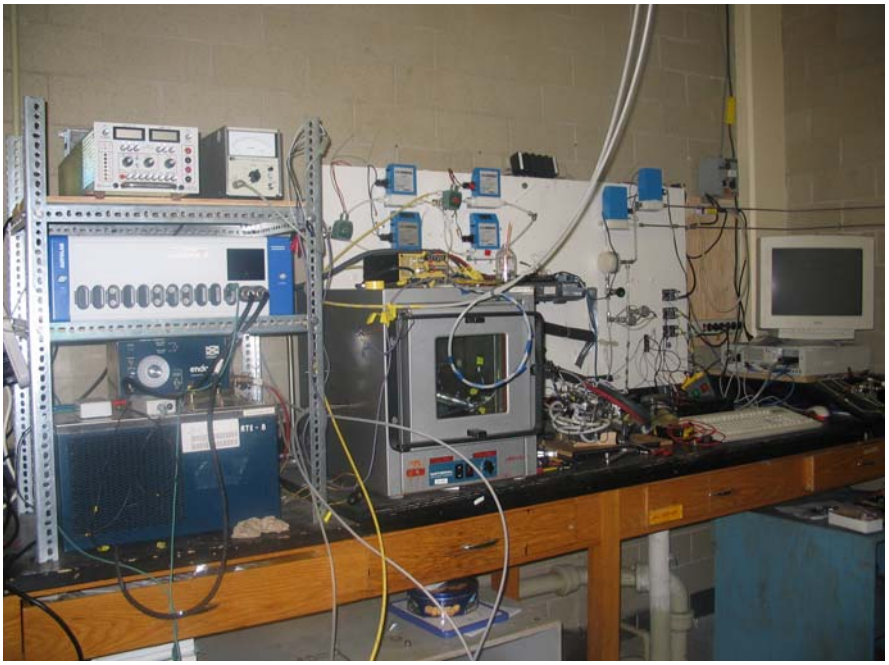

(A)

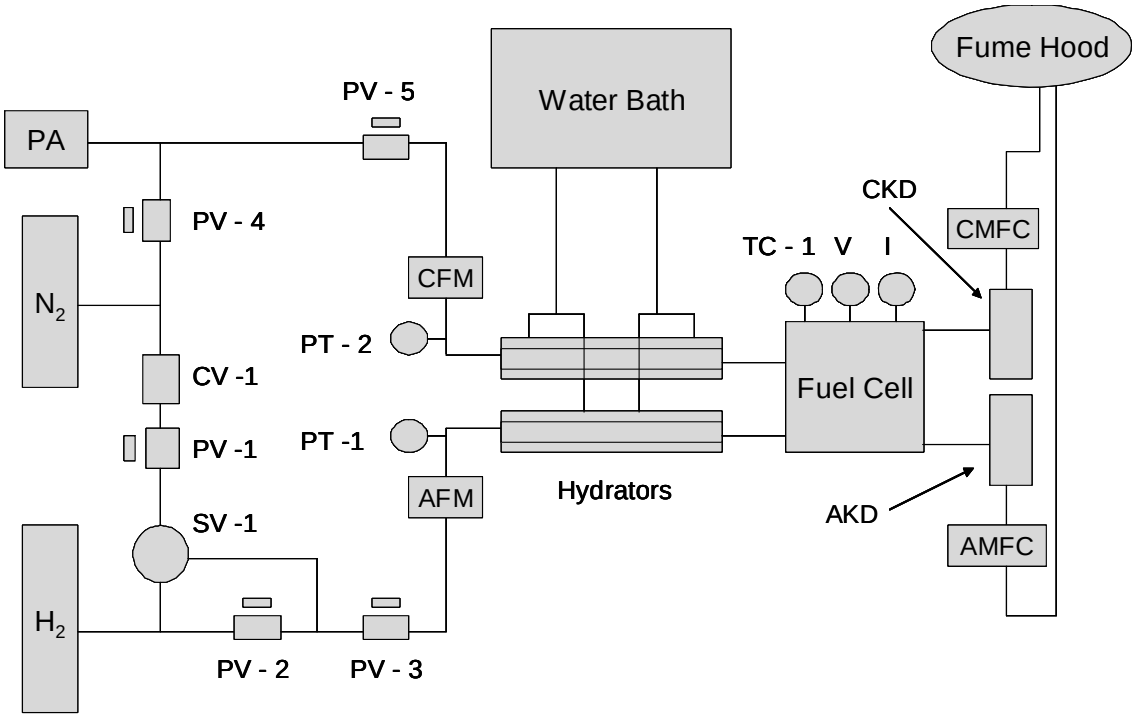

(B)

Figure 2.1: A) Photograph and B) Schematic diagram of the fuel cell test station used in this work. (SV: Solenoid Valve, PV: Plug Valve, CV: Check Valve, PT: Pressure Transducer, CFM: Cathode Flow Meter, AFM: Anode Flow Meter, TC: Thermo Couple, V: Voltage Signal, I: Current Signal, CMFC: Cathode Mass Flow Controller, AMFC: Anode Mass Flow Controller, CKD: Cathode Knockout Drum, AKD: Anode Knockout Drum) **[61]**

Once hydrated, the gas streams flow into the fuel cell. The cell itself was kept in an oven in order to maintain the cell temperature at 80°C. The anode and cathode current collectors were connected to an external load via load cables. The cell voltage is also measured at the current collectors with voltage taps. A shunt in series with the load allows

for current measurements.

Once gases leave the fuel cell carrying the water generated at the cathode, they enter knockout drums. These drums help condense water from the gas streams. This is done to prevent water from entering the mass flow controllers (MFCs) which are found downstream from the knockout drums. Each of the knockout drums has a valve to allow the operator to empty the drums of water. The mass flow controllers measure the outlet flow rates of the gases as well as provide the operator with the ability to control backpressure and flow through the system. Once the gases leave the MFCs, they are vented out in a fume hood.

A data acquisition system monitors temperature, gas flow rates, pressure, voltage, and current and calculated values such as power and efficiency are determined by a computer running a LabView program. This program is also capable of automatically recording data at any desired time interval **[61]**.

2.3 Experimental Materials

The materials selected for thermoplastic composite development include polymer matrix and conductive fillers. The detailed information about polymer matrix and fillers is discussed as follows.

2.3.1 Polymer Matrix

The polymer matrix chosen was an Equistar polypropylene copolymer Petrothene 36KK01, which has a melt flow index (MFI) of 7 and is manufactured for medium impact strength. Preliminary resin selection was based on industry recommendations and availability. This resin offers medium impact strength and suitable for thermoplastic composites. Table 2.2 illustrates the information about the virgin resin PP, and the specification sheet can be found in Appendix 1.

Table 2.2: Properties of Petrothene PP36KK01 Polypropylene [62, 63]

Property	Nominal Value	Units
Melt Flow Rate	70	g/10 mins
Tensile Strength @yield	3200 (22.0)	Psi (MPa)
Elongation @ Yield	6	%
Flexural Modulus	160,000 (1100)	Psi (MPa)
Rockwell Hardness	78	R
Specific Gravity	0.89-0.91	g/cm^3

2.3.2 Conductive Fillers

The conductive fillers were used in conjunction with Petrothene 36KK01 to develop

electrically conductive composites. Vulcan carbon blacks, carbon fibers, three types of synthetic graphite and two types of Ni-coated graphite were investigated in this study. The main properties of those fillers are presented in Table 2.3 **[64~67]**, and the specification sheets can be found in Appendix 2 - 4.

Table 2.3: Properties of Carbon Black, Carbon Fiber and Graphite Grades [64, 65, 66, 67]

Fillers	Reference	Name	Particle or Fiber Diameter	N2 Surface Area (m^2/g)	Supplier
Carbon Black	CB-1	Vulcan XC-72	30 nm	/	Cabot Corp.
Carbon Fibers	CF-1	Fortafil 243	7 microns	/	Fortafil Fibers
Graphite	GR-1	4012	60*325 mesh (44*250 microns)	1.5	ASBURY Carbons
	GR-2	4955	20*100 mesh (149*840 microns)	1.7	
	GR-3	4956	60*325 mesh (44*250 microns)	2.53	
Ni-coated Graphite	NCG-1	60% Ni	100*250 mesh (58*149 microns)	/	NOVAMET
	NCG-2	75% Ni	200*250 mesh (28*74 microns)	/	

Carbon black grade, Vulcan XC-72 (VCB) was supplied by Cabot Corporation. The main

carbon black characteristics in terms of processability and conductivity are the specific surface area, surface chemistry, and wetting properties.

Because of this material's high surface area, which increases with particle porosity, more porous carbon blacks should produce more conductive blends **[30]**. The physical and chemical properties of Vulcan carbon black are generalized in Table 2.4, and the specification sheet can be found in Appendix 2.

Table 2.4: Properties of Cabot VulcanXC72 Carbon Black [64]

Appearance	Black pellets, powdery
Odor	None
Density	1.7 -1.9 g/cm^3 @ 20℃
Bulk Density	20-550 kg/m^3
Mean Particle Size	30 nm

The carbon fiber used in this study was supplied by Fortafil Carbons, and specification sheets can be found in Appendix 3. It was anticipated that fibers will provide an ideal path for electron transport through the material. The carbon fiber selected for this study was Fortafil 243 chopped carbon fiber with 3-micron in length and aspect ratio of approximately 460. The properties of Fortafil 243 carbon fiber are generalized in Table 2.5.

Table 2.5: Properties of Fortafil 243 Chopped Carbon Fiber [65]

Specifications	**SI**
Tensile Strength	>3450 MPa
Tensile Modulus	>207 GPa
Ultimate Elongation	1.7%
Density	1.8 g/cm^3
Cross-sectional Area/Filament	$3.3 * 10^{-5}$ mm^2
Filament Diameter	6 microns
Electrical Resistivity	1.67 mOhm-cm
Fiber length	3 mm

Three types of synthetic graphite were supplied from Asbury with different size, and two kinds of nickel-coated graphite selected in this study were supplied from Inco-Novamet with 60% and 75% nickel by weight.

The properties of Asbury synthetic graphite and Inco-Novamet nickel-coated graphite are generalized in Table 2.6 and 2.7 respectively. Specification sheets for these materials can be found in Appendix 4 and 5.

Table 2.6: Properties of Asbury Synthetic Graphite [66]

Brand Name	Carbon Content (min)	Typical Size	Surface Area (m^2/gram)	Typical Resistively (Ohm-cm)
4012 (SG-1)	99	60*325 mesh	1.5	0.03
4955 (SG-2)	99	20*100 mesh	1.7	0.016
4956 (SG-3)	99	60*325 mesh	2.53	0.022

Table 2.7: Properties of Inco-Novemet Nickel-coated Synthetic Graphite [67]

Nickel Coated Graphite (NCG) (wt% of Nickel)	Screen Analysis	Apparent Density (g/cm^3)
60%	100*250 mesh	1.4 to 1.5
75%	200*325 mesh	1.7 to 1.9

2.3.3 Gas Diffusion Layer

The gas diffusion layer is used to: reduce contact resistance between the bipolar plate and the gold plate in conductive measurement of bipolar plates; collect the current from the electrode; and distribute the reactants over the area of the electrode. The chosen GDL for bipolar plate conductivity measurement was provided by Ballard Material Products Inc.,

and has the trade name AvCarb^{TM} 1071. AvCarb^{TM} 1071 is recommended to be used for PEM fuel cells **[68]**, and has a thickness of 280~432 microns. For the single fuel cell performance testing, the gas diffusion layer is supplied from SGL Carbon Group, and has the trade name SIGRACET Gas Diffusion Media GDL 10 BA, with a thickness of 400 microns. Specification sheets can be found in Appendix 6.

2.4 Sample Fabrication

2.4.1 Compounding

The composites were fabricated by mixing the conductive fillers and polymer resin received from suppliers. The specific sample fabrication processing flow chart is illustrated in Figure 2.2. The processing procedures include the material selection, compounding, compression or injection molding, and sample properties testing. For carbon black, Vulcan XC-72, which is a very fine particle, the first processing step was to make carbon black and Polypropylene VCB/PP master batch in the Haake Batch Mixer. The photographs of the Haake Batch Mixer are illustrated in Figure 2.3. The rational for the production of a master batch is to simplify the composite compounding process and reduce the pollution of lab equipment. Following a TGA analysis to identify the weight percent (wt%) of carbon black in master batch, other conductive fillers were added to the mater batch with certain ratio and concentration to make desired composites, followed by compression molding or injection molding of bipolar plates (or flat 'blank' plate from

which the plates could be made).

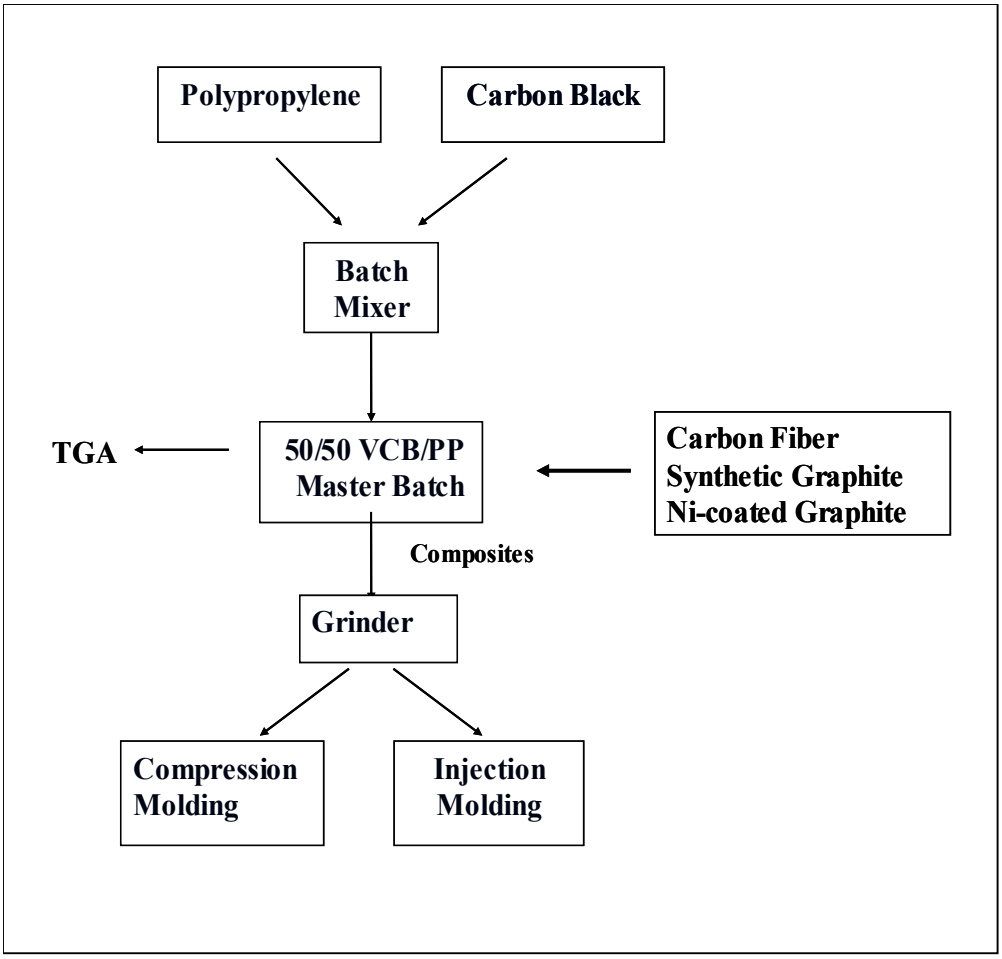

Figure 2.2: Flow chart of bipolar plate fabrication processing

Batch mixer compounding for PP-based blends was carried out at 210℃ in a 60-cm^3 Haake Batch Mixer. The rotation speed was 80 rpm and the mixing time was 15 min, including approximately 3 minutes for fillers loading. The PP resin or VCB/PP master

batch was first loaded into the chamber of the Haake Batch Mixer, then other carbon additives were added 1 minute later, thus allowing partial PP melting prior to solid incorporation.

Figure 2.3: Photographs of Haake Batch Mixer

2.4.2 Compression Molding of Bipolar Plates

Sample bipolar plates were fabricated with conductive composite granules via hot-pressing with temperature of 232°C - 243°C and compression forces up to 3000 Psi. The mold dimensions for making sample bipolar plates was 100.0 mm x 100.0 mm x 3.10 mm.

2.4.3 Injection Molding of Bipolar Plates

Injection molding of PP-based bipolar plates was performed using an Engel 85-ton injection molding machine at Polymer Technologies. The injection gate was positioned on the mold partition line to minimize the flow channel length. The PP-based blends were injected at 240°C in an oil-heated mold maintained at 120°C. Figure 2.4 shows the Engel 85-ton injection molding machine.

Figure 2.4: Photograph of Engel 85-ton injection molding machine

2.5 Design of Experiment

The software used for design of experiment was Stat Ease's DESIGN EXPERT 6.0 software package **[69]**, which allows for 2 or 3 factors prediction and evaluates synergetic effects of multiple fillers with maximum 50 wt% filler content. The fillers chosen were two kinds of graphite, synthetic graphite (Asbury) and Nickel-coated graphite (Inco-Novemet), Vulcan carbon black and carbon fiber. The specific filler ratio and weight percent of PP or fillers for different composites is generalized in Table 2.8, and specification sheets can be found in Appendix 8.

Table 2.8: Design of Experiment for various composite blends composites

Run	Percent of Fillers (wt %)			
	Synthetic Graphite/ Ni-coated Graphite	Vulcan Carbon Black	Carbon Fiber	PP
1	0	0	20	80
2	0	0	35	65
3	0	0	50	50
4	0	20	0	80
5	0	50	0	50
6	20	0	0	80
7	50	0	0	50
8	0	25	25	50
9	25	0	25	50
10	25	25	0	50
11	5.83	30.83	5.83	57.5
12	5.83	30.83	5.83	57.5
13	11.67	11.67	11.67	65
14	11.67	11.67	11.67	65
15	30.83	5.83	5.83	57.5
16	30.83	5.83	5.83	57.5

The objective of this experimental design was to compare the conductivity of different composites and to develop blends suitable for bipolar plates used for PEM fuel cell.

2.6 Testing Procedures and Analysis

2.6.1 Thermal Gravimetric Analysis (TGA)

Thermal gravimetric analysis was performed on a "TA SDT 2960 Simultaneous DTA-TGA". The method equilibrated at 75°C and increased at a rate of 20°C /min up to 1000°C in 5% oxygen and 95% helium environment. Data was collected at a rate of 10°C /min.

2.6.2 Scanning Electronic Microscopy (SEM)

The scanning electron microscope (SEM) was a LEO1530 field emission SEM with a Gemini column. Images were produced at 5 kV ranging from 100 X to 10000 X magnification.

The samples were freeze fractured using liquid nitrogen. The samples were freeze fractured in order to observe the interior material morphology. This involved taking a small bar of a sample and submerging it in liquid nitrogen. Once frozen, the sample was broken in half while still submerged or immediately on removal. At this point, one of the halves was chosen for mounting. Samples of the composite materials were fixed to an

aluminum stub with double sided tape or conductive adhesive. The presence of conductive paths from the material of interest to the aluminum stub is important to prevent charging. The detailed procedure for freeze fracturing can be found in Appendix 9.

2.6.3 Density Testing

The density of each sample was determined using an analytical balance and water displacement technique according to the ASTM D792 test procedures.

2.6.4 Current-Voltage (*I*-*V*) Performance Test

Conductive bipolar plates were also tested in a single fuel cell to evaluate the performance. Figure 2.5 shows the photograph of the actual assembled single cell fuel cell used in this study.

The dimensions of the composite bipolar plate and graphite bipolar plate were both 60.0 mm* 60.0 mm with an active area of 13.6 mm^2. The bipolar plates chosen for single fuel cell performance testing are 50%, 55% and 60% 1:1:1 SG-4012/VCB/CB composites. For 50% and 55% composites, their single cell performances were compared with the bipolar plates made from the same composite but with a copper sheet insert.

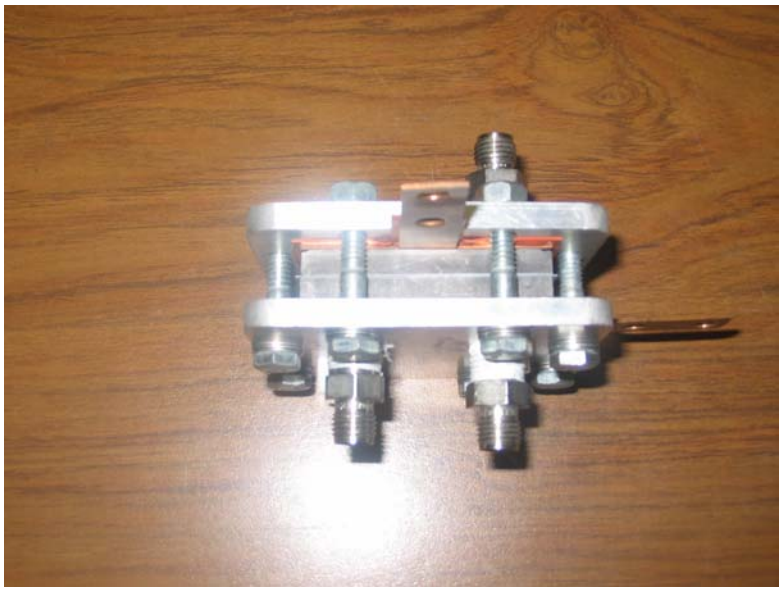

Figure 2.5: Photograph of the actual assembled single cell fuel cell used in this study

Bipolar plates were prepared via hot-pressing compression molding. The specific procedures for sample prototyping and the picture of the mold can be found in Appendix 10 and 11.

The membrane electrolyte assembly (MEA) was purchased from Ion Power. The fuel was wet hydrogen gas and dry oxygen gas. The flow rate of hydrogen/oxygen gas was 0.5 L/min. When the cell temperature reached 70 ℃, the current-voltage (I-V) polarization curves were recorded.

Safety is of the utmost importance when operating the fuel cell. The most significant risks

are hydrogen leaks or direct mixing of the hydrogen and oxygen reactant streams. The test station also has two safety alarms to alert the operator to hydrogen leaks. Details of the safety procedures and equipment start-up procedures can be found in an earlier work **[61]**.

2.6.5 Mechanical Properties Testing

Mechanical properties including tensile, flexural, and compressive modulus were tested using a Rheometric Scientific Mini-Mat tensile tester.

Flexural mechanical characterization was carried out at room temperature according to ASTM D-3039/D3030M-00 "Standard Test Method for Tensile Properties of Polymer Matrix Composites Materials", ASTM D-5934 "Standard Test Method for Determination of Modulus of elasticity for Rigid and Semi-Rigid Plastic Specimens by Controlled Rate of loading Using Three-Point Bending"; ASTM D-3410/D-3410M-03 " Standard Test Method for Compressive Properties of Polymer Matrix Composite Materials with Unsupported Gage Section by Shear Loading", respectively. Small deviations such as testing speed exist as appropriate for the material and sample size. Sample thickness was 3.0 mm, width was 5.0mm and length was 12 mm. Reported measurements were the average values obtained from five specimens.

2.6.6 Electrical Conductivity Testing Methods

2.6.6.1 Conductivity Testing Methods

Bipolar plate conductivity was measured by two different techniques. The first technique (Method 1) used ASTM D-991 "Volume Resistively of Electrically Conductive and Antistatic Products" to measure the in-plane conductivity of samples, and Equation 2.1 was used to calculate the conductivity:

$$\mathbf{EC} = \frac{\boldsymbol{I} * \boldsymbol{L}}{\boldsymbol{V} * \boldsymbol{W} * \boldsymbol{T} * \boldsymbol{k}} \qquad (2.1)$$

Where: **EC** = Electrical conductivity (in S/m)

V = Voltage drop (volts)

I = Current (Amps)

W = Sample width (mm)

T = Sample thickness (mm)

L = Distance between 2 probes (26mm)

k = 0.001

Figure 2.6 (a) and (b) illustrates the diagram and photo of the test apparatus for in-plane conductivity measurement. In Figure 2.6 (a), label C represents the test specimen, and labels D and E refer to the current and voltage electrodes, respectively. Figure 2.6 (b) is

the photo of in-plane conductivity measurement apparatus. Figure 2.7 illustrates the electrical circuit for calculating bipolar plate in-plane conductivity using Equation 2.1.

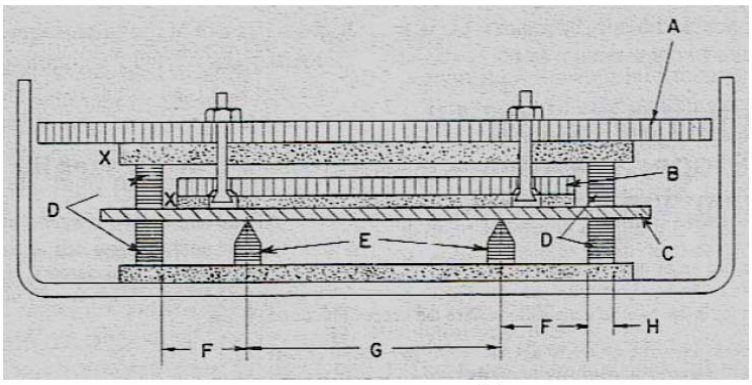

(a)

(b)

Figure 2.6: (a) Diagram of ASTM D-991 Conductivity Apparatus and (b) photograph of apparatus for in-plane conductivity measurement

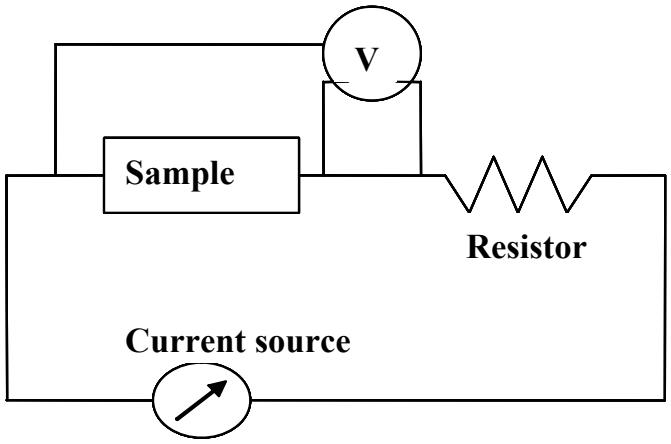

Figure 2.7: Diagram of in-plane conductivity measurement circuit

The second conductivity technique (method 2) was developed from the US Fuel Cell Council's recommended guidelines **[56]**. A photograph and two schematics of the experimental setup are shown in Figure 2.8 (a), (b) and (c), respectively.

The resistance measurement system includes a CARVER hydraulic press for providing a series of prescribed clamping pressures, a power source, and a dual input high precision digital multi-meter for capturing the electrical voltage and current.

Two pieces of gas diffusion layers are placed on either side of the sample, and the assembly was placed between two gold-nickel-copper plates. To insulate the electric circuit from the press, two polymeric insulation plates were placed between the plates of

the press and the gold plates. A clamping pressure up to 10000 lbs-force was applied and both voltage and current were independently monitored on both electrodes to calculate the total resistance.

The conductivity circuit, represented by Figure 2.8 (b), was used to calculate the volume conductivity using Equation 2.2.

$$\mathbf{EC} = \frac{\boldsymbol{I} * \boldsymbol{L} * \mathbf{1000}}{\boldsymbol{V} * \boldsymbol{W} * \boldsymbol{T}} \qquad (2.2)$$

Where: **EC** = Electrical conductivity (in S/m)

V = Voltage drop (volts)

I = Current (Amps)

W = Sample width (mm)

T = Sample thickness (mm)

L = Sample Length (mm)

(a)

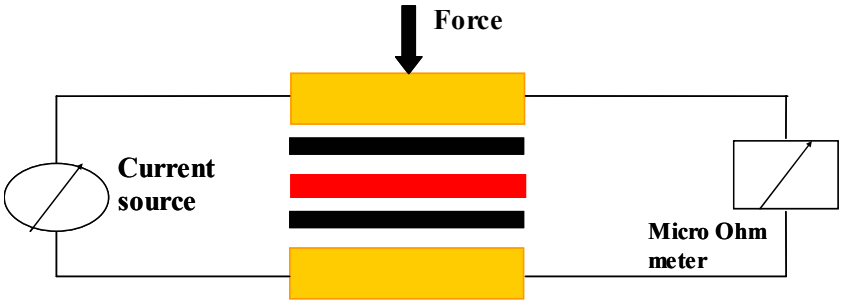

(b)

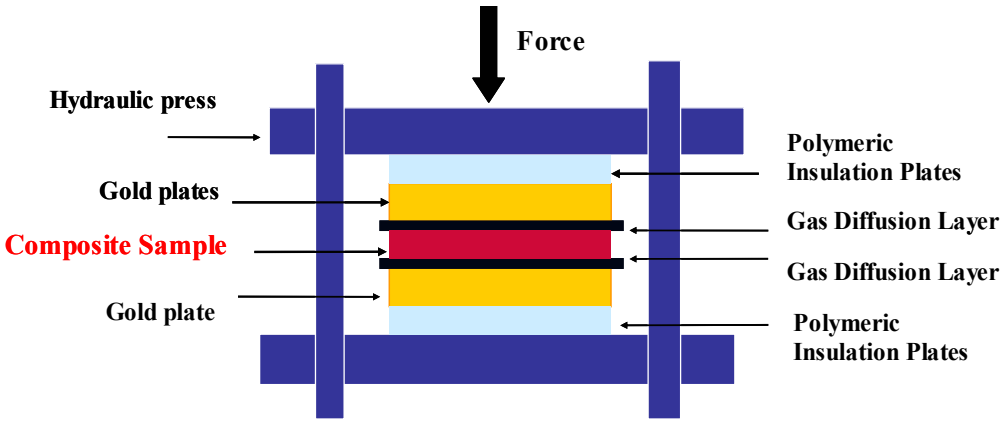

(c)

Figure 2.8: **(a) Photograph and (b) Schematic diagram of bipolar plate resistance measurement apparatus (c) Schematic diagram of bipolar plate resistance measurement set up**

2.6.6.2 Sample Dimensional Effects on Conductivity Measurement

In this research, the sample dimensional effects on bipolar plate conductivity were investigated. The specific experimental procedures are described as follows: A sample bipolar plate was fabricated with conductive composite pellets by hot-pressing at temperature of 232°C -243°C and compression forces up to 2000 Psi. The dimensions of three different molds used for making sample plates are as follows:

#1 100.0 mm x 100.0 mm x 3.10 mm

#2 59.5 mm x 24.3 mm x 5.95 mm

#3 70.0 mm x 28.0 mm x 1.76 mm

In order to determine the effect of surface area on bipolar plate resistance, the sample plates made by mold #1 was cut into three pieces with varied surface areas. The specific dimensions of those three pieces were:

#1a 100.0 mm x 49.0 mm x 3.10 mm

#1b 61.0 mm x 51.0 mm x 3.10 mm

#1c 51.0 mm x 38.0 mm x 3.10 mm

The sample plates made by mold #2 and #3 were used to determine the effect of surface area/thickness (S/T) and thickness independently on the resistance of the bipolar plate (R_{plate}).

Chapter 3: Results and Discussion

3.1 Polymer Blend Development - Design of Experiment

3.1.1 Synergetic Effect of Conductive Fillers

One of the basic concepts of this project was to demonstrate synergetic effects of different filler sizes and shapes. In order to compare effects of fillers on composite conductivity, Stat Ease's DESIGN EXPERT 6.0 software package was applied to predict the effect of 2 or 3 factors amongst different filler types, and to evaluate synergetic effects of multiple fillers on composite conductivity. Figure 3.1 illustrates through-plane conductivity of different PP-based blends.

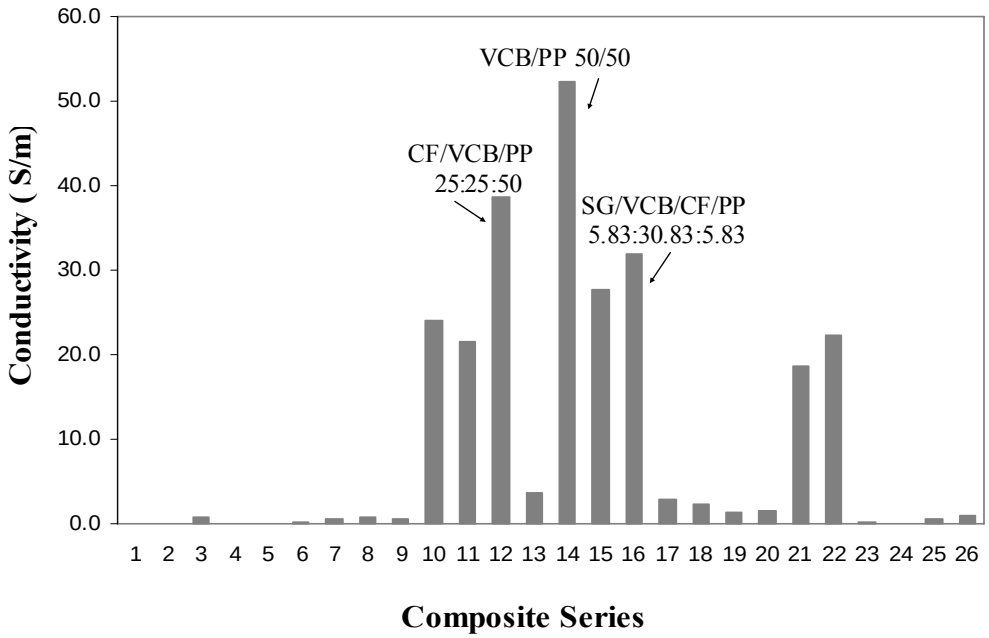

Figure 3.1: Through-plane conductivity of composite series from DOE

Table 3.1: Through-plane Conductivity of Composites from DOE

# of Sample	PP-based Composites (Filler ratio and wt %)	Conductivity (S/m)
1	CF/PP 20:80	0.0066
2	CF/PP 35:65	0.0097
3	CF/PP 50:50	0.7417
4	NCG/PP 20:80	0.0001
5	NCG/PP 50:50	0.0001
6	SG/PP 20:80	0.1418
7	SG/PP 50:50	0.5343
8	SG/CF/PP 25:25:50	0.8096
9	NCG/CF/PP 25:25:50	0.5989
10	NCG/VCB/PP 25:25:50	23.9872
11	SG/VCB/PP 25:25:50	21.4920
12	CF/VCB/PP 25:25:50	38.5894
13	VCB/PP 20:80	3.5714
14	VCB/PP 50:50	52.3269
15	SG/VCB/CF/PP 5.83:30.83:5.83	27.6244
16	SG/VCB/CF/PP 5.83:30.83:5.83	32.0102
17	SG/VCB/CF/PP 30.83:5.83:5.83	2.9388
18	SG/VCB/CF/PP 30.83:5.83:5.83	2.3854
19	SG/VCB/CF/PP 1:1:1	1.3808
20	SG/VCB/CF/PP 1:1:1	1.4936
21	NCG/VCB/CF/PP 5.83:30.83:5.83	18.6538
22	NCG/VCB/CF/PP 5.83:30.83:5.83	22.2692
23	NCG/VCB/CF/PP 30.83:5.83:5.83	0.2419
24	NCG/VCB/CF/PP 30.83:5.83:5.83	0.2866
25	NCG/VCB/CF/PP 1:1:1	0.9433
26	NCG/VCB/CF/PP 1:1:1	0.9251

Note: PP---Polypropylene
VCB---Vulcan Carbon Black SG---Synthetic Graphite
CF---Carbon Fiber NCG---Nickel-coated Graphite

Table 3.1 shows PP-based composites with varied filler ratio and concentration (wt %) as well as corresponding conductivities. Of note is that for blends with 3 fillers, each sample was replicated to check the reliability of testing results.

From Table 3.1 and Figure 3.1, as expected, carbon black concentration exhibits significant effect on blends conductivity, which means that the conductivities of different composites were increased as a function of carbon black concentration. For single filler blends, the conductivity of the 50% carbon black blend was significantly higher than that of the blend with 20% carbon black loading. For 2-filler composites, blends with carbon black show higher conductivity than those without carbon black.

One of the goals in this project was to investigate the synergistic effects among Vulcan Carbon Black (VCB), Carbon fiber (CF) and Synthetic Graphite (SG) or Nickel-coated Graphite (NCG). However, 3-filler based blends with varied filler ratios exhibit different conductivity. With the fixed filler loading, the conductivity of 3-filler blends with lower carbon black concentration was greatly less than those with the higher carbon black loading. For example, PP-based blend with a filler ratio of 5.83:30.83:5.83 SG/VCB/CF has a conductivity of 32.0 S/m, however, the conductivity of the blend with a filler ratio of 30.83:5.83:5.83 SG/VCB/CF was only 2.38 S/m. For composites with a ratio of 1:1:1 SG/VCB/CF, the conductivity was lower than other ratios of 3-filler blends, which is about 1.38~1.43 S/m. Thus, high carbon black content is critical to blend

conductivity.

From the point of view of composite formulation, the main challenge was to keep blends with a low enough viscosity to enable successful processing while ensuring that there were sufficient conductive particles to provide good electrical conductivity. This is an engineering 'trade-off', as increasing fill content will improve conductivity while decreasing processability.

In this case as the conductive additive concentration was increased, composite viscosity and conductivity showed similar increasing trends (and increased viscosity is not a desirable property). Thus, the conductivity of a blend is limited by the highest viscosity value at which the polymer blend can be compounded by the batch mixer, or twin-screw extrusion, or, more critically, injection molded to bipolar plates.

From Figure 3.1, 50/50 VCB/PP yields the highest conductivity (52 S/m) within all the blends, but 50/50 VCB/PP blend has some processing difficulty due to its high loading of carbon black. During mixing, the torque on the 50/50 VCB/PP blend was up to 90 N/m, compared to an average of 15~20 N/m during other mixture runs. Also, from sample finishing it can be identified that 50/50 VCB/PP blend has processability difficulty since the bipolar plate molded by hot-pressing had obvious cracks and voids in the sample as illustrated in Figure 3.2.

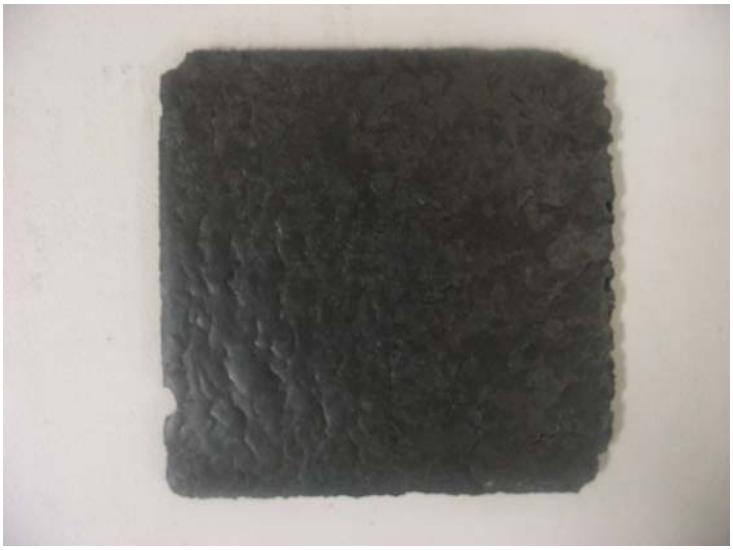

Figure 3.2: Photograph of bipolar plate of 50/50 VCB/PP blend

In addition to VCB and CF, there were two kinds of graphite used in this study, Asbury synthetic graphite and Inco-Novamet nickel-coated graphite. Both of these were used in the overall design of experimental program. Comparing SG-based blends and NCG-based blends, it was found that both conductivity and sample finishing of SG-based blends was better than for the NCG blends.

Figure 3.3 illustrates the SEM photo of 5.83:30.83:5.83 NCG/VCB/CF composite, in which there were obvious voids in the bipolar plate. Figure 3.3 also shows that the size of NCG particles was much bigger than that of carbon black or carbon fiber particles, and there was a gap between NCG particles with other filler particles or the polymer matrix, resulting in a poor dispersion and wetting of the fill. The reason is that the polar surface of NCG particles is incompatible with non-polar particles such as carbon black, carbon

fiber, or polymer matrix, resulting in poor dispersion and wetting of fill. Hence, the SG-based blends were selected for further study of conductivity and processability of different ratio 3-filler blends, and the blends with filler ratio of 1:1:1 SG:VCB:CF were chosen for further study.

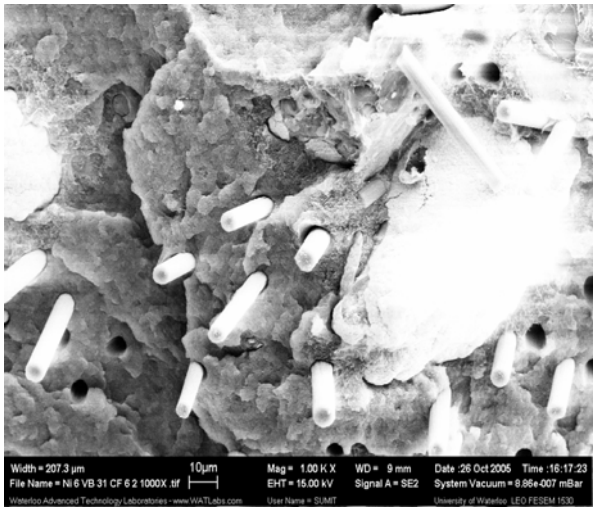

Figure 3.3: SEM Photo of NCG/VCB/CF composite at magnification of 1,000x

The reasons for choosing 1:1:1 filler ratio blends were based on the results from previous work and consideration of balance between conductivity and processability of blends.

Previous work in the lab had studied the synergetic effect of Vulcan carbon black, Acetylene carbon black and carbon fiber, the study results showed that 54% 1:1:1 filler ratio yield the highest conductivity which is 220 S/m **[70]**.

In this research project, with an expectation of acquiring both good conductivity and easy processing for bipolar plate, synthetic graphite was used to replace Acetylene Carbon Black as one of conductive fillers since graphite not only has excellent conductivity but also possesses good lubricant effect in processing. Although conductivity of 35% 1:1:1 SG/VCB/CF blend is very low, only 1.38~1.43 S/m, we expected that with increasing filler concentration up to 65% or even higher, as long as the composites can be processed successfully, could yield higher conductivity than previous work.

3.1.2 Thermal Gravimetric Analysis (TGA)

In order to improve processability of composites compounding, and considering 'cleaner' processing steps, VCB/PP master batches were fabricated before composites compounding. Vulcan carbon black is a very light material that is difficult to control and kept contained during processing. The twin screw extruder and batch mixer at the University of Waterloo have 'open' top fed hoppers in which it is also difficult to contain the materials added. A very small amount of unintended release in the facility is easily noticed and requires a significant clean-up effort. In this study, the master batch which was much easier to manage was then remixed with addition resin and fillers. Thus the VCB/PP master batch was mixed with other conductive fillers as well as PP with the specific filler ratio to make conductive composites.

Thermal gravimetric analysis (TGA) was applied to determine the actual carbon black

loading within the polypropylene matrix. Figure 3.4 illustrates a TGA graph for one of 13 runs of VCB/PP master batch samples.

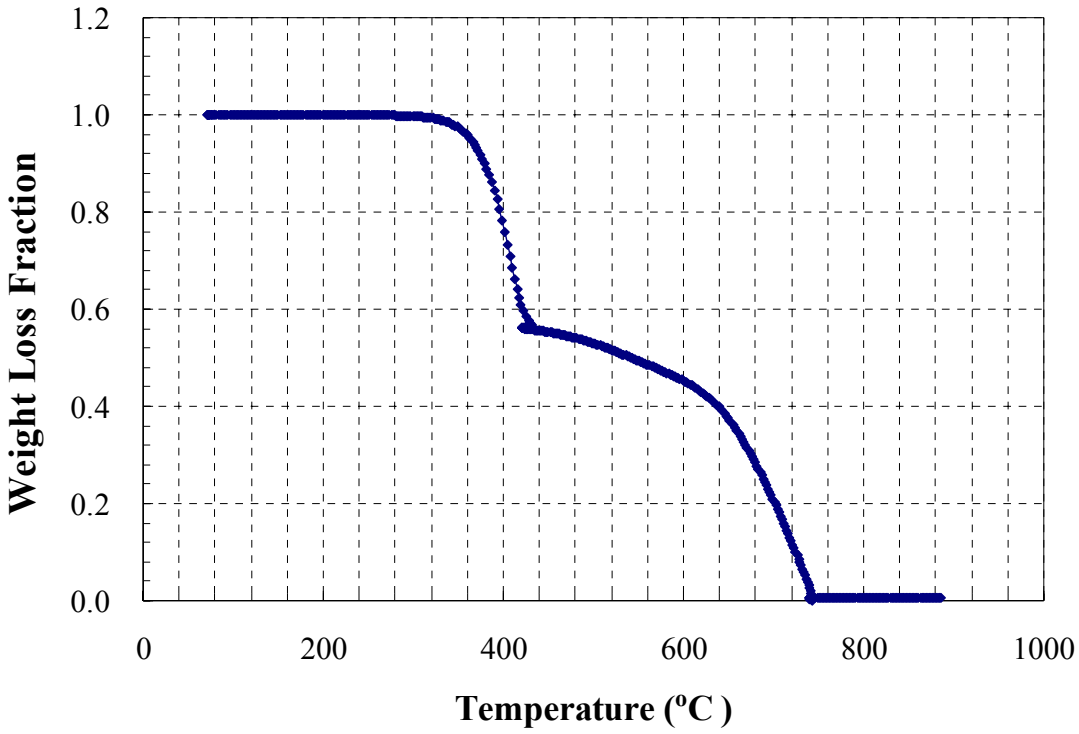

Figure 3.4: Graph of TGA for VCB/PP master batch

In Figure 3.4, the trends show that polypropylene resin has a distinct transition which means that PP starts to burn and off gas till it is completely consumed. The gap between two transitions represents the actual carbon black concentration within the polymer matrix. Table 3.2 summarized results for 13 runs of TGA for VCB/PP master batch samples (each run of TGA represents the two batches of VCB/PP master batch), and the

range of carbon black concentration is between 46.55%~56.62%. Note this concentration of carbon black in the master batch is near to the processing limit of the batch mixer, if the carbon black loading is higher than this range, the master batch of VCB/PP can produce more friction during the course of mixing due to its high shear viscosity, and in turn cause a higher torque in the batch mixer.

Table 3.2: TGA results for VCB/PP master batch

Run	Carbon Black (wt %)	PP (wt %)
1	46.55	53.45
2	47.68	52.32
3	50.48	49.52
4	51.53	48.47
5	49.38	50.62
6	47.58	52.42
7	52.92	47.08
8	51.08	48.92
9	56.62	43.38
10	56.57	43.43
11	55.99	44.01
12	56.34	43.66
13	55.99	44.01

3.1.3 Scanning Electron Microscopy (SEM)

Scanning electron microscopy (SEM) techniques are an effective way to view the microstructure of materials. Figures 3.5 through Figure 3.8 are various micrographs which show each fillers independently; as well the micrographs showing some edge effects, porosity of composite, carbon fiber pull-out, and fiber alignment.

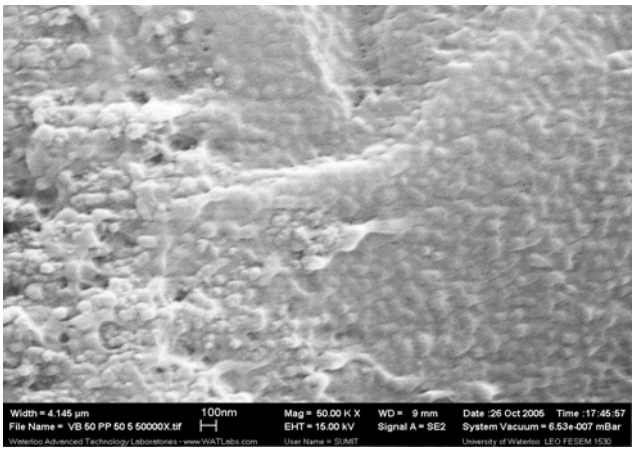

(a)

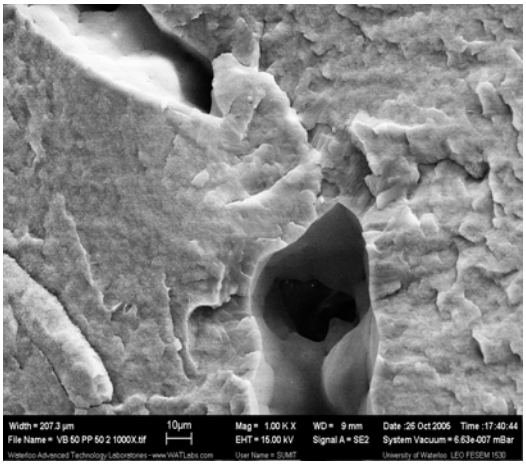

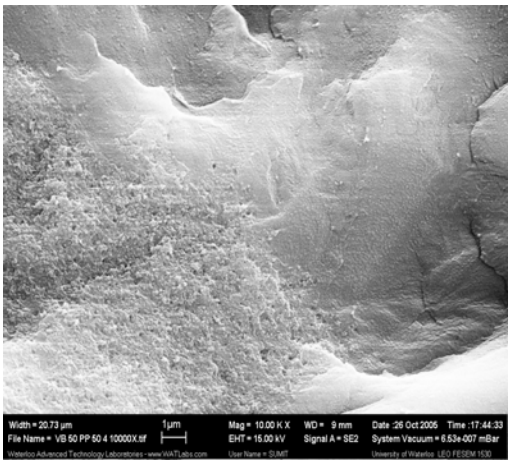

(b) **(c)**

Figure 3.5: SEM photos of 50/50 VCB/PP composite with magnification of (a) 100x, (b) 10,000x, and (c) 50,000x, respectively

In Figure 3.5, 50/50 VCB/PP composite shows voids within bipolar plate, which are due to the very high composite viscosity because of the high (50 wt%) carbon black concentration. This imagery also shows agglomeration of carbon black particles within the polymer matrix phase. This agglomeration will not likely result in high conductivity throughout the sample, and will lead to inconsistent mechanical properties. Future studies should consider additives which can assist in dispersion of carbon black particles.

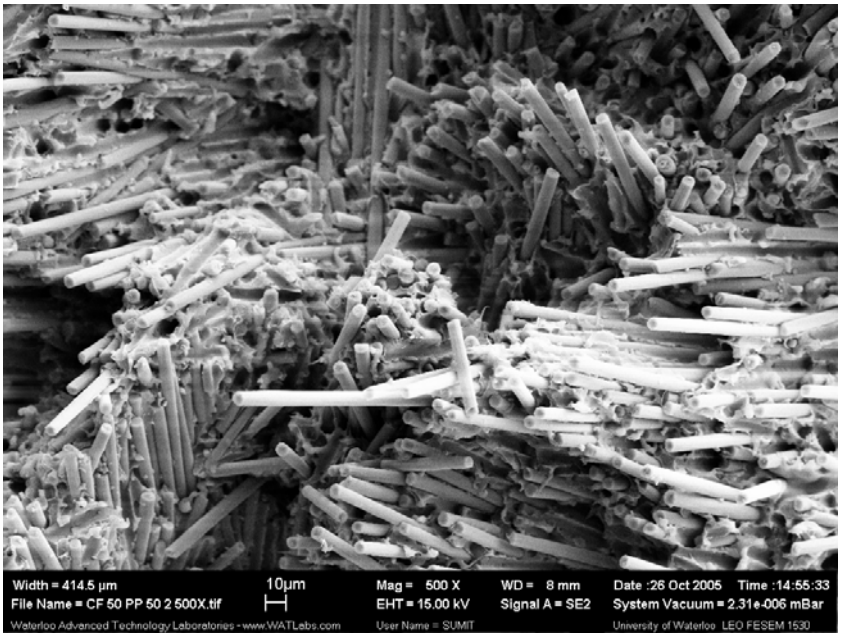

Figure 3.6: SEM photo of 50/50 CF/PP with magnification of 500x

From Figure 3.6, carbon fibers generally display a random orientation within the composite; however, some alignment of carbon fibers may be due to the bipolar plate compression molding process. Note that this sample was batch mixed and compression

molded, thus orientation was not expected.

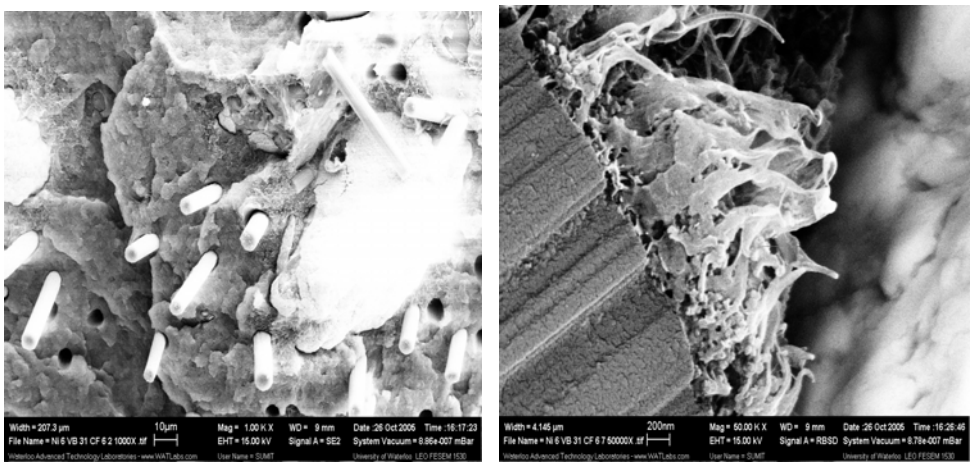

Figure 3.7: SEM photos of NCG/VCB/CF with magnification of 1,000x and 50,000x

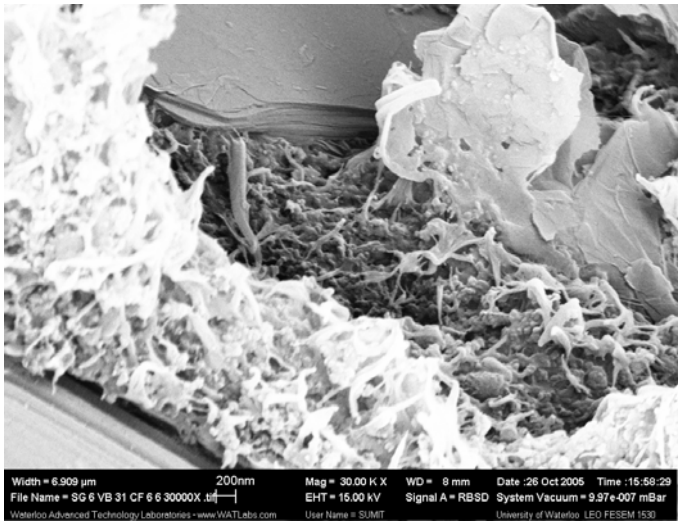

Figure 3.8: SEM photo of SG/VCB/CF with magnification of 30,000x

Figure 3.7 and 3.8 are the SEM images of NCG/VCB/CF and SG/VCB/CF composites. These pictures show a certain degree of contact among filler particles, such as Ni-coated

graphite, synthetic graphite, carbon fiber, and carbon black within the polymer matrix. With this contact, more electron flow paths are formed so electrons can pass, forming an electrically conductive circuit. As a result, in turn, the conductivity of the composite is improved. A continuous phase of conductive filler is critical for conductivity. This is consistent with conductivity measurement results that composites with three fillers demonstrate- higher conductivity than those with one filler or two fillers composites as shown in Figure 3.1 and Table 3.1

3.1.4 Density of Composites

Weight reduction of the bipolar plate is one of the key objectives of this project; hence, densities of the developed composites should be less than that of graphite plate. Figure 3.9 and Table 3.3 illustrate the density of 26 composites from the DOE which is in the range of 0.80~1.30 g/cm^3.

The difference in density values depends on the type of fillers and their concentration within the composite, and the single, double or triple fillers composite exhibits different tendency of composite density variation. For single filler composites, the density increases with the increasing of filler content. For 50:50 composites, compared to other blends, SG/PP composite has the highest density value at 1.2589 g/cm^3. For 2 filler blends, except for NCG/CF/PP 25:25:50 with a density of 0.9 g.cm^3, the densities of other composites are in the range of 1.20~1.26 g/cm^3. For 3 filler blends, except for 1:1:1

NCG/VCB/CF blend with a density of 0.9 g/cm^3, the densities of other blends are in the range of 1.0~1.2 g/cm$^{3.}$ These results demonstrate that conductive thermoplastics composites can satisfy a low density target for a bipolar plate, since the benchmark graphite plates have a density of 1.88 g/cm^3.

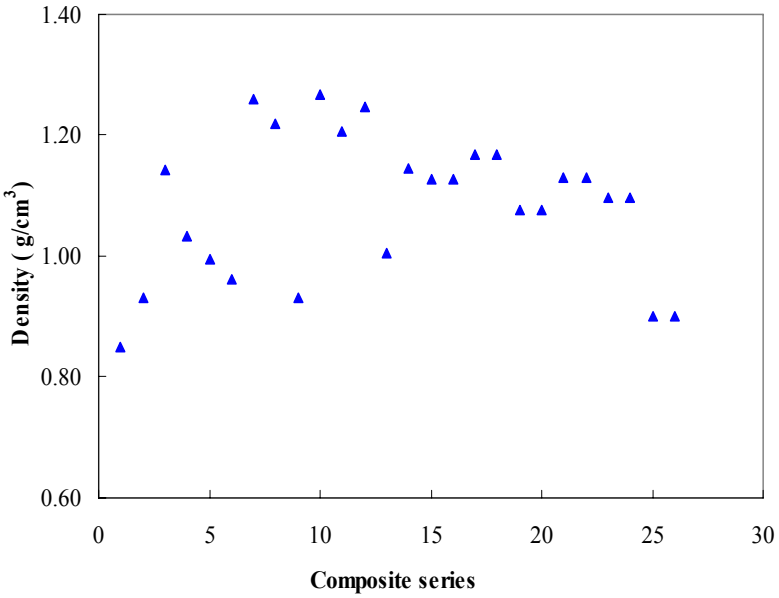

Figure 3.9: Densities of composites from Design of Experiment

3.2 Improvement of Composite Blends

The results of composites from the initial series of samples allowed for the selection of the best composites for further testing within this project. Since a combination of carbon black, carbon fiber, and synthetic graphite seemed to yield an optimal processability/conductivity balance, the next part of this work was devoted to improvement of the composite formulation.

Table 3.3: Densities of 26 composites from Design of Experiment

# of Sample	PP-based Composites (Filler ratio and wt %)	Density (g/cm^3)
1	CF/PP 20:80	0.8498
2	CF/PP 35:65	0.9321
3	CF/PP 50:50	1.1432
4	Ni/PP 20:80	1.0343
5	Ni/PP 50:50	0.9952
6	SG/PP 20:80	0.9620
7	SG/PP 50:50	1.2589
8	SG/CF/PP 25:25:50	1.2179
9	Ni/CF/PP 25:25:50	0.9324
10	Ni/VCB/PP 25:25:50	1.2672
11	SG/VCB/PP 25:25:50	1.2059
12	CF/VCB/PP 25:25:50	1.2467
13	VCB/PP 20:80	1.0059
14	VCB/PP 50:50	1.1443
15	SG/VCB/CF/PP 5.83:30.83:5.83	1.1275
16	SG/VCB/CF/PP 5.83:30.83:5.83	1.1275
17	SG/VCB/CF/PP 30.83:5.83:5.83	1.1674
18	SG/VCB/CF/PP 30.83:5.83:5.83	1.1674
19	SG/VCB/CF/PP 1:1:1	1.0757
20	SG/VCB/CF/PP 1:1:1	1.0757
21	Ni/VCB/CF/PP 5.83:30.83:5.83	1.1295
22	Ni/VCB/CF/PP 5.83:30.83:5.83	1.1295
23	Ni/VCB/CF/PP 30.83:5.83:5.83	1.0966
24	Ni/VCB/CF/PP 30.83:5.83:5.83	1.0966
25	Ni/VCB/CF/PP 1:1:1	0.9011
26	Ni/VCB/CF/PP 1:1:1	0.9011

3.2.1 Conductivity with Increasing Filler Concentration

From the results of initial screening of runs, a 35% 1:1:1 SG/VCB/CF blend was chosen for further study. Although the conductivity of this composite is 1.38 S/m, and therefore slightly lower in comparison to other blends, this blend possesses relatively better processability. This conductivity was among the top 1:1:1 SG or NCG/VCB/PP blends in conductivity as shown in Figure 3.1.

According to percolation theory, a conductive blend will reach a threshold where the filler content will be high enough that the conductive filler can form a continuous network to allow for electrons to pass. In this case the blend with 35% filler concentration was too low to reach to the percolation threshold; hence, there is a further experimental series of runs to investigate the effects of filler concentration on composites conductivity and mechanical properties.

The specific experimental program maintained a 1:1:1 filler ratio, but increased the total fillers concentration within polymer matrix phase. Polypropylene (Equistar 36KK01) was still chosen as polymer matrix, while three different graphite grades were used. These were all provided from Asbury Carbons. The fillers SG-4012, SG-4955, and SG-4956 were used and these runs were selected to investigate the effects of filler loading as well as types and sizes of graphite on blend processability and conductivity. Three series of PP-based blends were compounded with the batch mixer with a combination of VCB, CF,

and SG-4012 or SG-4955 or SG-4956 in a ratio of 1:1:1. The total filler loading varied from 40% to 45%, 50%, 55%, 60% and 65%. The conductivity measurement results are illustrated in Table 3.4, 3.5 and 3.6, and the corresponding graphs are shown in Figure 3.10, 3.12 and 3.13, respectively. Samples were injected molded to form both 'blanks' for mechanical testing, and bi-polar plates.

For in-plane conductivity measurements, samples were tested in two directions: one test was in the sample direction which parallels to the injection molding direction, and another was the samples direction perpendicular to injection molding direction. As illustrated in Table 3.4 and Figure 3.10, in-plane conductivity of samples in injection molding direction was greater than that perpendicular to the injection molding direction. There was a limited difference between in-plane conductivity with respect to the molding direction, but the trend was reliable since all the testing results showed the same trend from 45% filler loading up to 65%.

Table 3.4: In-plane conductivity of 1:1:1 SG-4012/VCB/CF blends

Fillers level (wt %)	In-plane Conductivity (S/m)	
	∥ Injection Direction	⊥ Injection Direction
45%	291.86	257.96
50%	443.72	375.82
55%	702.25	634.64
60%	973.21	917.37
65%	1971.91	1916.81

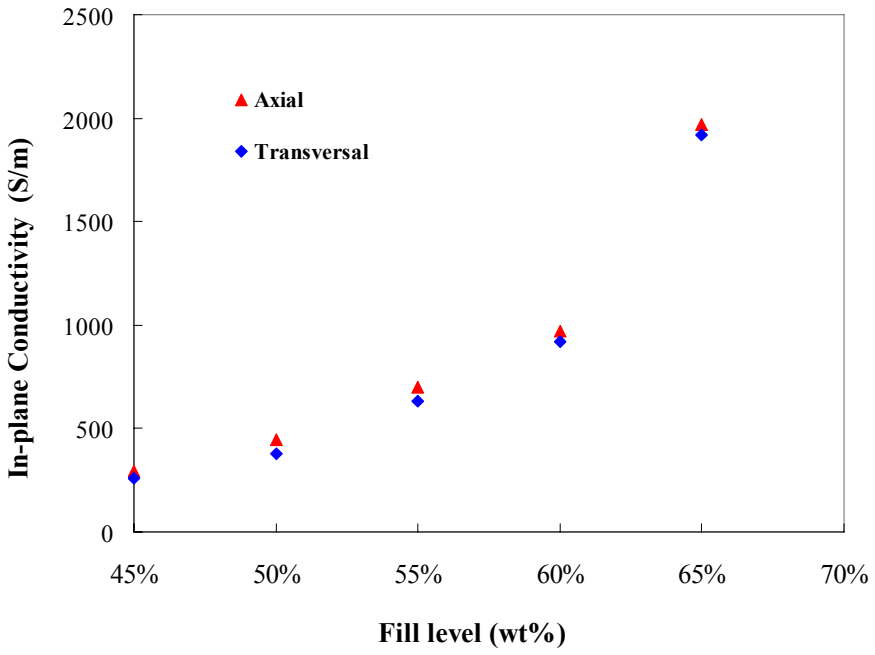

Figure 3.10: In-plane conductivity of 1:1:1 SG-4012/VCB/CF composite measured in two directions (Injection molding direction and Perpendicular to injection molding direction)

The reason for conductivity difference in two directions is that for samples having the same direction as injection molding, the fillers (specifically the fiber fill) are oriented in the direction of flow induced during the injection molding process. This is the same as the direction of electrical conductivity measurement, and oriented fillers allow electrons to flow through easier than the direction perpendicular to injection molding process. Figure 3.11 is the SEM image of 55% 1:1:1 SG-4012/VCB/CF composites with magnification of 200x, in which shows carbon fiber alignment along injection flow direction.

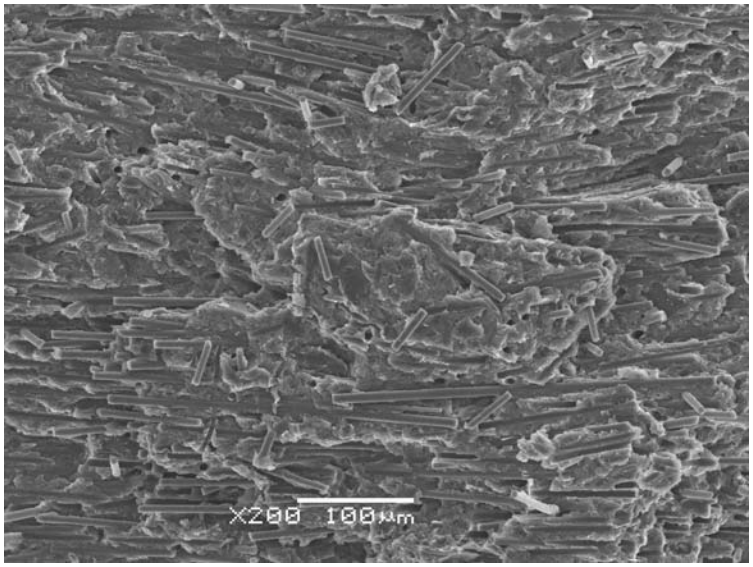

Figure 3.11: SEM photo of 55% 1:1:1 SG-4012/VCB/CF composites with magnification of 200x

The conductivities of the different PP-based blends as a function of filler (SG/VAB/CF) concentration are illustrated in Figure 3.12 and 3.13 as well as in Table 3.5 and 3.6. As expected, the blend conductivity increases with increasing filler concentration. Conductivity values around 150 S/m in though-plane and 1900 S/m in in-plane are reached with 65% filler concentration by weight. However, 65% filler loading reaches the processing limit of the apparatus used. It is important to determine which blend formulation will offer the best combination in terms of conductivity and process ability. From the results, 65% of 1:1:1 SG-4012/VCB/CF obtains the volume conductivity of 156 S/m and in-plane conductivity of 1971.91 S/m, respectively.

The effect of different synthetic graphite grades on composite conductivity was also investigated in this project. The comparison of in-plane conductivity for these samples is based on samples with the same directions as injection molding process.

Figure 3.12, shows that with filler concentration less than 60%, SG-4012 and SG-4956 composites have higher conductivity than that of SG-4955, although SG-4012 and SG-4956 have very close conductivity values. At 65% filler loading, different graphites exhibit distinct differences.

Table 3.5: In-plane conductivity of 1:1:1 SG/VCB/CF composites

Fill level (wt %)	In-plane Conductivity (S/m)		
	SG-4012	**SG-4955**	**SG-4956**
45%	291.86	172.81	411.27
50%	443.72	293.63	467.14
55%	702.25	509.37	717.96
60%	973.21	800.24	901.50
65%	1971.91	1431.42	1354.20

The highest conductivity value is obtained by SG-4012, which is 1971.9 S/m, followed by SG-4955 at 1431.42 S/m and SG-4956 at 1354.2 S/m. Of note is that for SG-4012 composite, when the filler level increases from 60% to 65%, the in-plane conductivity increases significantly from 973.2 to 1971.9 S/m which almost doubles the conductivity

at 60% concentration. The possible reason for this is that after 60% filler level, a percolation threshold is reached because there are more conductive particles within polymer matrix, and this resulted in higher conductivity. For the other two graphite composites, at 65% filler loading, their in-plane conductivities did increase but not as significantly as SG-4012. This is not a surprising result, since SG-4012 has large crystal domains aligned in the flat graphite flake, resulting in highly anisotropic material properties. Because the best conductivity value was obtained using SG-4012, this graphite was used for all the additional PP-based blends developed in this study, and this filler was selected as the composite blend for the metal insert technique testing.

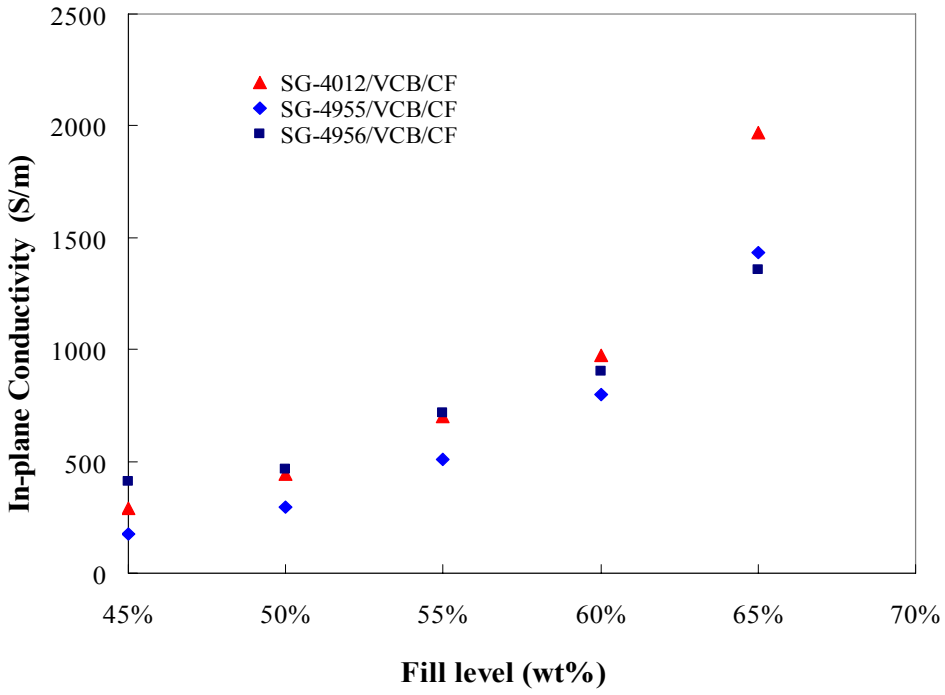

Figure 3.12: In-plane conductivity of 1:1:1 SG/VCB/CF composites (three kinds of SG were applied)

For through-plane conductivity, there is not much difference with different synthetic graphite results. As shown in Figure 3.13, with increasing of filler concentration, composites through-plane conductivity increases correspondingly.

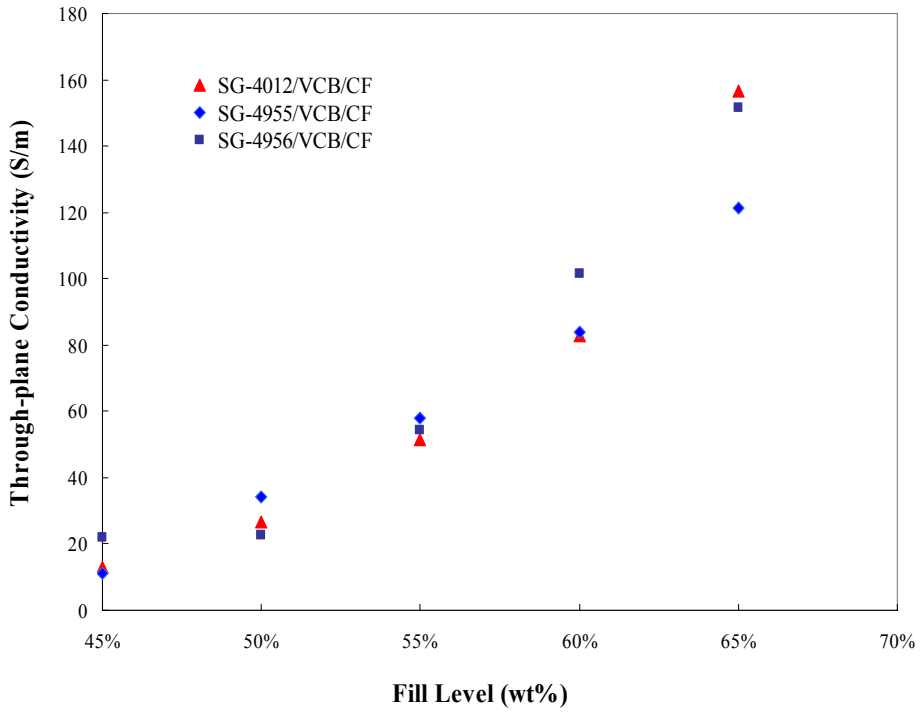

Figure 3.13: Through-plane conductivity of 1:1:1 SG/CF/VCB composites with different graphite and varied filler level

When filler concentration is below 55%, composites have very close conductivity values which only appear to depend on individual filler loading levels. After 60% filler levels, different graphite based composites exhibit different trends. SG-4956 has higher through-plane conductivity than the others, and the other two SG based composites have

very close conductivity values. At 65% filler loading, SG-4012 and SG-4956 composites have higher conductivity than that of SG-4955. The highest through-plane conductivity is obtained by 65% SG-4012/VCB/CF, 156.5 S/m, which is similar to the in-plane conductivity results. Comparing to in-plane conductivity, the through-plane conductivity DOE Target of 10,000 S/m was not achieved.

Table 3.6: Through-plane conductivity of 1:1:1 SG/VCB/CF composites

Fill level (wt %)	Through-plane Conductivity (S/m)		
	SG-4012	SG-4955	SG-4956
45%	12.80	11.17	21.86
50%	26.82	34.08	22.85
55%	51.41	58.06	54.19
60%	82.78	83.86	101.43
65%	156.5	121.40	151.72

There are several possible reasons for the variation in the test results. First, the testing method is different between in-plane and through-plane conductivity. In through-plane conductivity measurement, the contact resistance between gold plate and bipolar plate becomes more significant than the volume resistance of the bipolar plate, and depends more significantly on the area of the sample used. If contact resistance between surfaces is high, the total measured volume conductivity can be significantly affected, leading to

low through-plane conductivity. This phenomenon is discussed further in Chapter 3 Section 3.4 “Effect of Sample Dimensions on Conductivity Measurement”.

Second, these bipolar plate samples are injection molded, and the through-plane conductivity measurement direction is perpendicular to the injection molding direction. With the injection molding process, conductive particles within the composite are aligned along the injection molding direction, which makes it more difficult for electrons to go through the bipolar plate and lead to low through-plane conductivity. As well, there is a certain concentration of the resin on the surface of the sample which creates a non-conductive barrier layer.

Figure 3.14 (a) and (b) demonstrates the SEM images of 55% 1:1:1 SG-4012/VCB/CF composite, in which we can see the carbon fiber alignment as well as a surface layer on the edge of bipolar plate.

For injection molded bipolar plates, carbon fibers show very regular alignment along the injection molding direction as shown in Figure 3.14 (a) and result in through-plane conductivity that is much lower than in-plane conductivity. On the surface of the bipolar plate, a non-conductive polymer layer with around 20 μm in thickness can be identified very clearly in Figure 3.14 (b), which also induces the low through-plane conductivity.

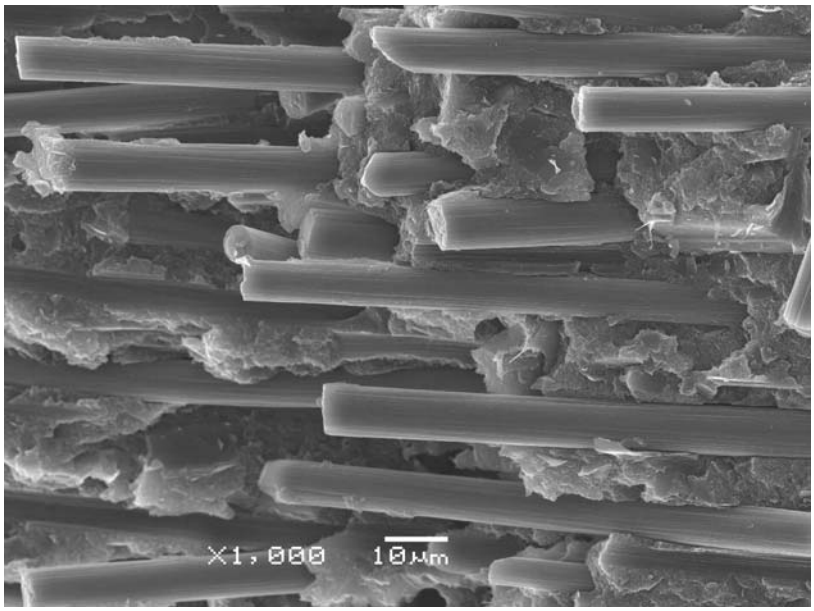

(a)

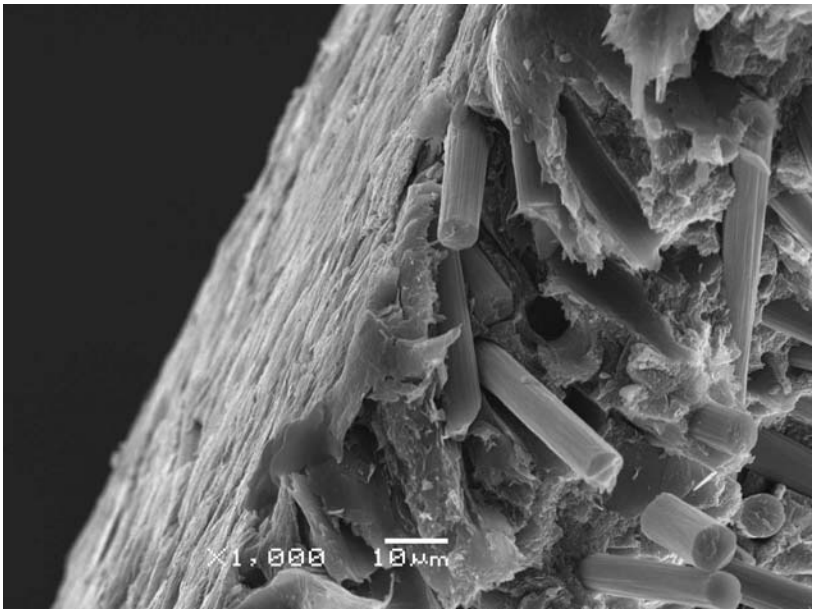

(b)

Figure 3.14: SEM photos of 55% 1:1:1 SG-4012/VCB/CF composite show (a) carbon fiber alignment (b) a polymer surface layer

3.2.2 Mechanical Properties of Composites

Mechanical properties are one of most important properties of a bipolar plate in a PEM fuel cell. The plate must retain mechanical stability in order to prevent the stack from leaking, and so that the plate does not damage the membrane. The 1:1:1 SG-4012/VCB/CF composites with filler loading up to 65% were tested for their mechanical properties which include tensile strength, compression strength, and 3-point bending. The test results are illustrated from Figure 3.15 to Figure 3.20.

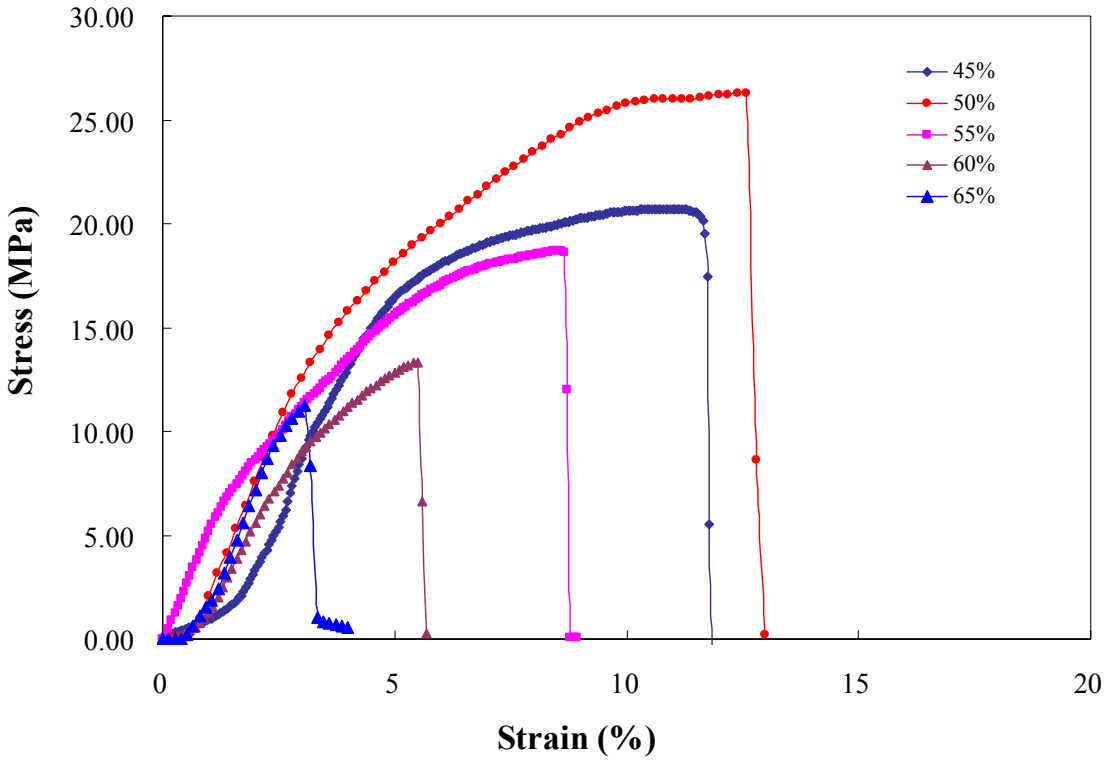

Figure 3.15: Tensile Stress-strain curves of 1:1:1 SG-4012/VCB/CF composites

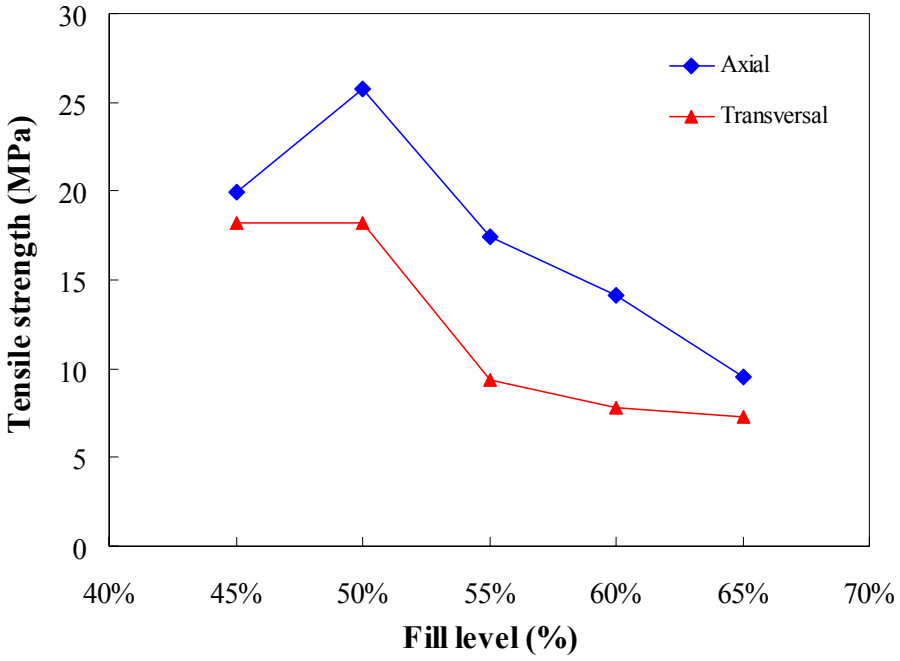

Figure 3.16: Tensile strength of 1:1:1 SG-4012/VCB/CF composites

Figure 3.15 and 3.16 illustrates the tensile stress-strain curves and tensile strength of 1:1:1 SG-4012/VCB/CF composites with filler loading from 45% up to 65%. Of note is that the tensile strength is tested in two directions, similar to that of in-plane conductivity measurement: one test is in the sample direction which is parallel to the injection molding direction (axial direction), and another is in the samples direction perpendicular to injection molding direction (transverse direction).

Figure 3.15 compares the tensile stress-strain curves of 1:1:1 SG-4012/VCB/CF composites with filler loading from 45% up to 65%. It is clear that the composite with

50% filler concentration exhibits the highest fracture strength and ductility, followed by 45%, 55%, 60% and 65% composite. Also, in stress-strain curve (Figure 3.15), the slope of 65% filler loading composite is steeper than others which means it has higher tensile modulus and is stiffer and more brittle comparison to other composites.

In Figure 3.16, samples in the axial direction show higher fracture strength in comparison to those samples in transverse direction, which is due to the filler particle alignment along injection flow induced in the injection molding process. Similar to the trend shown in Figure 3.15, from 45% to 65% filler concentration, the highest tensile strength value (25.7 MPa) is obtained at 50% filler loading; from 45% to 50%, tensile strength is increased because of filler reinforcement effect with the higher filler loading tensile strength is decreased with filler levels increasing.

The tensile modulus of composites is illustrated in Figure 3.17. Similar to tensile strength, the tensile modulus of samples in axial direction is greater than those samples in transverse direction. With filler concentration increasing, the composites tensile modulus exhibits a fluctuation from 417 MPa to 584 MPa. Compared to 45% filler loading, the 50% composite has higher tensile modulus; however, the modulus is decreased when filler loading reaches 55% and 60%, and at 65%, samples in axial direction exhibit the highest tensile modulus (584 MPa) while the samples perpendicular to injection flow show a decrease in tensile modulus.

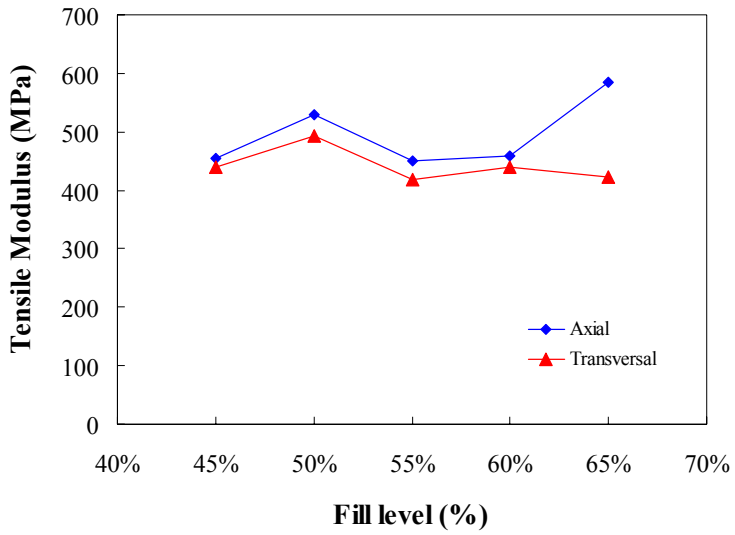

Figure 3.17: Tensile modulus of 1:1:1 SG-4012/VCB/CF composites

The compression and flexural strength are the measure of a material's ability to sustain loading prior to failure. The testing results are illustrated in Figure 3.18, 3.19 and 3.20.

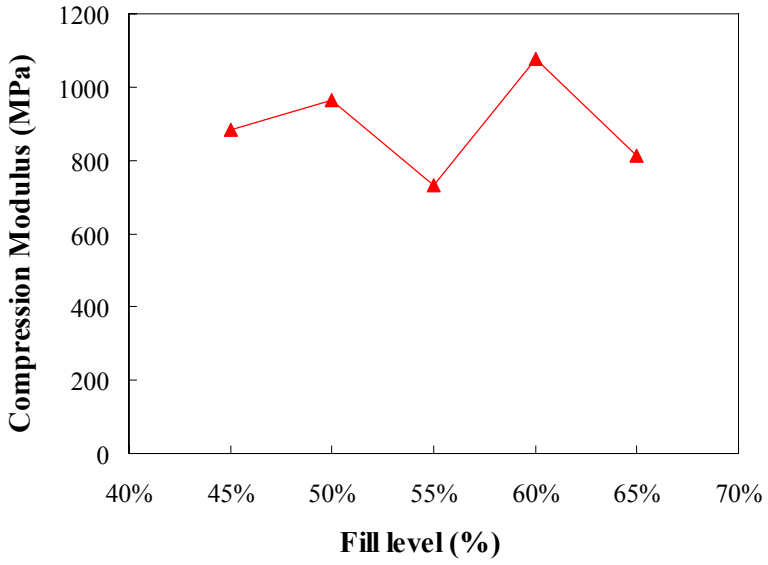

Figure 3.18: Compression modulus of 1:1:1 SG-4012/VCB/CF composites

Of note is that for compression and flexural strength test, samples were done in the axial direction. In Figure 3.18, the compression modulus shows the fluctuation from 731 MPa to 1076 MPa for composites from 45% to 65% filler loading. The maximum compression modulus was obtained at 60% filler loading, and 55% composite yields the minimum modulus value.

Figure 3.19 and 3.20 show the test results for the flexural strength and flexural modulus of composites. From 45% to 50% filler level, flexural strength increases significantly, from 36 MPa to 53 MPa, and then decreases with higher filler loading but is still higher than that of 45% composite.

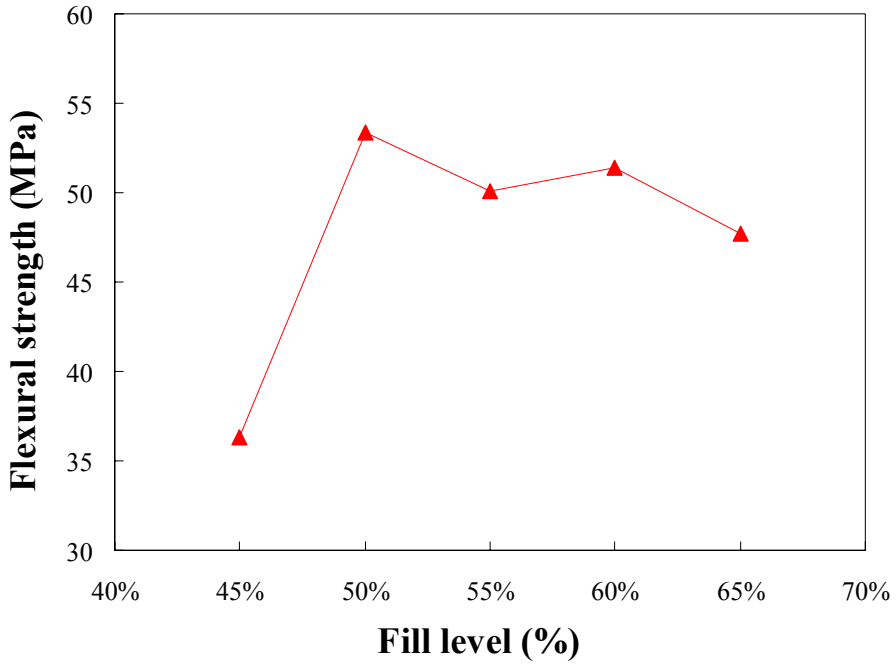

Figure 3.19: Flexural strength of 1:1:1 SG-4012/VCB/CF composites

The flexural modulus of composites increases consistently from 2.25 to 6.82 GPa with the increase of filler concentration. The highest value of 6.82 GPa is obtained at 65% composite filling, indicate that this kind of material is stiffer than other composites.

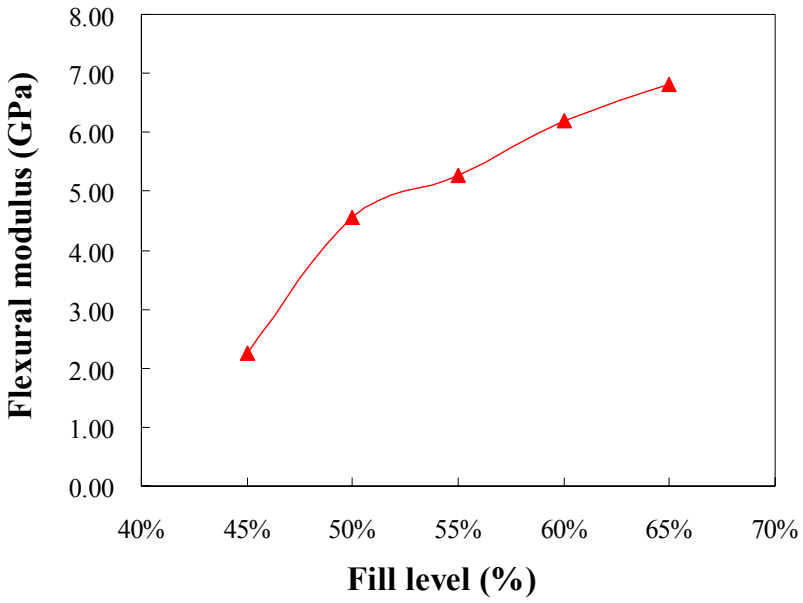

Figure 3.20: Flexural modulus of 1:1:1 SG-4012/VCB/CF composites

3.2.3 SEM of the 1:1:1 SG/VCB/CF Composite Blend

As was discussed earlier, SEM techniques are an effective way to view the microstructure of composites; the injection molded bipolar plate with 55% filler concentration was chosen for SEM. The reasons for choosing this blend are: first, it is one of composites for blends development; second, it is also used for metal insert bipolar plates preparation as well as in-situ single cell performance testing with and without a metal insert. The SEM samples for this blend are prepared from three different parts in one injection molded

bipolar plate, which are the upper (near to the injection gate), middle and lower part of one plate. Two directions are inspected using SEM, one is along the injection molding direction (Axial direction), and another is perpendicular to injection molding direction (Transversal direction). Figure 3.21, 3.22 and 3.23 are various SEM images which show each part of a bipolar plate independently; as well the micrographs show edge effects, surface layer, carbon fibers pull-out and fibers alignment.

Figure 3.21 displays the SEM images of upper part of injection molded 55% 1:1:1 SG-4012/VCB/CF bipolar plate in (a) transversal direction and (b) axial direction, respectively. For the upper part of the bipolar plate, in the transversal direction, the alignment of carbon fibers can be identified and the composite shows relatively uniform micro-structure; while in the axial direction, in the boundary area and the middle of sample, the composite exhibits fairly different structures as shown in Figure 3.21 (b)-1. The two interesting phenomena are: First, in injection molding direction, the carbon fibers show different orientations. In the boundary area of sample (upper and bottom of bipolar plate interface), carbon fibers orientate along the injection molding direction, while in the middle of the sample, carbon fibers show a relatively random orientation compared to those in the boundary area of the sample, which might be induced by different velocity of injection flow. Second, most synthetic graphite particles located in the middle of bipolar plate, and showed a certain degree of alignment.

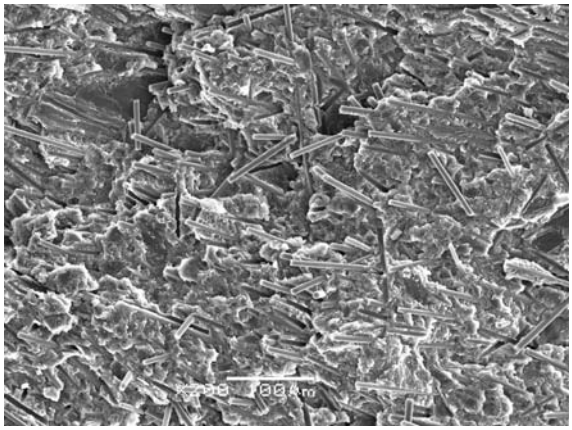

(a) Overall

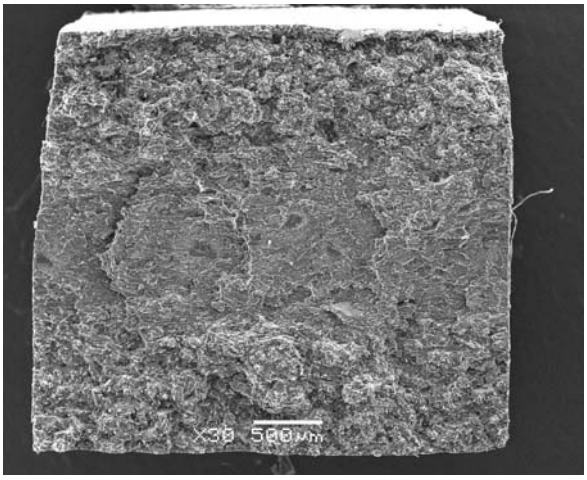

(b)-1 Overall

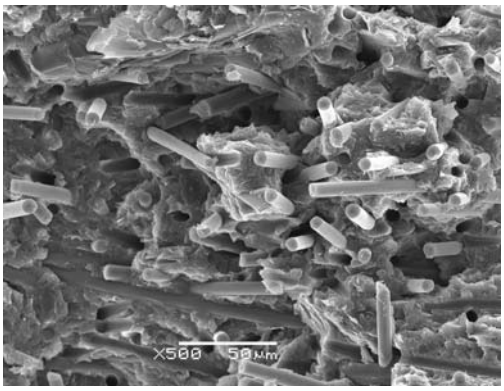

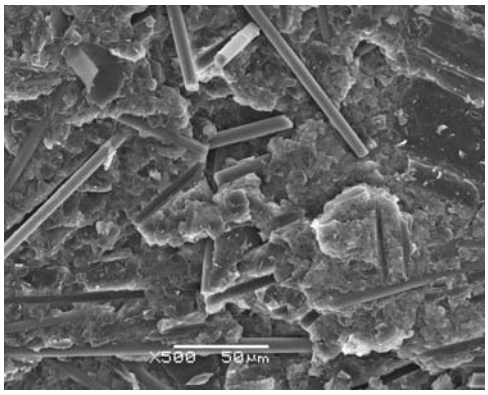

(b)-2 Boundary **(b)-3 Middle**

Figure 3.21: SEM photos of upper part of injection molded 55% 1:1:1 SG-4012/VCB/CF bipolar plate in (a) Transversal direction and (b) Axial direction

Figure 3.22 displays the SEM images in the transversal and axial directions of the middle part of the injection molded 55% 1:1:1 SG-4012/VCB/CF bipolar plate. Similar to Figure 3.21, the microstructure of the bipolar plate is quite different at different locations even at the same interface of the sample. SEM images in Figure 3.22 (a) exhibit that in the transversal direction carbon fibers show totally different alignment at different locations which is similar to those for SEM images in the axial direction as shown in Figure 2.23 (b).

The SEM images of the lower part of bipolar plate are displayed in Figure 3.23, and showed similar results to those in Figure 3.22.

Injection molding is an effective method for fabricating bipolar plates, however, the SEM images of bipolar plates indicate that the micro structures of injection molded bipolar plates are not uniform. It was also found from those SEM images that the distribution and orientation of conductive particles was not uniform within the composite, which might be the possible reason for low conductivity results.

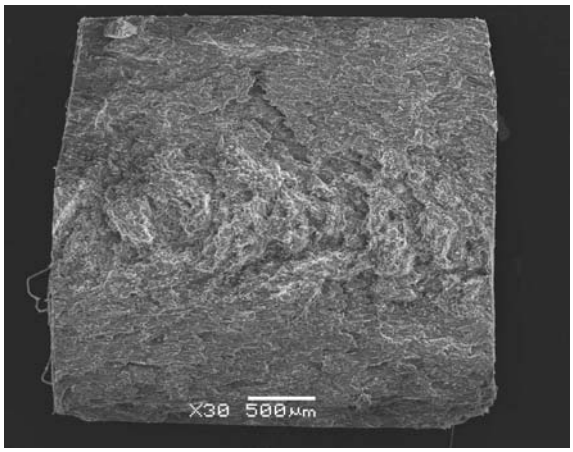

(a)-1 Overall

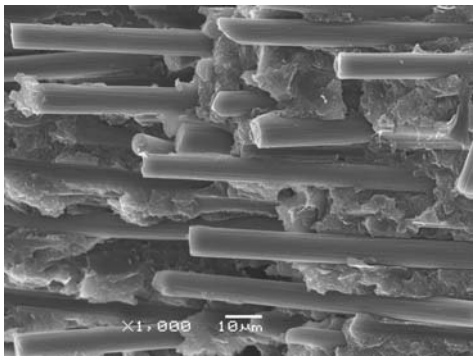

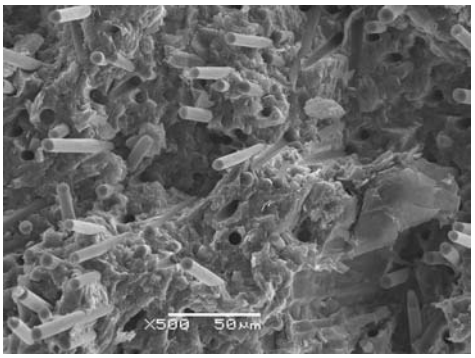

(a)-2 Boundary **(a)-3 Middle**

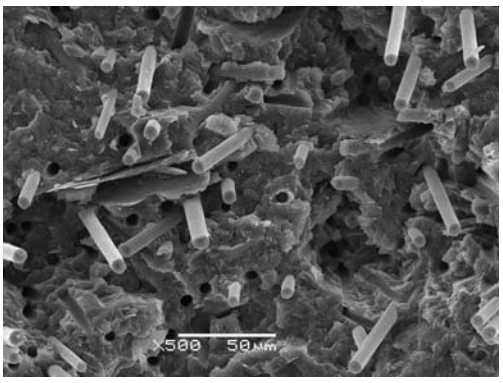

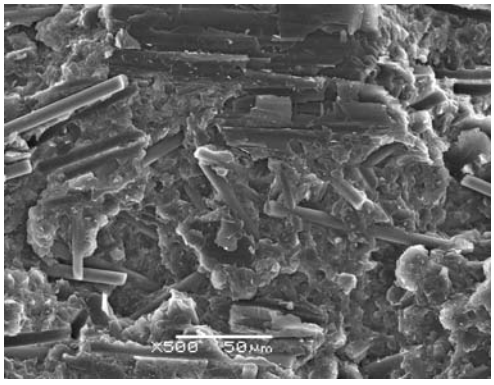

(b)-1 Boundary) **(b)-2 Middle**

Figure 3.22: SEM photos of middle part of injection molded 55% 1:1:1 SG-4012/VCB/CF bipolar plate in (a) Transversal direction and (b) Axial direction

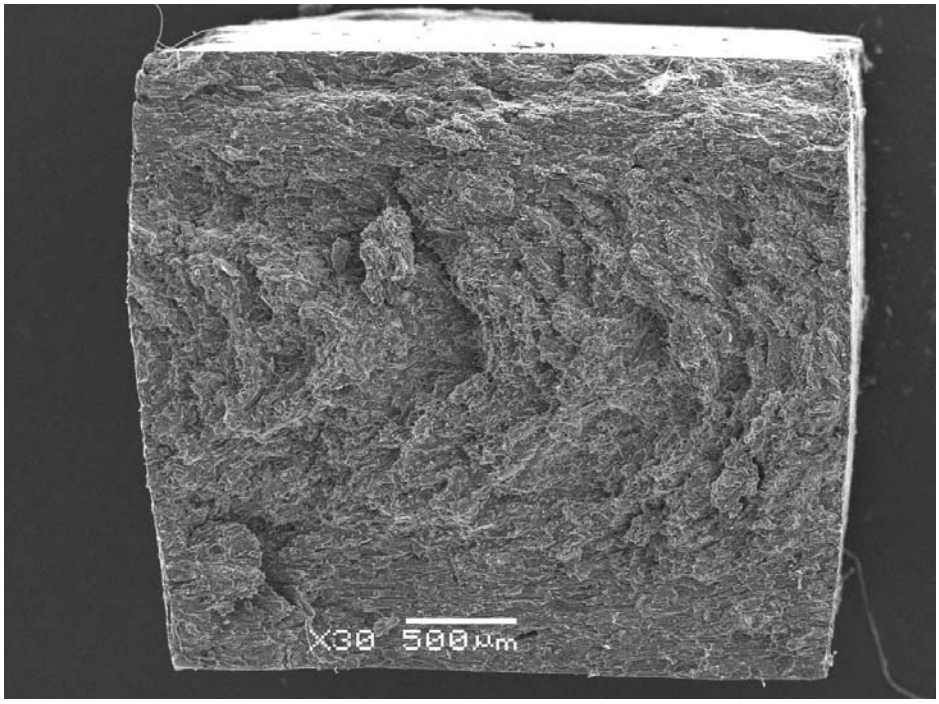

(a) Overall

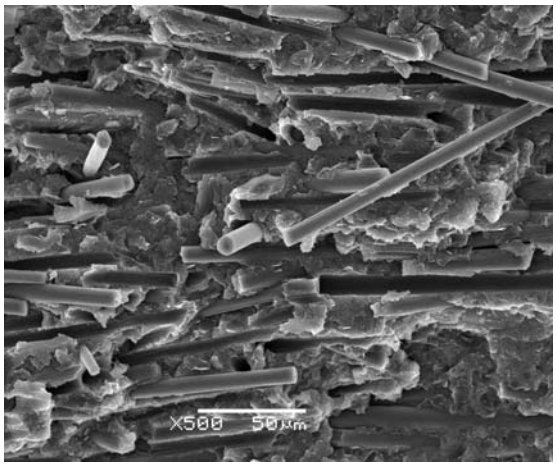

(b) Boundary

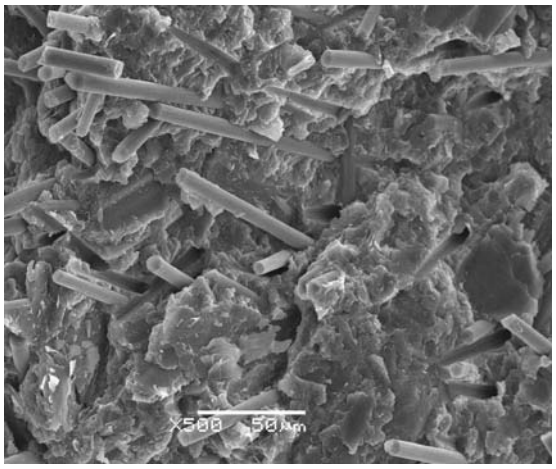

(c) Middle

Figure 3.23: SEM photos of lower part of injection molded 55% 1:1:1 SG-4012/VCB/CF bipolar plate in transversal direction

3.2.4 Density of Composites

With increasing filler concentration, the density of composite bipolar plates increases from 1.17 to 1.33 g/cm^3, as shown Figure 3.24.

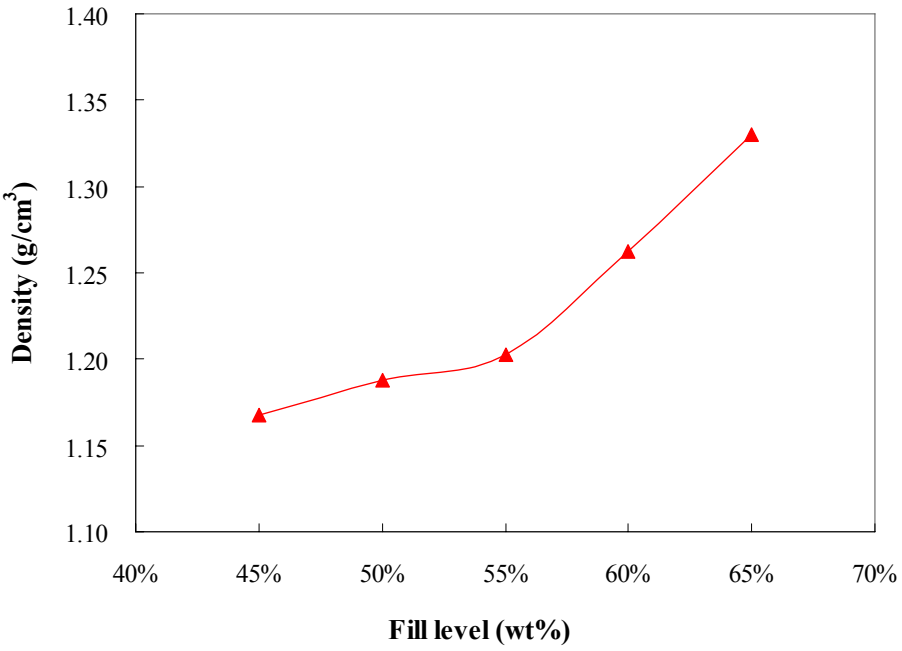

Figure 3.24: Density of 1:1:1 SG-4012/VCB/CF bipolar plates

Increasing the filler level will reduce the resin content. Since the density of polypropylene (0.89~0.91 g/cm^3) is much lower than that of synthetic graphite SG-4012 (1.2~1.4 g/cm^3), carbon black (1.7~1.9 g/cm^3), and carbon fiber (1.8 g/cm^3), the density of a composite bipolar plate increases with filler concentration. The density of the plate significantly affects the overall weight of the fuel-cell stack. The maximum density of the plate for 65 wt% 1:1:1 SG-4012/VCB/CF composite is 1.33 g/cm^3; which is still far

lower than that of a pure graphite bipolar plate (1.88 g/cm^3).

3.3 Metal Sheet Insert Techniques for Bipolar Plate Development

The objective of this project was to develop a highly conductive, light weight and low cost bipolar plate. Metal sheet insert techniques were also investigated to improve the conductivity of a bipolar plate. This technique is based on the concept that with metal sheet insert within the bipolar plate, the electrons can easily go through the metal sheet to form an electric circuit; hence the conductivity of the bipolar plate can be improved significantly, making the plates more suitable for use in a PEM fuel cell. The potential advantages of metal sheet insert in a bipolar plate are as follows:

- highly conductive;
- light in weight;
- no corrosion problems;
- strong mechanical properties;
- mass produced flow path by injection molding, specifically through the use of an insert over-molding technique; and
- low cost

The Figure 3.25 illustrates the diagram of a metal sheet insert bipolar plate. The black straight line, big black dot, and small black dot are conductive fillers in the composite, mainly carbon fibers, synthetic graphite as well as carbon black, which were specifically

studied in this project. The gray line refers to metal sheet insert in the bipolar plate, such as metal mesh or copper sheet. As can be seen in the graphic, conductive particles within the composite can easily form an electric circuit with the aid of the metal sheet, so that electrons can go through the bipolar plate and the conductivity is significantly improved.

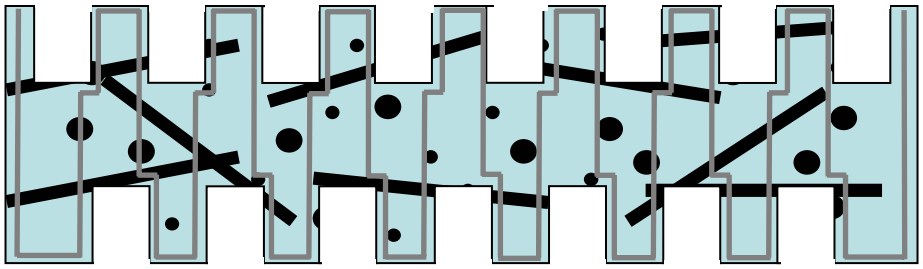

Figure 3.25: Schematic diagram of conceptual metal sheet insert bipolar plate

3.3.1 Experimental Metal Sheet Insert Techniques

3.3.1.1 Materials

The composite used was the 1:1:1 SG-4012/VCB/CF composite, with total filler loading from 45% up to 65%, and in which 65% composite has in-plane and through-plane conductivity 1916 S/m and 156 S/m, respectively. The metal-mesh and copper sheet selected for use in this study were selected based on the material availability.

3.3.1.2 Sample Fabrication

Metal sheet insert bipolar plates were prepared as follows:

first, two pieces of composite sheets with dimension of 100.0* 24.0* 3.0 mm from injection molded bipolar plate samples were cut, and then a metal sheet with length and width of 92.0 mm and 18.0 mm was compression molded between the two sheets of composite materials. The entire sample was oven heated to 190°C for 40 minutes to ensure that composite sheets were soften, and then the materials were transferred to compression molding for cold-pressing for 5 minutes. Samples were cut into the final metal sheet insert bipolar plates with a dimension of 100* 24* 2.8~3.1 mm.

Due to the viscosity of different composites, even with the same clamping pressure, the final samples thickness were not identical, thus the sample thickness varied from 2.8~3.1 mm, but the effect of varied thickness is not significant from conductivity data perspective for the metal sheet insert bipolar plates.

3.3.2 Properties of Metal Sheet Insert Bipolar Plate

3.3.2.1 Conductivity of Metal Sheet Insert Bipolar Plate

The metal sheet insert bipolar plates were tested for both in-plane and through-plane conductivity, and compared with those without metal sheet inserts. The testing results are summarized in Table 3.7 and 3.8. Figures 3.26 through 3.31 illustrate the graphs of conductivity of metal sheet insert bipolar plates.

With the metal mesh insert technique, the in-plane conductivity of composite increases significantly, as shown in Table 3.7 and Figure 3.26. For 65% 1:1:1 SG--4012/VCB/CF composite with a metal mesh insert, for example, the in-plane conductivity is increased from 3651 S/m to 17523 S/m, which is consistent with our expectation for conductivity improvement with the metal sheet insert.

Table 3.7: Conductivity of metal-mesh inserts bipolar plates

Filler loading (%) 1:1:1 SG--4012/VCB/CF	Conductivity of Metal Mesh Insert Bipolar Plate (S/m)			
	In-Plane		Through-Plane	
	Before	After	Before	After
45%	475.8	9184.8	21.2	23.0
50%	835.7	14738.2	62.1	43.1
55%	1404.3	14489.9	126.9	79.8
60%	1974.9	16715.2	184.0	143.0
65%	3651.5	17523.3	416.2	163.6

With the aid of metal mesh, electrons can go through the bipolar plate more easily to form an electric circuit. As a result, the bipolar plate becomes more conductive. However, the through-plane conductivity decreases with the metal mesh insert, which is the opposite trend to that for in-plane conductivity. The possible reason for this is although metal mesh is more conductive than composite, for the metal mesh inset bipolar plates the contact resistances between metal mesh and composite reduce through-plane conductivity.

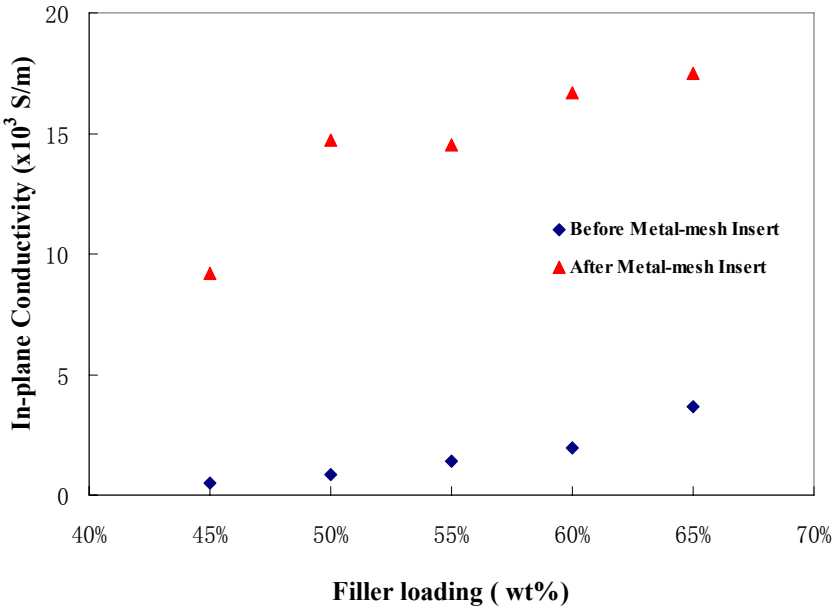

Figure 3.26: In-plane conductivity of metal-mesh inserts bipolar plate

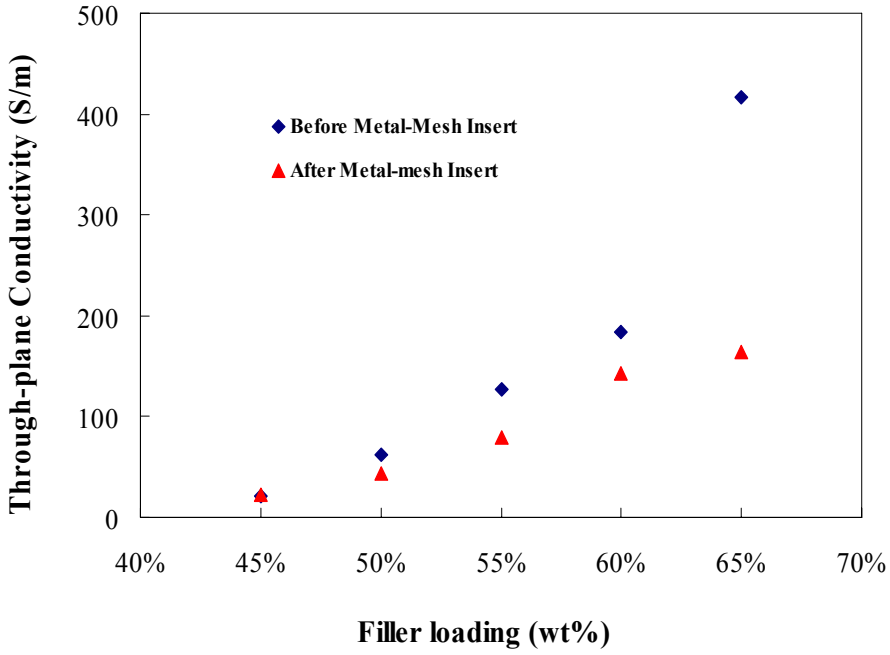

Figure 3.27: Through-plane conductivity of metal-mesh inserts bipolar plate

The conductivity values for copper sheet insert bipolar plates are summarized in Table 3.8 and illustrated in Figure 3.28 and 3.29 for in-plane and through-plane conductivity, respectively. Also, the comparison of effects between metal mesh insert and copper sheet insert on in-plane and through conductivity is demonstrated in Figures 3.29 and 3.30.

Table 3.8: Conductivity of copper sheet inserts bipolar plate

Filler loading (%) 1:1:1 SG-4012/VCB/CF	Conductivity of Copper Insert Bipolar Plate (S/m)			
	In-Plane		Through-Plane	
	Before	After	Before	After
45%	478.8	46602.1	19.4	22.5
50%	831.7	106056.2	54.3	39.2
55%	1371.3	369241.8	120.8	74.6
60%	1858.2	859044.7	217.2	138.9
65%	3903.1	891084.3	345.6	158.0

Similarly to metal mesh insert bipolar plates, in-plane conductivity of copper sheet insert bipolar plate increases as well, but more significantly, as shown in Table 3.8 and Figure 3.28. For the same composite, 65%1:1:1 SG-4012/VCB/CF, with copper sheet insert, the plate in-plane conductivity reaches $8.91 * 10^5$ S/m, which is approximately 50 times that of with metal mesh insert (as 17523.3 S/m) and 220 times than that of the same composite (as 3903.1 S/m). Once again, with the copper sheet insert, obtained in-plane conductivity results confirmed our concept for conductivity improvement with the metal

insert. On the contrary, the copper sheet insert decreases the through-plane conductivity as illustrated in Figure 3.29, which is similar to that with metal mesh insert due to the contact resistance between copper sheet with composite.

Another possible reason for though-plane conductivity reduction is the molding process. Since the copper sheet is sandwiched in between the two composite plates and heated up to 190~200℃ for 40 minutes in an oven, an oxidation layer formed on the surface of copper sheet, which is non-conductive and therefore may affect though-plane conductivity.

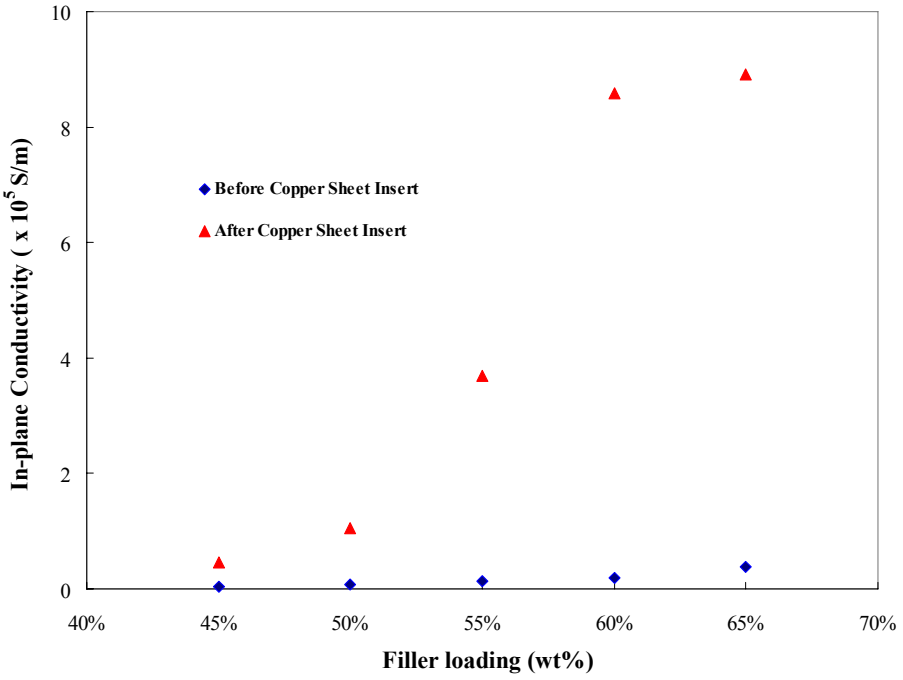

Figure 3.28: In-plane conductivity of copper sheet insert bipolar plate

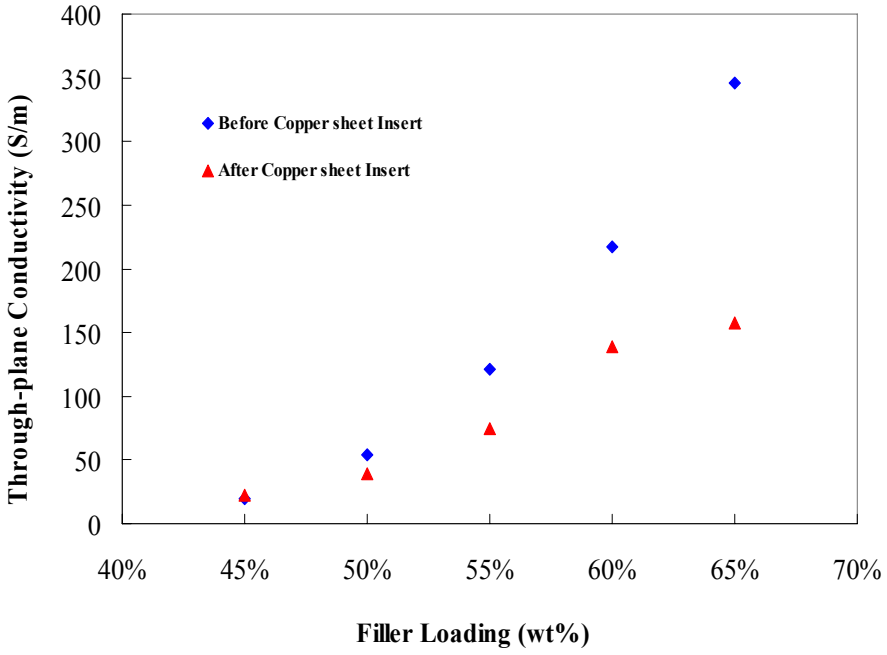

Figure 3.29: Through-plane conductivity of copper sheet insert bipolar plate

Figure 3.30 and 3.31 show the comparison between the metal mesh insert and copper sheet insert bipolar plates. As a result, copper sheet is a more effective material than metal mesh for improving bipolar plate in-plane conductivity.

However, both metal mesh and copper sheet inserts decrease the through-plane conductivity. The possible reasons for this are increased contact resistance between metal mesh or copper sheet with composite, an oxidation layer formed on metal surface, or improper molding process. An injection molding process is suggested for fabricating metal insert bipolar plate to increase through plane conductivity.

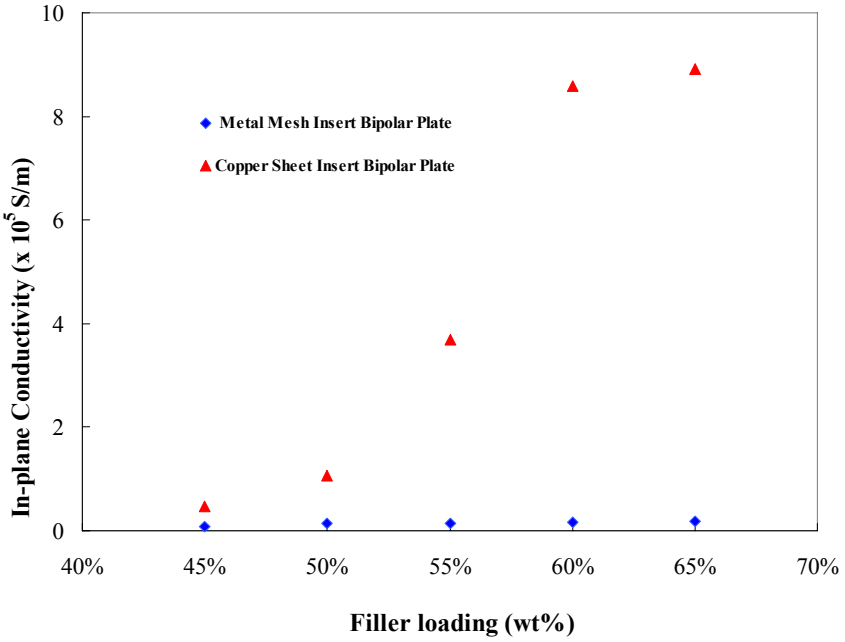

Figure 3.30: Comparison of in-plane conductivity of metal mesh insert plate with copper sheet insert bipolar plate

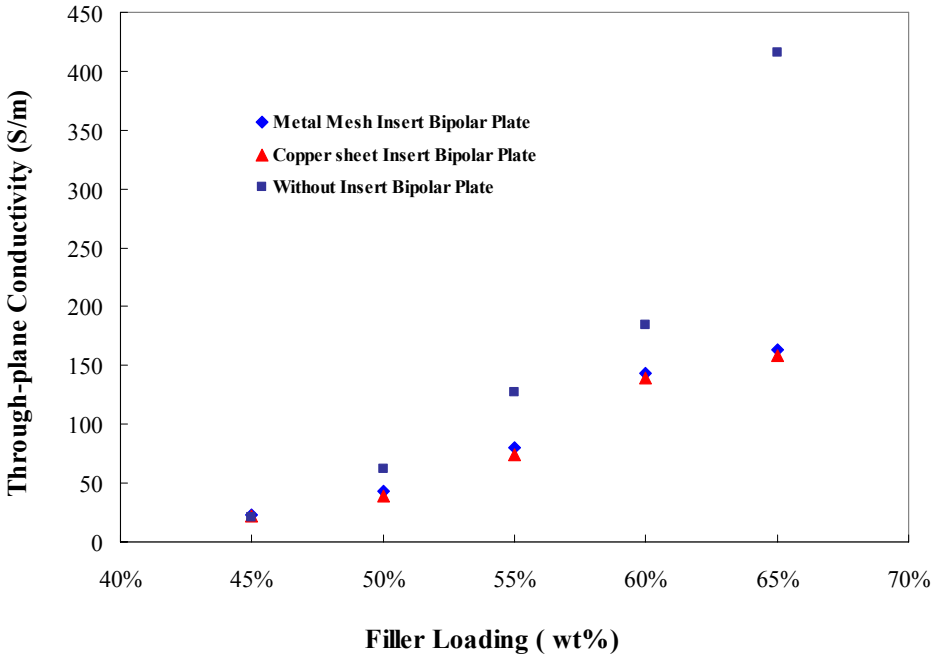

Figure 3.31: Comparison of through-plane conductivity of bipolar plate with or without metal sheet insert technique

3.3.2.2 In-situ Testing of Metal Insert Bipolar Plates

In this project, the performance characteristics of metal copper sheet insert bipolar plates were evaluated in a single fuel cell, and compared with graphite and composite bipolar plates.

The polymer composite bipolar plate had a thickness of 2.5~2.8 mm and approximately 13.9 cm^2 active area. The composites chosen for the in-cell testing were 50%, 55% and 60% 1:1:1 SG-4012/VCB/CF, and 50% and 55% composites were also made with copper sheet insert. Figure 3.32 shows the composite bipolar plates and copper insert bipolar plates used in this study.

Figure 3.33 presents the polarization curves for single cells assembled with graphite, 50%, 55% and 60% composite bipolar plates. The open circuit voltage (OCV) of the single cells was almost the same, around 0.80 V, however, graphite and 60% composite had a higher OCV at 0.86 V. This would indicate that there may be increased resistance in the cell hardware - specifically the bi-polar plate or the electrical contact with the GDL and electrode.

The single cells of different polymer types exhibit almost the same performance at lower current densities. With the increasing of current densities, all the composite bipolar plates showed lower performance than graphite bipolar plates, and voltages of single cells using

50% and 55% composite bipolar plates decreased more rapidly than those of single cells using graphite and 60% composite bipolar plate. Clearly this is as a result of the lower conductivity of the plate material, and is therefore an expected result.

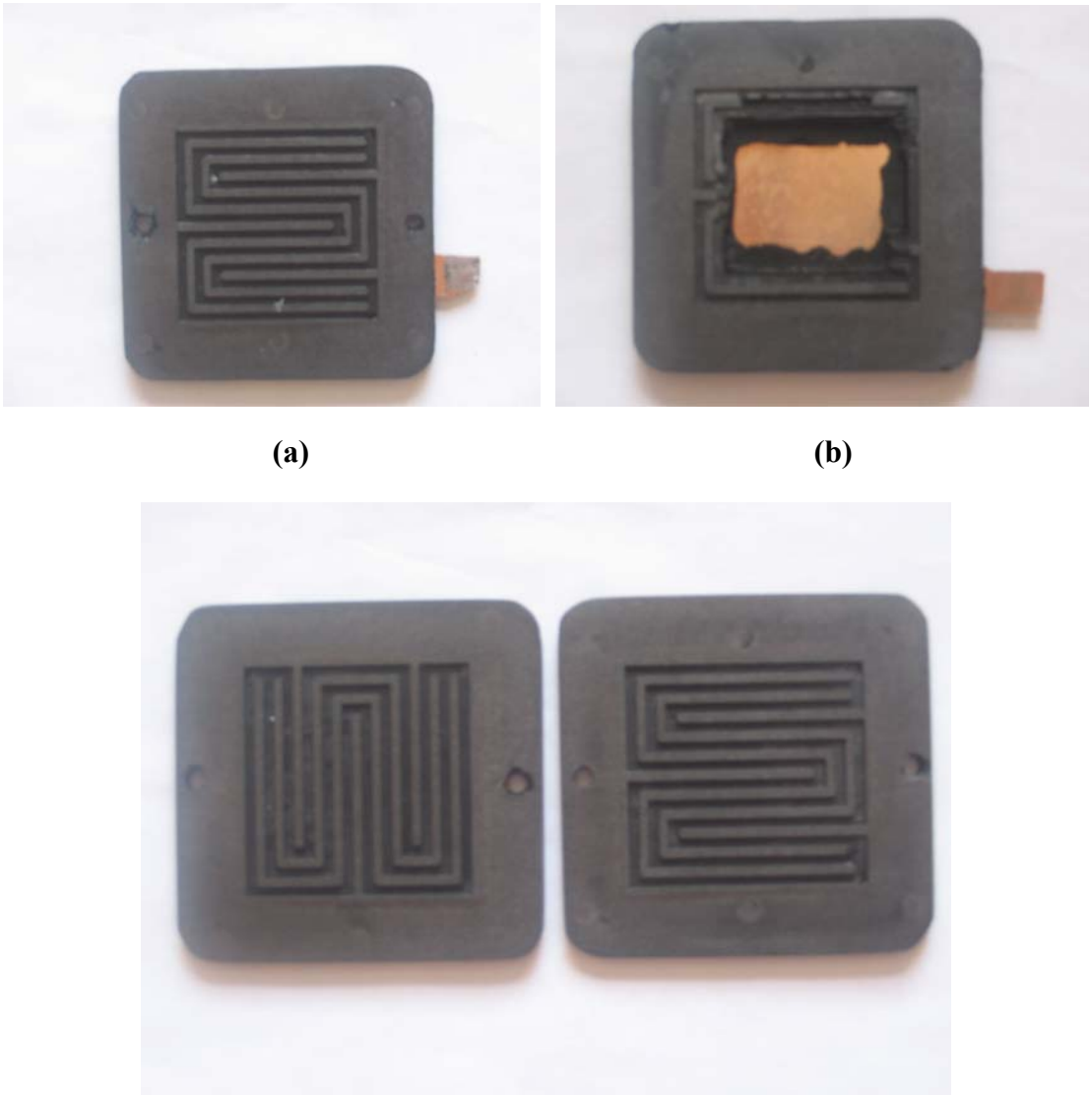

(a) **(b)**

(c)

Figure 3.32: Photographs of the compression-molded bipolar plate (single side) (a) With copper sheet insert (b) Inside of the copper sheet insert bipolar plate (c) With 1:1:1 SG-4012/VCB/CF composites

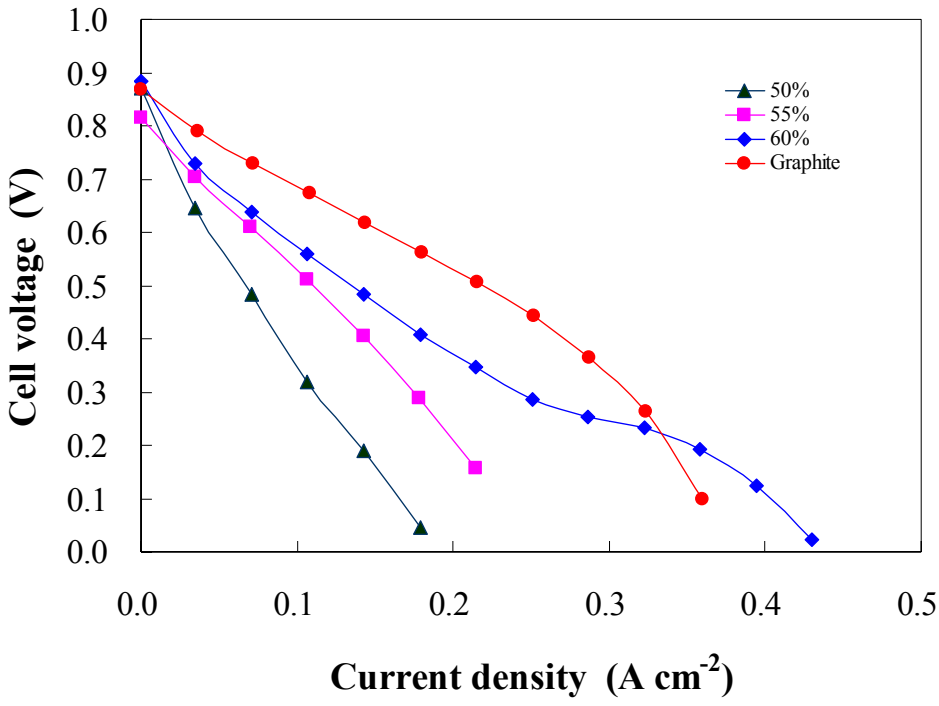

Figure 3.33: Comparison of *I-V* performance of graphite bipolar plate and 50%, 55% and 60% composite bipolar plates in a single cell test

At the cell voltage around 0.5 V, the current density of the single cells using graphite, 50%, 55% and 60% composite bipolar plates was 0.22, 0.14, 0.11 and 0.07 A cm^{-2}, respectively. The interesting phenomenon is the performance of single cell using 60% composite bipolar plate. When the current density reached 0.25 A cm^{-2}, the voltage of single cell decreased at a slower rate than before, and at the same voltage of 0.359 V, it exhibited a higher current density than a single cell using a graphite bipolar plate. This may indicated that the thermoplastic plate has better water removal characteristics either because of the nature of the GDL/plate interface or the surface energy of the material

allowing for easier water transport.

Figure 3.34 shows the distribution of power vs. current density for both graphite and composite bipolar plates. The maximum output power was 0.48, 0.80, 1.04 and 1.55W for 50%, 55% and 60% composite bipolar plate and graphite bipolar plate, respectively.

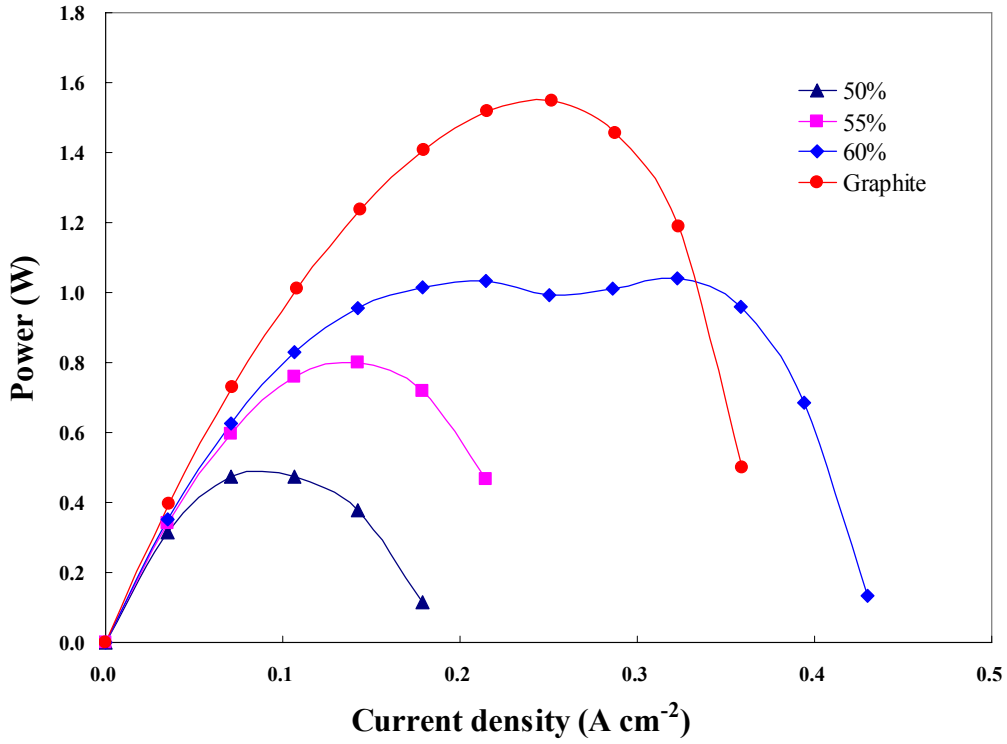

Figure 3.34: Comparison of performance of graphite bipolar plate and 50%, 55% and 60% composite bipolar plates in a single cell test

In this study, the performance of single cells using copper sheet insert composite bipolar

plates was also investigated, and compared with that of single cells using composites and graphite bipolar plates, see Figure 3.35 and Figure 3.36. Similar to the results shown in Figure 3.33 and 3.34, the OCV of single cells are almost the same at 0.8 V.

At low current density, all single cells exhibited the similar performance, however, with the increasing of current density, all the single cells using composite bipolar plates showed lower performance than the graphite plate cell. Compared to the single cells with composite bipolar plates, the performance of the copper sheet insert bipolar plate did show a certain degree of improvement, but it was not very significant. Even 55% copper sheet insert bipolar plate has a lower single cell performance than that of 60% composite plate. The possible reason is that the molding process (compression laminating) is not suitable for the copper sheet insert bipolar plate. Compression molding was applied to prepare samples; however, with the inspection of inside of plates (as shown in Figure 3.32-b), there is a gap between the copper sheet and composite plate, which may increase the contact resistance between those layers and lead to poor performance of the single cell using copper insert plates.

An alternative molding process was suggested for fabricating copper insert bipolar plates. For example, injection over-molding the copper sheet may lead to better performance of injection molded plates. This process would result in a molding process made under higher pressure which can significantly reduce the gap between copper sheet and

composite, there would be not resin 'skin' or film between the copper plate and the conductive composite (i.e. the conductive fill should be direct contact). Note that this trial also made use of a flat plate, and formed plate as shown in the above Figure 3.32-a would also reduce the conductive length through the conductive polymer, and then lower the resulting IR loss.

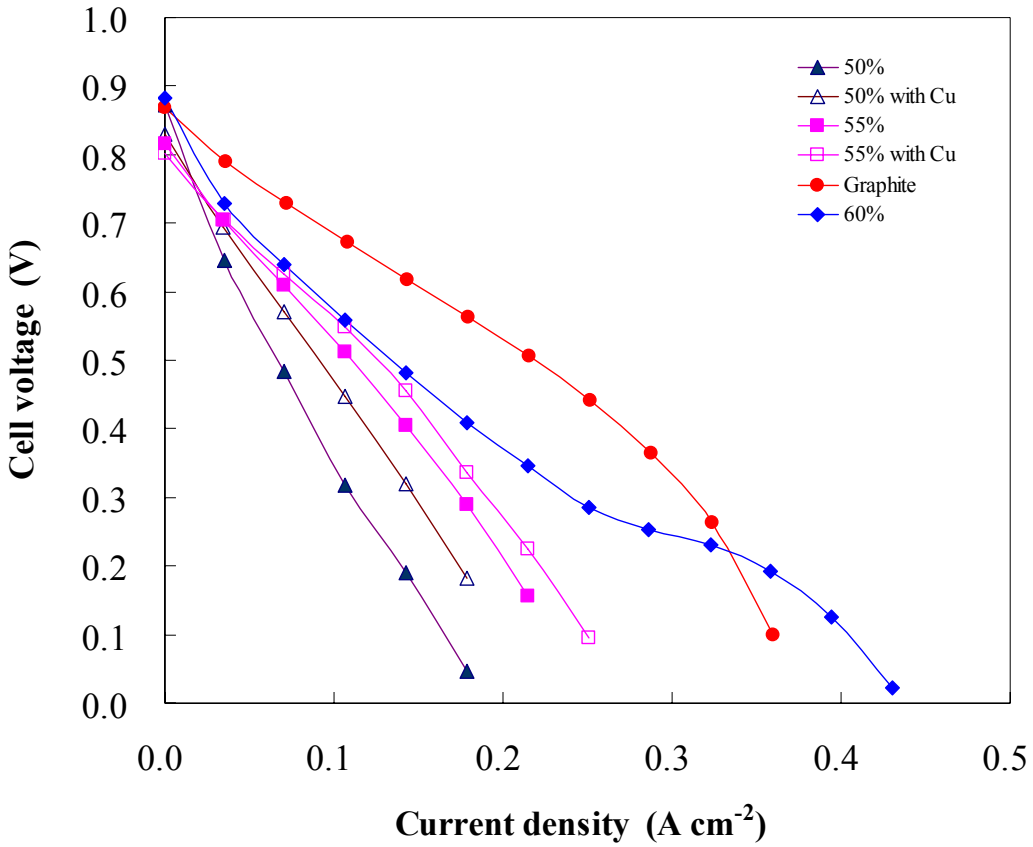

Figure 3.35: Comparison of *I-V* performance of graphite plate with composite and copper sheet insert composite bipolar plates in a single cell test

Figure 3.36 depicts that the maximum output power for graphite and composite bipolar plates, and copper insert composite bipolar plates. The results indicated a better performance for copper sheet insert composite plates in comparison to those without copper sheet insert. However, the graphite plate still exhibited the maximum output power density.

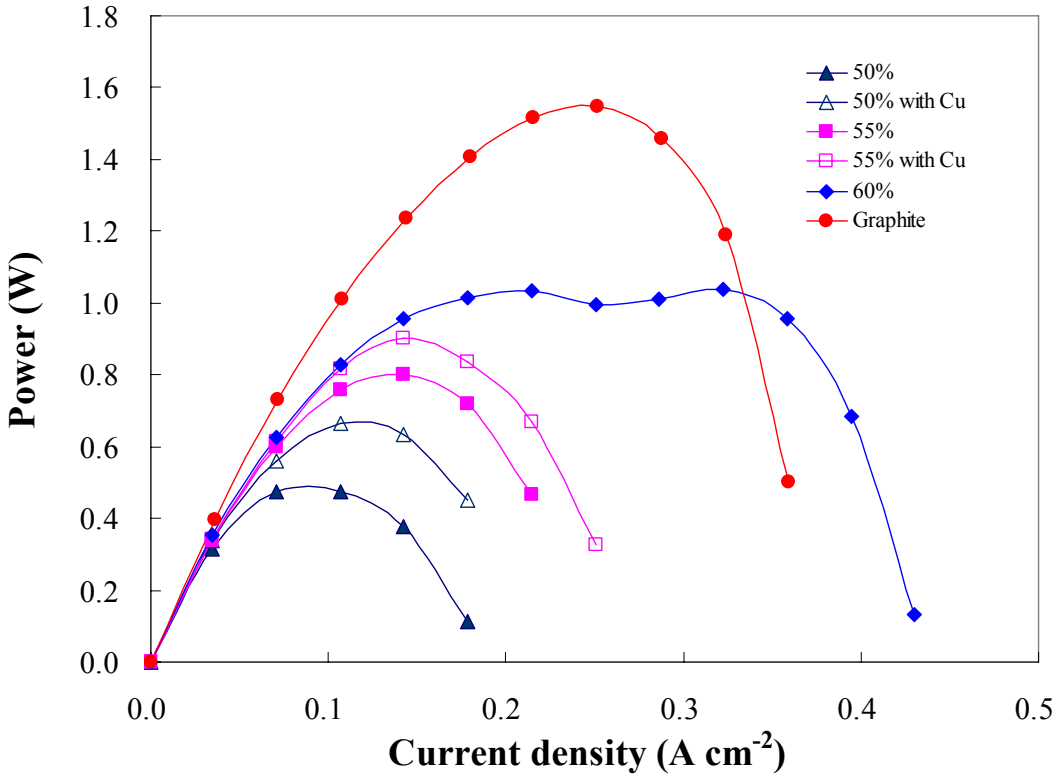

Figure 3.36: Comparison of performance of graphite plate with composite and copper sheet insert composite bipolar plates in a single cell test

3.4 Effect of Sample Dimensions on Conductivity Measurement

3.4.1 Introduction

As one of the most important properties of bipolar plates; electrical conductivity is important to identify possible factors that may have a significant effect on bipolar plate electrical resistance measurement techniques.

Contact resistance between the gas diffusion layer and the bipolar plate, and the sample's dimensional factors could have significant effects on plate resistance measurement, even when the bipolar plates are made of the same material. Sample dimensional factors include surface area (S), thickness (T), and ratio of surface area over thickness (S/T), while electrical contact resistances include the one between gas diffusion layer and the bipolar plate, and the one between gold plate and gas diffusion layer.

During this project, the effects of sample thickness T and surface area S on resistance of bipolar plates were investigated, as well as the effect of loading pressure applied in the testing system. Special attention was also devoted to reducing all interfacial contact resistances. Symbols and their definition used in this research are generalized in Table 3.9.

The bipolar plate samples chosen for this work were developed from previous work. The thermoplastic resin chosen was Equistar Polypropylene copolymer (Petrothene

PP36KK01), which is the same as the one applied in this project, and the conductive fillers are Vulcan carbon black(VCB), Acetylene carbon black(ACB) and Carbon fiber (CF) provided by Cabot Corporation, Chevron Phillips Chemical's and Fortafil, respectively. The specific conductive composite is made of 71% PP and 29% fillers with a ratio of VCB: ACB: CF at 21: 4: 4.

Table 3.9: Symbols and their definitions

Symbols	Definition
S	Surface area (mm^2)
T	Thickness (mm)
P	Clamping pressure (Psi)
R_{Meau}	Measured resistance
R_{Plate}	Resistance of bipolar plate sample
R_{GDL}	Resistance of Gas Diffusion Layer(GDL)
$R_{Au\text{-}Cu}$	Resistance of Gold-nickel-copper plate
$R_{Au/GDL}$	Contact resistance caused by an interface between GDL and gold plate
$R_{P/GDL}$	Contact resistance caused by an interface between GDL and bipolar plate sample

Each specimen was sandwiched between two gas diffusion layers, and the assembly was placed between two gold plates in a hydraulic press with loading forces up to 10,000 lbs during measurement. A constant current was passed through the two copper plates, and

the potential difference between the two copper plates was measured. Figure 3.37 illustrates the resistance components associated with the conductivity measurement for bipolar plate, and the resistances classification and nomenclature are summarized in Table 3.10

Table 3.10: Nomenclature and classification of resistances

Resistance	Nomenclature	Classification	Value
R_{Meau}	Measured Resistance	Total resistance	Depends on measured voltage and current
R_{Plate}	Resistance of sample plate	Sample	Depends on sample
R_{GDL}	Resistance of gas diffusion layer	GDL	Very Small
$R_{Au\text{-}Cu}$	Resistance of gold plate	Apparatus	Very Small
$R_{Au/GDL}$	Resistance caused by an interface of GDL and gold plate	Contact resistance	Varied
$R_{P/GDL}$	Resistance caused by an interface of GDL and bipolar plate	Contact resistance	Varied

From Figure 3.37, the total electrical resistance of the entire system is a summation of (1) the bulk resistance of the two gold plates, $2R_{\text{Au-Cu}}$, (2) the bulk resistance of two gas diffusion layers, $2R_{\text{GDL}}$, (3) the bulk resistance of bipolar plate, R_{Plate}, (4) the two interfacial contact resistances between gas diffusion layer and the bipolar plates, $2R_{\text{P/GDL}}$, (5) the two interfacial contact resistances between gold plate and gas diffusion layer, $2R_{\text{Au/GDL}}$. The expression for the total measured resistance for the assembly is given as:

$$R_{\text{Meau}} = V_{\text{Meas}} / I_{\text{Meas}}$$

$$= 2R_{\text{Au-Cu}} + 2R_{\text{GDL}} + 2R_{\text{P/GDL}} + 2R_{\text{Au/GDL}} + R_{\text{Plate}} \qquad (3.1)$$

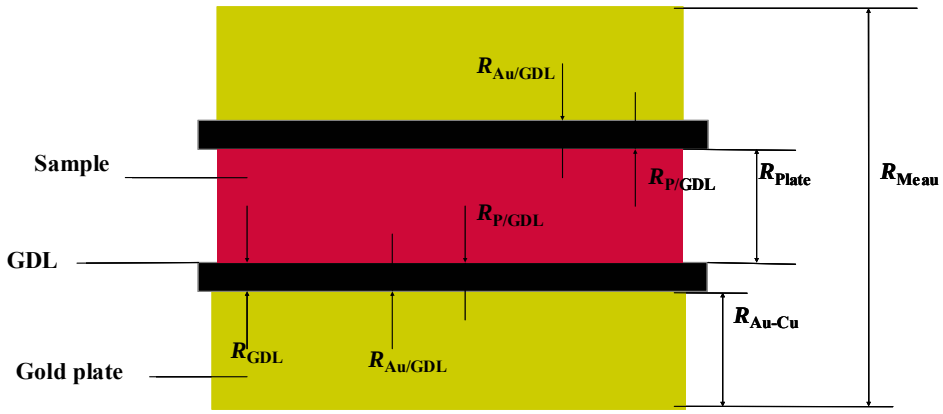

Figure 3.37: Schematic diagram of resistance measurement of bipolar plate

From Table 3.10, the values of R_{GDL} and $R_{\text{Au-Cu}}$ are very small (<<1), since the gas

diffusion layer and gold plate are very conductive. Therefore we can neglect the effect of R_{GDL} and $R_{Au\text{-}Cu}$ on the total measured resistance, R_{Meau}, and the Eqn. (3.1) can be simplified to Eqn. (3.2):

$$R_{Meau} = V_{Meas} / I_{Meas}$$
$$= 2R_{Au/GDL} + 2R_{P/GDL} + R_{Plate} \quad (3.2)$$

In Eqn. (3.2), the measured resistance, R_{Meau}, is determined by the contact resistance between the gas diffusion layer and the gold plate, $R_{Au/GDL}$, the contact resistance between the bipolar plate and gas diffusion layer, $R_{P/GDL}$, as well as the bulk resistance of the bipolar plate sample, R_{Plate}. If the values of the two contact resistances are as small as possible, the measured resistance essentially is equal to the bulk resistance of bipolar plate. In other words, the bulk resistance of bipolar plate can be accurately measured by minimizing the contact resistances in the testing system caused by the interface between the bipolar plate and gas diffusion layers and the interface between the gas diffusion layer and gold plates.

3.4.2 R_{GDL} and $R_{Au\text{-}Cu}$ Measurement

From Eqn. (3.1), in order to measure the bulk resistance of bipolar plates R_{Plate} accurately, the bulk resistances of the gold plates ($R_{Au\text{-}Cu}$) and gas diffusion layers (R_{GDL}) must be evaluated and subtracted from the total measured resistance of the assembly. $R_{Au\text{-}Cu}$ can

be determined by independent measurement involving only the two gold plates put together as shown in Figure 3.38 (a).

The bulk resistance of the gas diffusion layers, R_{GDL}, can also be determined by independent measurement involving only the gas diffusion layer sandwiched between the two gold plates shown in Figure 3.37 (b). Based on this new set up in Figure 3.37 (b), the total measured resistance, R'_{Meau}, is expressed in Eqn. (3.3).

$$R'_{Meau} = V'_{Meas} / I'_{Meas}$$
$$= 2\,R_{Au\text{-}Cu} + 2R_{Au/GDL} + R_{GDL} \qquad (3.3)$$

If we subtract R'_{Meau} from the total measured resistance, R_{Meau}, then Eqn. (3.3) is further expressed as:

$$R_{Meau} - R'_{Meau} = R_{GDL} + 2R_{P/GDL} + R_{Plate} \qquad (3.4)$$

According to the testing results as showed in Table 3.11, the average value of $R_{Au\text{-}Cu}$ is only $3.2 * 10^{-6}$ ohm, which is insignificant with respect to the total resistance of the system and is therefore negligible.

Table 3.11: Testing results of resistance of gold plate (R_{Au-Cu})

Resistance (Ω)	#1	#2	#3	Ave.
R_{Meau}	0.0000055	0.0000068	0.0000072	0.0000065
R_{Au-Cu}	0.0000027	0.0000034	0.0000036	0.0000032

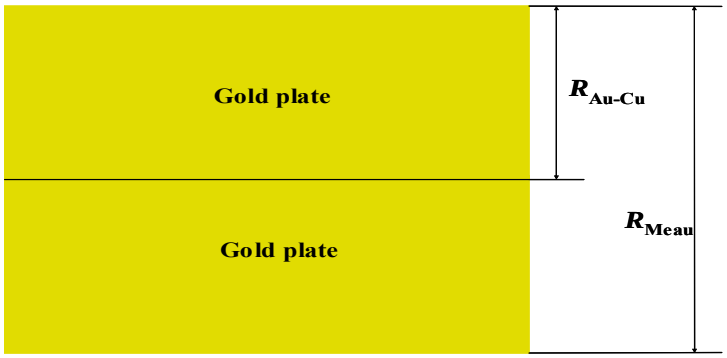

(a)

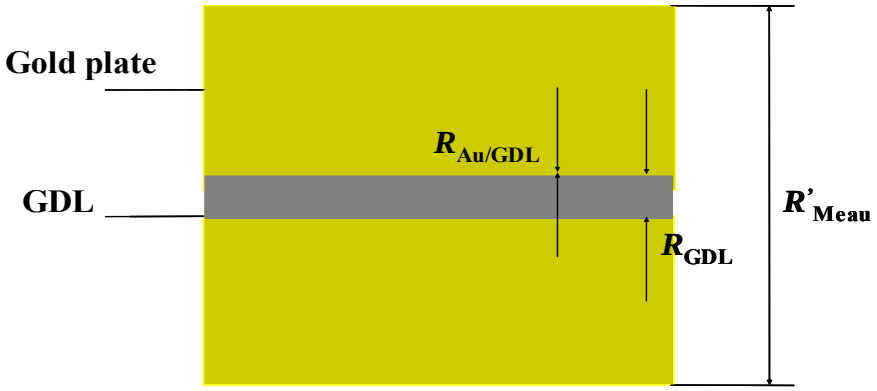

(b)

Figure 3.38: (a) Schematic diagram of resistance measurement analysis of gold plate and (b) gas diffusion layer

For a piece of gas diffusion layer with a dimension of 100.43 mm*100.35 mm*0.42 mm, sandwiched between two gold plates with a series of loading forces, the measured resistances for this arrangement are shown in Table 3.12. The resistance data are in the range of $2.1*10^{-5} \sim 8.4*10^{-5}$ Ω, which are very low values compared to the total resistance experienced in actual fuel cell operation environments.

Table 3.12: Resistance measurement of GDL (R_{GDL})

GDL Dimensions	Force (lbs)	Pressure (Psi)	R_{GDL}(Ω)
Length: 100.43mm **Width:** 100.35mm **Thickness**: 0.42mm	1000	64	0.000084
	2000	128	0.000056
	3000	192	0.00042
	4000	256	0.000035
	5000	320	0.000021

Based on the values of R_{GDL} and $R_{Au\text{-}Cu}$, the contributions of R_{GDL} and $R_{Au\text{-}Cu}$ to the total measured resistance of bipolar plate assembly are negligible. Moreover, since gas diffusion layers are highly conductive materials compared to the bipolar plates, the contribution of bulk resistance of the gas diffusion layer can also be regarded as negligible within the resistance measurement assembly. As a result, Eqn. (3.4) is further simplified to:

$$R_{\text{Meau}} \approx 2R_{\text{P/GDL}} + R_{\text{P}} \qquad (3.5)$$

In Eqn. (3.5), the total measurement resistance of bipolar plates and gas diffusion layer assembly is the summation of (1) the bulk resistance of bipolar plate, R_{Plate}, (2) the two interfacial contact resistances between gas diffusion layer and bipolar plate, $2R_{\text{P/GDL}}$. It is obvious that except for the intrinsic bulk electrical resistance of the bipolar plate, R_{Plate}, the interfacial contact resistances between the gas diffusion layer and bipolar plate, $2R_{\text{P/GDL}}$, also have a significant effect on the total measured resistance. Hence, it is very important to identify the factors that affect the $R_{\text{P/GDL}}$, and to minimize the effect of interfacial contact resistance on the total measured resistance.

3.4.3 Effect of Surface Area (S) on Bipolar Plate Conductivity

Figure 3.39 shows the total resistance as a function of surface area for GDL/Bipolar plate assembly, where bipolar plates have various thicknesses and the applied loading force is 5000 lbs.

With increasing surface area, the measured resistance (Ω) is decreased. As the surface area increases, the contact area between the GDL and bipolar plate increases correspondingly. In this case, the contribution of interfacial contact resistance between the GDL and bipolar plate becomes more significant than that of the bulk resistance of bipolar plate with respect to the total measured resistance. With increasing surface area,

the bulk resistance of the bipolar plate is decreased, which lead to the decrease of the total measured resistance of system. It seems that as the contact area or surface area of bipolar plate reaches infinity, the bulk resistance can become negligible (based on Eqn.1) and the total measured resistance can be regarded as that of the two interfacial contact resistances between gas diffusion layers and bipolar plates.

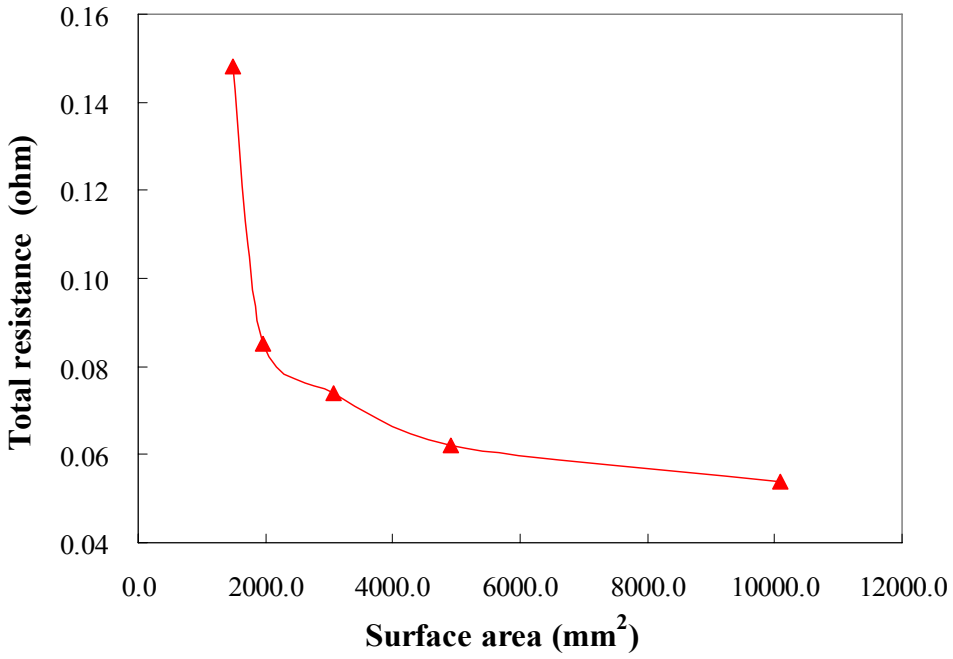

Figure 3.39: Total measured resistance with surface area for gas diffusion layer and bipolar plate assembly

3.4.4 Effect of Thickness (T) on Bipolar Plate Conductivity

The effect of thickness on resistance measurement was also investigated in this work. With the same surface area, the resistances of bipolar plates with different thicknesses

were measured. Figure 3.40 shows the bipolar plate resistances as a function of thickness for samples with the same surface area. The measured resistance increases with increasing thickness of the bipolar plate, contributing to increased bulk resistance. The sum of the bulk resistances and the two contact resistances between the bipolar plate and gas diffusion layer, R_{plate} and $2R_{P/GDL}$, forms the dominant part of the total resistance shown in Figure 3.40. The lower value of R_{meau} corresponds to the thinner bipolar plate, 0.8mm, and the higher R_{meau} value corresponds to the bipolar plate with 4.70mm thickness. In this case, the bulk resistance of the bipolar plate has a more significant contribution to the total measured resistance than the contact resistance. However, if the thickness of the bipolar plate is as thin as possible, similarly, the bulk resistance is also negligible, and the measured resistance is equal to the two contact resistances between the GDL and bipolar plate.

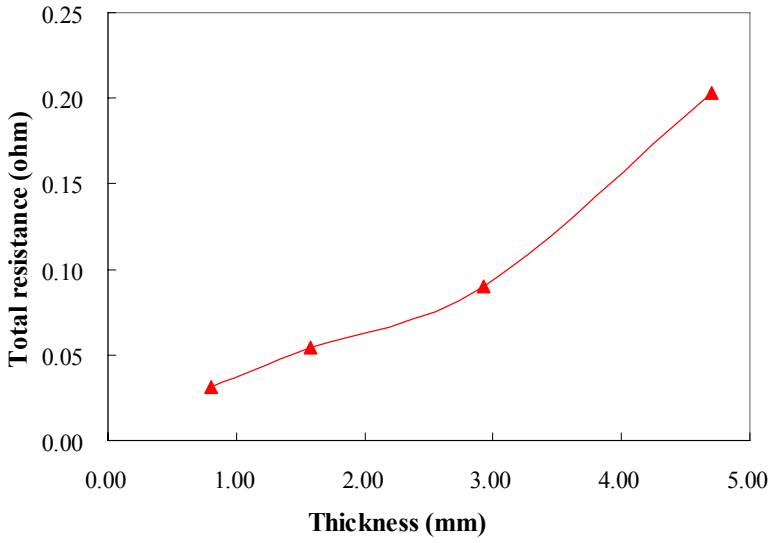

Figure 3.40: Thicknesses effect on resistance of bipolar plates

3.4.5 Effect of S/T on Bipolar Plate Conductivity

Figure 3.41 represents the resistance of the GDL/bipolar plate assembly as a function of the ratio of surface area over thickness (S/T). With increasing S/T, the measured resistance (Ω) is decreasing. This tendency is similar to that of Figure 3.39 in which the measured resistance decreases with increasing surface area. Similarly, with increasing S/T, the bulk resistance of the bipolar plate will decrease significantly, and the contact resistance between the gas diffusion layer and bipolar plate has more contribution on the total measured resistance. It is clear that due to the geometry difference of the various bipolar plates, the measured resistance can be significantly different. If there were procedures recommending plate geometry it would be much easier to successfully compare conductivity results between different composite materials.

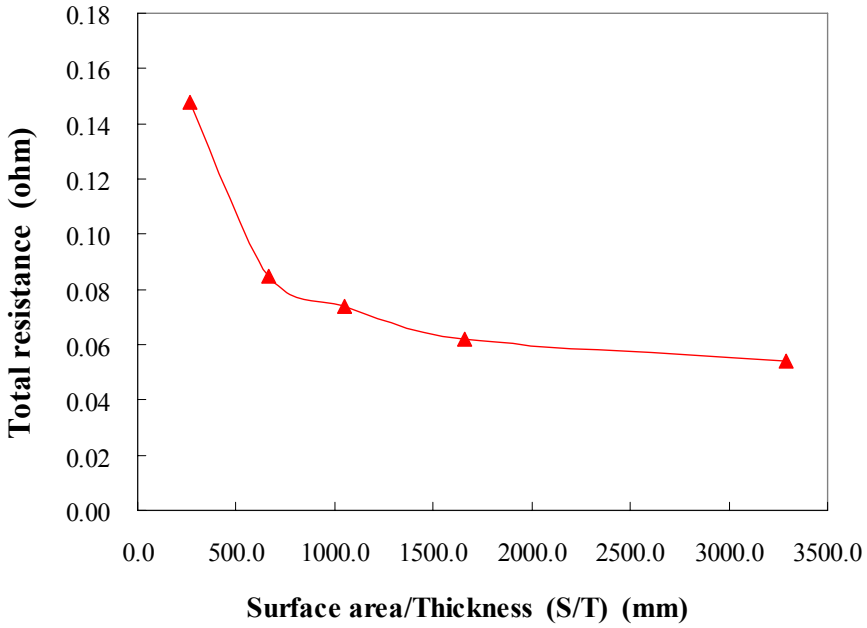

Figure 3.41: Resistance of GDL/bipolar plate assembly at various sizes and S/T

3.4.6 Effect of Clamping Pressure on Bipolar Plate Conductivity

The resistances of the bipolar plates were also measured at conditions with different loading forces. Forces applied to the interface leads to the increase in the contact area between the bipolar plate and gas diffusion layer, which in turn decreases the interfacial contact resistances.

Loading forces that were applied include 1000, 2000, 3000, 4000 and 5000 lbs respectively. The converted applied pressures vary depending on force and sample dimensions. The measured resistance results are shown in Figure 3.42.

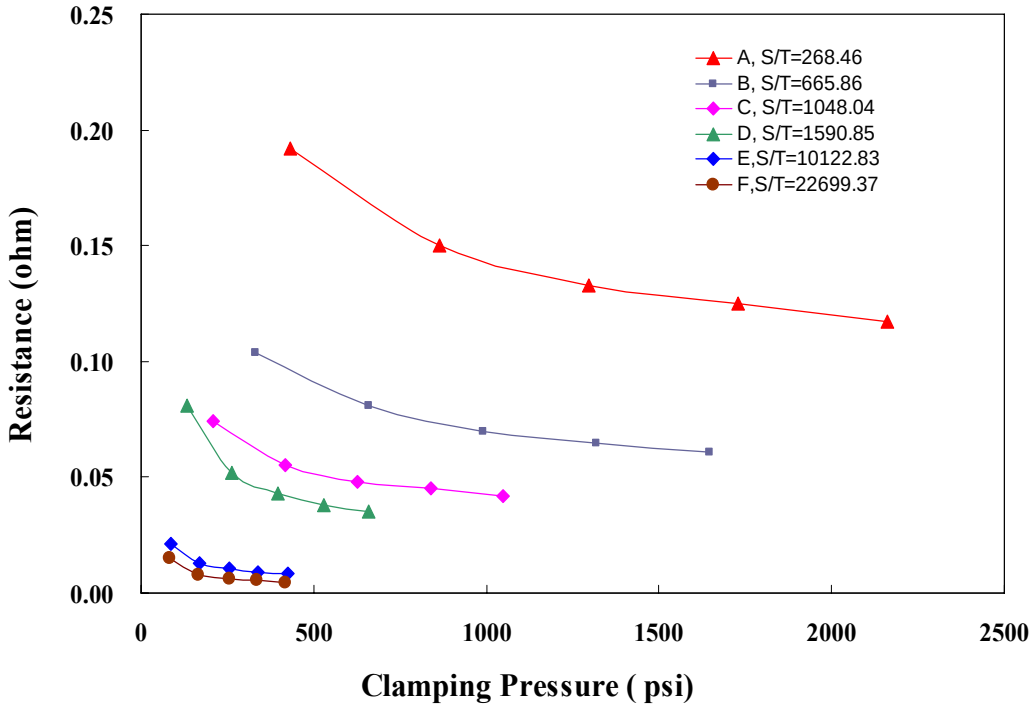

Figure 3.42: Effect of clamping pressure on measured resistance

As expected, the measured resistance decreases with increasing clamping pressure for all bipolar plate samples with different ratio of surface area over thickness (S/T). The highest resistance was observed for the bipolar plate with smaller S/T ratios (for example, S/T=268.46 mm). For a wide range of clamping pressures the change in measured resistance is not very significantly. While with increasing S/T values (from 268.46 mm to 22699.37 mm), the measured resistance decreases dramatically, in other words, the higher value of S/T, the lower the resistance measured.

Additionally, for higher S/T ratios, the measured resistance can be decreased over a narrow range of clamping pressures. In the case of bipolar plates with higher values of S/T, the contribution of contact resistance between the gas diffusion layer and the bipolar plate to the measured resistance is more significant than the bulk resistance of bipolar plate. The contact resistance between the gas diffusion layer and bipolar plate with unknown conductivity can be estimated as S/T reaches very large (infinite) values, which in turn can enable the actual bulk resistance of the bipolar plate to be measured accurately.

Chapter 4: Conclusions and Recommendations

4.1 Conclusions

With proper selection of polymer matrix and conductive fillers, the development of thermoplastic conductive bipolar plates for PEM fuel cells has been demonstrated. As one of the most important components for a PEM fuel cell, the conductivity of bipolar plates needs to be improved if a thermoplastic plate can be successfully implemented. However, the development of thermoplastic plates remains of interest as there is a need to reduce the weight and costs of bipolar plates for successful commercialization of PEM fuel cells.

In this project, the synergetic effect of different conductive fillers on composite conductivity has been investigated. The conductive fillers investigated for this project were: the three kinds of synthetic graphite with different size, Vulcan carbon black, and carbon fiber. Study results showed that three-filler composites exhibit better performance than single or two-filler composites. It was found that 1:1:1 SG-4012/VCB/CF composites showed better performance than other blends. The highest conductivity was obtained with a 65% fill level 1:1:1 SG-4012/VCB/CF composite, specifically 1900 S/m in in-plane and 156 S/m in through-plane conductivities were obtained, respectively. At 65% filler level, mechanical properties as Young's modulus, tensile strength, flexural strength and flexural modulus for 1:1:1 SG-4012/VCB/CF composite were 584.3 MPa,

9.50 MPa, 47.7 MPa and 6.82 GPa, respectively, and these results meet with mechanical properties requirement for bipolar plates. The highest density for bipolar plate materials developed during this project was 1.33 g/cm^3 and is far less than that of graphite bipolar plate, thus some weight reduction in the fuel cell stack can be expected.

A novel development of the use of a metal insert bipolar plate was also investigated during this project. With metal mesh or copper sheet inserts, there was very limited improvement shown in through-plane conductivity; however, in-plane conductivity of metal insert bipolar plate was improved significantly, and the highest in-plane conductivity (891,084 S/m) was obtained by 65% 1:1:1 SG-4012/VCB/CF composite. From the result one can envision the development of bipolar plates with metal inserts for high conductivities, and low cost injection molded flow field paths.

The performance of composite and copper sheet insert bipolar plates was investigated in a single cell fuel cell testing. From current-voltage polarization (*I-V*) curves, all the composites bipolar plates showed lower performance than graphite bipolar plate. Although the copper sheet insert bipolar plates are very conductive in in-plane conductivity, there were limited improvements in a single cell performance compared to composite bipolar plates.

During this work, the significance of contact resistance between the plate and GDL

materials was identified. Investigation was then conducted with the aim to understand the relative significance of contact resistance to bulk conductivity, which is important for fuel cell bipolar plate design and material selection. This work therefore conducted a specific investigation into the factors and procedures affecting bipolar plate resistance measurements. Bipolar plate surface area (S) and surface area over thickness (S/T) ratio were found to show significant effects on the interfacial contact resistances. At high S/T ratio, the contact resistant was most significant. Other factors such as thickness, material properties, surface geometry and clamping pressure also were found to affect the bipolar plate resistance measurements significantly.

4.2 Challenges and Recommendations

Research into the development of thermoplastic conductive bipolar plates is still at a developmental stage, and the biggest challenge remains to improve polymer composite conductivity. The possible suggestions are discussed in the section below:

- **Polymer matrix selection**

  The polymer matrix applied in this project was a Polypropylene with MFI of 7. Since higher filler loadings are required for improving the composite conductivity, the use of polymers with a higher melt flow index value may be a more promising choice to achieve high dispersion of conductive fillers within polymer matrix. Other choices of polymers, such Nylon, PE or PPS could be considered in future research

efforts. A small amount of rubber or elastomer additive in the process of compounding could be investigated in the future for reducing composite brittleness especially with high filler loading.

- **Processing agent or dispersion agent**

  SEM pictures of the composite materials developed during this project showed agglomeration of carbon black within polymer matrix. This agglomeration could be one reason for relative low conductivity of composites. With proper selection of processing agent or dispersion agent, the degree of conductive fillers agglomeration within polymer matrix could be reduced.

- **Conductive filler selection**

  This work has shown that different shape and size conductive fillers can affect conductivity of composite. The different aspect ratios of carbon fibers could be investigated. Carbon nano-fibers could be a possible choice for improving composite conductivity with a small amount of additional fill material.

- **Sample prototype for metal insert bipolar plate**

  The work has shown that metal insert bipolar plates exhibit very high in-plane conductivity results; however, their performance in a single cell testing was not as encouraging. The reason for this could be that the molding method (i.e. compression

molding) for prototyping the metal insert bipolar plates was not suitable, and injection over molding metal sheet is suggested in future research.

References

1. U.S. Fuel Cell Council, *Fuel Cell Glossary*, **1999**, August 19
2. O. Savadogo, *J. New. Mater. Electrochem. Syst.*, **1998**, 1, 47
3. J.M. King, M.J. O' Day, "Applying fuel cell experience to sustainable power products", *J. of Power Sources*, **2000**, 86, 16-22
4. D.P. Davies, P.L. Adcock, M. Turpin, S.J. Rowen, "Bipolar plate materials for solid polymer fuel cells", *J. of Applied Electrochemistry*, **2000**, 30(1), 101-105
5. I. Bar-On, R. Kirchain, R. Roth, "Technical cost of analysis for PEM fuel cells" *J. of Power Source,* **2002**, 109(1), 71-75
6. J. Larminie, A. Dicks, *Fuel Cell Systems Explained,* Wiley, West Sussex, UK, **2000**
7. M.J. Ajersch, M.W. Fowler, *Fuel Cell Science, Engineering and Technology,* **2003**
8. V. Mehta, J.S. Cooper, "Review and analysis of PEM fuel cell design and manufacturing", *J. of Power Sources*, **2003**, 114, 32-53
9. *Fuel Cell Handbook (Sixth Edition)*, EG & G Technical Services, Inc. Science Applications International Corporation, **2002**
10. A. Hermanna, T. Chaudhuria, P. Spagnolb, *International Journal of Hydrogen Energy*, **2005**, 30, 1297 -1302
11. D. Busick, M. Wilson, in: D.H. Doughty, L.F. Nazar, M. Arakawa, H. Brack, K. Naoi (Eds.)**,** *New Materials for Batteries and Fuel Cells*, Materials Research Society Symposium Proceedings, Pennsylvania, Materials Research Society, **2000**, 575, 247-251
12. K. Robberg, V. Trapp, in: W. Vielstich, H.A. Gasteiger, A. Lamm (Eds.), *Handbook of Fuel Cells—Fundamentals, Technology and Applications*, vol. 3: Fuel Cell

Technology and Applications, Willey & sons, New York, **2003**, 286-293

13. R.L. Borup, N.E. Vanderborgh. *Mater. Res. Soc. Symp. Proc.*, **1995**, 393, 151-155
14. A. Kumar and R.G. Reddy, "Fundamentals of Advanced Materials for Energy Conversion," Eds. D. Chandra and R.G. Bautista, TMS, Warrendale, **2002**, 41
15. Y. Hung, K.M. El-Khatib, H. Tawfik, "Corrosion-resistant lightweight metallic bipolar plates for PEM fuel cells", *J. of Applied Electrochemistry*, **2005**, 35, 445-447
16. Y. Hou, M. Zhang, M. Rong, "Improvement of Conductive Network Quality in Carbon Black-Filled Polymer Blends", *J. of Appl. Polym. Sci.*, **2002**, 84, 2768 - 2775
17. T.M. Besmann, J.W. Klett, T.D. Burchellet, "Carbon/Carbon Composite Bipolar Plate for Proton Exchange Membrane Fuel Cells", *J. of Elec. Soc*., **2000**, 147 (11), 4083-4086
18. R. Hornung and G. Kappelt, "Bipolar plate materials development using Fe-based alloys for solid polymer fuel cells", *J. Power Sources*, **1998**, 72, 20
19. D.P. Davies, P.L. Adcock, M. Turpin, S.J. Rowen, "Stainless steel as a bipolar plate material for solid polymer fuel cells"**,** *J. of Power Sources*, **2000**, 86, 237
20. R.C. Makkus, A.H.H. Janssen, F.A. de Bruijn, R.K.A.M. Mallant, "Use of stainless steel for cost competitive bipolar plates in the SPFC", *J. of Power Sources*, **2000**, 86, 274
21. J. Wind, A. LaCroix, S. Braeuninger, P. Hedrich, C. Heller, M. Schudy, in: W. Vielstich, H.A. Gasteiger, A. Lamm (Eds.), *Handbook of Fuel Cells—Fundamentals, Technology and Applications*, vol. 3: Fuel Cell Technology and Applications, Willey & sons, New York, **2003**, 294 - 307
22. D.G. Baird, J.H. Huang, J.E. McGrath, *Plastic Engineering*, **2003**, 59 (12), 46-55

23. A.S. Woodman, E.B. Anderson, K.D. Jayne, and M.C. Kimble, "Development of Corrosion Resistant Coatings for Fuel Cell Bipolar Plates", *American Electroplaters and Surface Finishers Society, AESF SUR/FIN '99 Proceedings*, **1999**

24. D.P. Davies, P.L. Adcock, M. Turpin, S.J. Rowen, "Bipolar plate materials for solid polymer fuel cells", *J. of Appli. Electro.,* **2000**, 30(1), 101-105

25. J. Wind, A. LaCroix, S. Braeuninger, P. Hedrich, C. Heller, M. Schudy, in: W. Vielstich, H.A. Gasteiger, A. Lamm (Eds.), *Handbook of Fuel Cells—Fundamentals, Technology and Applications*, vol. 3: *Fuel Cell Technology and Applications*, Willey & sons, New York, **2003**, 294 -307

26. S. Lee, C. Huang, Y. Chen, C. Hsu, *J. of Fuel Cell Science and Technology*, **2005**, 2, 291

27. J. Huang, D.G. Baird , J.E. McGrath, "Development of fuel cell bipolar plates from graphite filled wet-lay thermoplastic composite materials", *J. of Power Sources*, **2005**, 150, 110 –119

28. K. Robberg, V. Trapp, in: W. Vielstich, H.A. Gasteiger, A. Lamm (Eds.), *Handbook of Fuel Cells—Fundamentals, Technology and Application*s, vol.3: Fuel Cell Technology and Applications, Wiley & Sons, New York, **2003**, 308-314.

29. H. Kuan, C.M. Ma, K.H. Chen, S. Chen, "Preparation, electrical, mechanical and thermal properties of composite bipolar plate for a fuel cell", *J. of Power Sources*, **2004**, 134, 7 -17

30. F. Mighri, M.A. Huneault, "Electrically Conductive Thermoplastic Blends for Injection and Compression Molding of Bipolar Plates in the Fuel Cell Application", *Polymer Engineering and Science*, **2004**, 44 (9), 1755 -1765

31. M. Lee, L. Chen, "The Development of a Heterogeneous Composite Bipolar Plate of a Proton Exchange Membrane Fuel Cell", *J. of Fuel Cell Science and Technology*, **2005**, 2, 14 -19
32. http://www.azom.com/details.asp?articleID=2484
33. http://www2.dupont.com/Automotive/en_US/products_services/engineeringPlastics/zeniteLCP.html
34. H. Wolf, M. Willert-Porada, "Electrically conductive LCP–carbon composite with low carbon content for bipolar plate application in polymer electrolyte membrane fuel cell", *J. of Power Sources*, **2006**, 153, 41 - 46
35. Y. Agari, T. Uno, **"**Thermal conductivity of polymer filled with carbon materials: Effect of conductive particle chains on thermal conductivity", *J. Appl. Polym. Sci*., **1985,** 30, 2225
36. R.M. Simon, *Polym. News*, **1985,** 11, 102
37. D.M. Bigg, *Polym. Eng. Sci.*, **1977**, 17, 842
38. M.L. Clingerman, E.H. Weber, J.A. King, K.H. Schulz, "Development of an Additive Equation for Predicting the Electrical Conductivity of Carbon-Filled Composites", *J. of Appl. Polym. Sci.*, **2003**, 88, 2280 - 2299
39. X. Jing, W. Zhao, L. Lan, *J. Mater. Sci. Lett.*, **2000**, 19, 377
40. H.S. Gokturk, T.J. Fiske, D.M Kalyon, **"**Effects of particle shape and size distributions on the electrical and magnetic properties of nickel/polyethylene composites", *J. Appl. Polym. Sci.*, **1993**, 50, 1891
41. J.Y. Yi, G.M. Choi, *J. Electroceram.*, **1999**, 3, 361
42. E.P. Mamunya, V.V. Davidenko, E.V. Lebedev, *Compos. Interfaces*, **1997**, 4, 169

43. E.P. Mamunya, V.F. Shumskii, E.V. Lebedev, *Polym. Sci.*, **1994**, 36, 835

44. R.H.J. Blunk, D.J. Lisi, "Enhanced conductivity of fuel cell plate through controlled carbon fiber orientation", *AICHE Journal*, **2003**, 49, No. 1

45. R.H.J. Blunk, C.L. Tucker, Y. Yeong-Eun, and D.J. Lisi, "Fuel Cell Separator Plate Having Controlled Fiber Orientation and Method of Manufacture," U.S. Patent Application No. USSN 09/871,189 (filed May 31, 2001a)

46. R.H.J. Blunk, M.H. Abd Elhamid, Y.M. Mikhail, and D.J. Lisi, "Low Contact Resistance PEM Fuel Cell," U.S. Patent Application No. USSN 09/997,190 (filed Nov. 20, 2001b)

47. Y. Zou, J. Zhang, J. He, Y. Zheng et. al., "A Study of a composite bipolar plate for PEMFC", *New Carbon Materials*, **2004**, 19, 303-307

48. J. Zhang, Y. Zou, J. He, "Influence of graphite particle size and its shape on performance of carbon composite bipolar plate", *J. of Zhejiang University Science*, **2005**, 6A(10), 1080-1083

49. F.R. Spinelli, "Conductive Carbon Black", in *Plastics Additives and Modifiers Handbook*, Chap. 47, J. Edenbaum ed., Chapman & Hall, New York, **1996**, 615-643

50. G. Geuskens, J.L. Gielens, D. Geshef, R. Deltour, *Eur. Polym. J.*, **1987**, 23, 993

51. J. Scholta, B. Rohland, V. Trapp, U. Focken, **"**Investigation on novel low-cost graphite composite bipolar plate", *J. of Power Source,* **1999,** 84, 231-234

52. http://www.incosp.com/novamet_products/graphite_powders/

53. M.S. Dresselhaus, G. Dresselhaus, K. Sugihara, I.L. Spain, H.A. Goldberg, *Graphite Fibers and Filaments*, Springer Series in Materials Science, New York, **1988**.

54. B.E. VerWeyst, C.L. Tucker, P.H. Foss, J.F. O'Gara, "Fiber Orientation in 3-D

Injection Molded Features: Prediction and Experiment", *Int. Polymer Processing,* **1999**, 14, 409

55. L. Song, M. Xiao, X. Li, Y. Meng, "Short carbon fiber reinforced electrically conductive aromatic polydisulfide/expanded graphite nano-composites", *Materials Chemistry and Physics*, **2005**, 93, 122–128
56. U.S. Fuel Cell Council, **2003**. Electrical Conductivity Testing Protocols Task Force Draft Guidelines, Materials & Components Working Group
57. N. Cunningham and M. Lefevre, "Measuring the through-plane electrical resistivity of bipolar plates (apparatus and methods)", *J. of Power Sources*, **2005**, 143, 93-102
58. H.L. Wang, M.A. Sweikart, John A. Turner, "Stainless steel as bipolar plate material for polymer electrolyte membrane fuel cells", *J. of Power Sources*, **2003**, 115, 243-251
59. V. Mishra, F. Yang, R. Pitchumani, "Measurement and Prediction of Electrical Contact Resistance Between Gas Diffusion Layers and Bipolar Plate for Applications to PEM Fuel Cells", *J. of Fuel Cell Science and Technology*, **2004**, Vol. 1 / 3
60. L.J. Blomen, M.N. Mugeroa, *Fuel cell system*., New York: Plenum; **1993**
61. S. Kundu, "Structure-Property-Performance Relationships in Fuel Cell Materials", Masters Thesis, Chemical Engineering, University of Waterloo, August **2004**
62. Equistar, Petrothene Data Sheet, http://www.equistarchem.com/htm1/polymer/polyproplyene/Impact_IM.htm
63. Equistar, Petrothene Material Safety Data Sheet, http://www.equistarchem.com/html/polymer/polypropylene/Impact_IM.htm
64. Cabot, Carbon Black Vulcan XC72 Data Sheet,

http://www.cabot-corp.com/cws/product.nsf/PDSDOCKEY/~~~VXC72?OpenDocument&bc=Products+%26+Markets/Carbon+Black/Data+Sheets+%26+MSDS&bcn=23/4294967220/3033&entry=product

65. Fortfail Carbon fiber Data Sheet, as provided with material
66. Asbury Synthetic graphite Data Sheet, as provided with material
67. Nickel coated graphite Data Sheet, http://www.incosp.com/novamet_products/graphite_powders/
68. AvCarb™ 1071 Data Sheet, http://www.avcarb.com/
69. Stat Ease's DESIGN EXPERT 6.0 software package User Guide
70. T. Mali, M.W. Fowler, M. Stevens, C. Tzoganakis, L. Simon, "Advanced Material Testing of Thermoplastic Composite Bipolar Plats for Polymer Electrolyte Membrane Fuel Cells (PEMFC)", **2005**, University of Waterloo.

Appendix

Appendix 1: Properties of Petrothene PP36KK01 Polypropylene

Table 1: Properties of Petrothene PP36KK01 Polypropylene

Property	Nominal Value	Units	ASTM Test Method
Melt Flow Rate	70	g/10 mins	D 1238
Tensile Strength @yield	3200 (22.0)	Psi (MPa)	D 638
Elongation @ Yield	6	%	D 638
Flexural Modulus	160,000 (1100)	Psi (MPa)	D790
Izod Impact, Notched @23 ℃	9.5 (500)	ft-lb/in (J/m)	D 256
Izod Impact, Notched @-18 ℃	1.4 (75)	ft-lb/in (J/m)	D 256
unnotched @-18 ℃	31 (1655)	ft-lb/in (J/m)	D 4812
Gardner Impact @-18 ℃	320 (36)	in-lb (J)	D 5420
Rockwell Hardness	78	R	D 785
Heat Deflection @ 66 psi	73 (163)	℃ (℉)	D 648
Heat Deflection @ 264 psi	56(134)	℃ (℉)	D 648
Specific Gravity	0.89-0.91		

Appendix 2: Physical and Chemical Properties of Cabot VulcanXC72

Appearance	Black Pellets (VulcanXC 72)
Odor	None
PH	4-11 [50g/l water, 68℉(20℃)](non-oxidized carbon black 2-4 (oxidized carbon black)
Vapor Pressure	Not determined
Boiling Point/Range	Not applicable
Melting Point/Range	Not applicable
Water solubility	Insoluble
Density	1.7 -1.9 g/cm^3 @ 20℃
Bulk Density	20-550 kg/m^3
Specific Gravity	Not determined
Mean Particle Size	30 nm
% Volatile (by weight)	< 2.5% @ 950℃(non-oxidized carbon black) 2-11% (oxidized carbon black)

Appendix 3: Properties of Fortafil 243 Chopped Carbon Fiber from Fortafil Carbons

Specifications	**English**	**SI**
Tensile Strength	>500 ksi	>3450 MPa
Tensile Modulus	>30.0 Msi	>207 GPa
Ultimate Elongation	1.7%	1.7%
Density	0.0065 lb/in^2	1.8 g/cm^3
Cross-sectional Area/Filament	$4.7 * 10^{-8}$ in^2	$3.3 * 10^{-5}$ mm^2
Filament Shape	Round	/
Filament Diameter	$0.24 * 10^{-3}$ in^2	6 microns
Electrical Resistivity	/	1.67 mOhm-cm
Physical Form	Flakes	/

Appendix 4: Properties of nickel-coated graphite from Inco-Novamet

NOVAMET® Nickel-Coated Graphite

(25%, 60%, 75%)

Typical Analysis (Wt. %)

Ni	O	C
20-80	<0.06	balance

Hazardous Ingredients

Hazardous Ingredients	Calculated Composition	C.A.S. No	PEL[1] –mg/m^3	TLV2 –mg/m^3
Nickel (Ni)*	20-80	7440-02-0	1	1.5*
Carbon (C) and/or Synthetic Graphite (C)	Balance	7440-44-0 7782-42-5	15 (total dust) 5 (respirable)	10 (inhalable) 2 (resp. dust)

* As inhalable fraction

Physical and Chemical Data

Grey-black, odorless powder, ranging in size from 20 to 200 microns in diameter.

Ingredient	Mol. Wt.	Specific Gravity	m.p.°C	b.p.°C	Sol. In H_2O g/100ml
Ni	58.71	8.9	1453	2732	0
C	12.01	1.92 – 2.2	n. av.	n. av.	0

Physical Hazards

Metal powders heat treated in reducing atmospheres may become spontaneously combustible.

Health Hazards

LD_{50} ORAL RAT >9000 mg/kg

Inhalation:

The National Toxicology Program has listed nickel as reasonably anticipated to be a carcinogen based on the production of injection-site tumors. The International Agency for Research on Cancer (IARC) found there was inadequate evidence that metallic nickel is carcinogenic to humans but since there was sufficient evidence that it is carcinogenic to animals, IARC concluded that metallic nickel is possibly carcinogenic to humans. Epidemiological studies of workers exposed to nickel powder and to dust and fume generated in the production of nickel alloys and of stainless steel have not indicated the presence of a significant respiratory cancer hazard.

The inhalation of nickel powder has not resulted in an increased incidence of malignant lung tumours in rodents.

Typical Properties of Nickel Coated Graphite

Screen Analysis

60% NCG	95% - 100 + 250
75% NCG	90% - 200 + 325

Apparent Density

62% NCG	1.4 to 1.5 g/cm3
75% NCG	1.7 to 1.9 g/cm3

Packaging

Size	Weight
1 gal / 4 liter can	11 lb / 5 kg
5 gal / 20 liter pail	55 lb / 25 kg

Note: All containers are lined with a polyurethane bag.

Appendix 5: Properties of Asbury synthetic graphite

Type	Carbon Content (min)	Typical Size	Surface Area (m^2/gram)	Typical Resistivity (Ohm-cm)
Natural Flake				
3610	99	60 x 325 mesh	1.5	0.067
FC3243	99	60% -325 mesh	3.0	0.036
230U	99	20 micron	6.5	0.068
5601	99	12-15 micron	7.0	0.066
Micro 850	99	3-5 micron	13.0	0.088
Synthetic				
4012	99	60 x 325 mesh	1.5	0.03
A60	99	60% -325 mesh	3.0	0.036
A99	99	20 micron	6.5	0.047
4437	99	12-15 micron	11.5	0.058
4827	99	1 micron avg.	113.18	0.1842
Hybrid				
4955	99	20 x 100 mesh	1.7	0.016
4956	99	60 x 325 mesh	2.53	0.022
4957	99	97% -200	8.38	0.040
Fibers				
AGM 94	94	1/8" and 150 micron	0.93 / 0.99	0.0014
AGM 95	94	1/8" and 400 micron	0.93 / 0.96	0.0068
AGM 99	99	150 micron	1.87	0.0014
Carbon Black				
5303	99	30 nm	254	.341

Appendix 6: Data sheet of gas diffusion layer AvCarb™ 1071

AvCarb™ properties, styles and grades

Yarn Filament Properties:

Grade(s)	HC	HCB
Diameter *(microns)* :	7.5	7.5
Cross-section :	Round	Round
Density *(gm/cc)* :	1.72 – 1.75	1.75 – 1.77
Surface Area *(gm/M²)* :		0.62
Tensile Strength kN/cm² *(ksi)* :	210 *(300)*	192.5 *(275)*
Tensile Modulus mN/cm² *(msi)* :	21 *(30)*	26.6 *(38)*
Elongation @ Break *(%)* :	1.0	0.72
Electrical Resistivity *(ohm-cm)* :	Controllable	1.1×10^{-3}
Thermal Oxidative Stability : *(wgt. loss/hr @ 500°C in air)*	Oxidizes	<1.0
Carbon Content *(%)* :	88 – 95	99.5

Representative AvCarb™ Carbon Fabric Applications:

Fabric Designation	Application
1071 HCB	Gas Diffusion Layer (PEM Fuel Cells), Other Electrochemical Applications
1209 HC	Ablative Insulation (Solid Fuel Rocket Motors)
1209 HCB	High Temperature Furnace Hardware Reinforcement
1243 HCB	Friction (Motion Control)

Typical AvCarb™ Fabric Styles / Grades:

Fabric Style	1071	1209	1243	1500	1580
Grade(s) :	HCB	HCB*	HCB*	HCB*	HCB*
Weave Construction :	Plain	Plain	Plain	5 Harness Satin	8 Harness Satin
Weave Count :					
Warp – per cm	17.3 – 21.3	9 – 10.6	11 – 12.6	9.8 – 13.8	10.2 – 14.2
Fill – per cm	16.5 – 20.5	7.1 – 7.9	10.6 – 11.4	9.0 – 13.0	9.5 – 13.5
Basis Wt. – gm/m² :	105 – 125	270 – 330	200 – 240	319 – 387	340 – 404
Thickness – microns :	280 – 432	675 – 825	650 – 750	675 – 1040	675 – 1040
Width – cm :	117	117	107	117	117
Availability :	Inventory	Inventory	Inventory	Special Order	Special Order

* Also available in HC grade

Appendix 7: Data sheet for GDL SIGRACET GDL10 BA

Properties	Unit	Typical Value	Variance
Thickness	micron	400	+/- 70
Areal Weight	g/m^2	85	+/- 12
Air Permeability	$cm^3/(cm^2*s)$	85	+/- 40
Spec. Electr. Resistivity	$m\,\Omega\,cm^2$	< 12	/

Appendix 8: DOE results from software for different filler loading including nickel coated graphite

Std	Run	Block	SG/Ni	VCB	CF	PP
13	1	Block 1	0.058333	0.308333	0.058333	0.575
6	2	Block 1	0	0	0.2	0.8
15	3	Block 1	0.116667	0.116667	0.116667	0.65
14	4	Block 1	0	0.5	0	0.5
16	5	Block 1	0	0.25	0.25	0.5
12	6	Block 1	0.308333	0.058333	0.058333	0.575
7	7	Block 1	0	0	0.35	0.65
3	8	Block 1	0	0	0.5	0.5
10	9	Block 1	0.25	0	0.25	0.5
8	10	Block 1	0.25	0.25	0	0.5
2	11	Block 1	0.2	0	0	0.8
1	12	Block 1	0.5	0	0	0.5
11	13	Block 1	0.116667	0.116667	0.116667	0.65
5	14	Block 1	0	0.2	0	0.8
4	15	Block 1	0.058333	0.308333	0.058333	0.575
9	16	Block 1	0.308333	0.058333	0.058333	0.575

Appendix 9: Procedures for freeze fracturing composite SEM samples

a) Cut bipolar plates made from different composites into strips with10cm in length, 3mm in width and 3mm in thickness;
b) Use a tweezers hold the sample strip, and dip into liquid nitrogen below the liquid lever for 3 minutes;
c) Break the sample strip, cut SEM sample around 4-5 mm in length from fracture surface, and stick the sample into SEM sample holder with fracturing surface upward.

Appendix 10: Procedures for hot-pressing molded bipolar plates for a single cell performance testing

a) Preheat the mold in hot pressing up to190 ~ 200 ℃;

b) Spray releasing agent on the surfaces of mold;

c) Put injection molded plate sheet into the chamber of mold and keep hot pressing temperature within 190 ~ 200 ℃ around 15 minutes;

d) In order to push air bubbles out of mold, load pressure and release the mold for a couple of times. Pressure applied are from 5000, 10000 to 15000 psi;

e) Shut off hot-pressing heating, and keep load pressure at 15000 psi;

f) Take out mold from hot pressing until the temperature reaches to 120℃;

g) Release bipolar plate sample.

Appendix 11: Photos of mold for fabricating composite bipolar plate for single cell fuel cell performance testing